ACCELERATED MORPHOLOGICAL MODELLING

A SCHEMATIZED CASE STUDY INTO THE MEDIUM- AND LONG-TERM MORPHOLOGICAL ACCELERATION TECHNIQUES MORFAC AND MORMERGE

ARCADIS & UNIVERSITY OF TWENTE

M.Sc. Thesis R.J.A. Wilmink

Wednesday, 1 July 2015
Final report

ARCADIS

UNIVERSITY OF TWENTE.

ACCELERATED MORPHOLOGICAL MODELLING

A schematized case study into the medium- and long term morphological acceleration techniques Morfac and Mormerge

Thesis

Submitted to acquire the degree of Master of Science
To be presented in public
On 7 July 2015 at 15.00 hours
At University of Twente, Enschede, the Netherlands

By

Rinse Johannes Andreas Wilmink

University of Twente
Faculty of Engineering Technology
Master Programme: Civil Engineering and Management, Water Engineering and Management

Student number: s1095153

Cover images: Harbour moles and adjacent beaches at IJmuiden, The Netherlands (North Sea). Pictures obtained from Beeldbank Rijkswaterstaat.

This thesis has been approved by the supervisors.

Members of graduation committee:

Dr. ir. J.S. Ribberink	Chairman, University of Twente Water Engineering and Management, Marine and fluvial systems
Dr.ir. P.C. Roos	Supervisor, University of Twente Water Engineering and Management, Marine and fluvial systems
Dr. A.P. Tuijnder	Supervisor, Arcadis, River, Coast and Sea & University of Twente
Dr. ir. B.T. Grasmeijer	Supervisor, Arcadis, River, Coast and Sea

This Master Thesis is initiated and supported by Arcadis. Their cooperation is hereby gratefully acknowledged.

UNIVERSITY OF TWENTE.

Abstract

In simulating the long-term morphology of a natural coastal and offshore system, the most restrictive element is the available computational capacity. Computations for long-term simulations of the morphology take a long time and a lot of computational power. To overcome this crucial disadvantage for long-term morphological simulations, input reduction for real-time measurement signals and an acceleration of morphological changes can be applied. This thesis attempts to test both approaches. Based on progressive insight in morphodynamic modelling, two techniques for accelerating the morphological changes are commonly used nowadays, i.e. Morfac and Mormerge. The performance of both methods and their possibilities and limitations for a uniform sandy coast, including a navigation channel and a harbour entrance is the subject of this study.

This thesis first provides answers to introductory questions as which input conditions should be combined into 'input scenarios' to run morphological simulations that represent the reality and how do Morfac and Mormerge simulate the medium- and long-term morphology. Then, using a schematized Delft3D model in 2DH mode for the coastal and offshore area of IJmuiden, there has been investigated in what way a tidal signal can be reduced, how many wave classes should be included to obtain accurate results, which acceleration factor is still acceptable to achieve accurate results and what are the distinguishing elements that decide which method is most appropriate for a certain simulation. All simulations will produce a ten yearly morphodynamic development of the study area by tidal forcing (and if included, waves as well). The simulations are compared to a reference simulation. To quantify the accuracy, four performance indicators will be calculated. These performance indicators are: Nash-Sutcliffe coefficient (NS), Root Mean Square error (RMS), linear correlation coefficient (R) and the slope of the linear regression line (B). An acceptable accurate result is obtained when the NS is above 0.95, the RMS lower than 0.5, R over 0.99 and B lower than 1.05. By means of a Multi-Criteria-Analysis (MCA) a comparison will be performed between Morfac and Mormerge. The assessment criteria of the MCA are: accuracy, ease of use, applicability (physical justification of what is happening) and simulation time.

The reference simulation chosen in this study is named the brute-force simulation. This brute-force simulation uses the reduced tidal input condition, a measured wave signal and an acceleration factor of ten to simulate the morphological development for ten years. Incorporating these elements for the brute-force simulation is the most time efficient and closest to reality as possible for the time limit of this study.

Morfac and Mormerge both accelerate the sediment transport rate by a factor. This approach is considered legitimate because of the differences in timescales of the hydro- and morphodynamics. The difference between the techniques is in the computation of particular conditions (for example varying wave heights or directions). Morfac calculates the conditions one after another using the bathymetry of the previous condition at the start of the new condition. The acceleration factor applied is for every condition multiplied by a weight (percentage of occurrence of that particular condition). The sequence of conditions is determined randomly. Mormerge calculates these conditions parallel by weighting the bottom change of all conditions every flow time step by its percentage of occurrence of that condition. A fixed acceleration factor is applied in Mormerge.

For the input reduction, a (double consecutive) morphological tide has been derived which matches the morphological development of the study area for approximately one spring-neap tidal cycle simulation as close as possible in terms of the linear correlation coefficient. This morphological tide has been made

harmonic to avoid shocks of the model from one tide to another and it consists of the M_2, M_4, M_6 and M_8 tidal constituents. For the long-term simulations, the harmonic morphological tide is easy to implement. The validation of the harmonic morphological tide, when focusing on water levels and flow velocities, matches the double tide of the spring-neap tidal cycle very well. The Nash-Sutcliffe coefficients averaged over 41 temporal observation points in the domain for the water levels and flow velocities are 0.98 and 0.95 respectively. The Brier Skill Score of the morphological development by the harmonic morphological tide compared to the morphological development of the simulated spring-neap tidal cycle is 0.96 (were a value of 1 is a perfect prediction with respect to the brute-force simulation). In addition, a real-time wave signal has been converted into directional and magnitudinal bins. The results of short simulations of all combinations of directional and magnitudinal bins (wave conditions) have been used to determine the sequence of importance for the morphological development of the study area by different wave conditions. This sequence is determined by the OPTI-routine which resulted in four wave scenarios (including one, two, six or ten wave classes).

The long-term simulations performed showed the formation of nearshore banks, migration of the nautical channel, sedimentation around the harbour moles and a deep scour hole directly in front of the harbour moles. This study showed that for water depths of approximately > 6 m, the acceleration factor and acceleration method are not decisive for the accuracy of the results with respect to the brute-force simulation (in water depths over 6 m, the sediment transport is more tide driven). The model is accelerated to its maximum factor possible using the input reduction for the tide; at least one harmonic morphological tide has to be simulated for the result to be valid. No deviating results were obtained. The inclusion of additional wave classes (determined by the OPTI-routine) resulted in an increased model performance. At least six wave classes had to be included to obtain results within the acceptable range of accuracy.

A Multi-Criteria Analysis has been performed to determine which method is most appropriate to use and what are the distinguishing elements that are decisive in choosing a particular method. Each performance criterion (accuracy, ease of use, applicability and simulation time) has a specific weight in the MCA and are ranked from + + to - -. The outcomes of the MCA are therefore a weighted average of the rankings. Accuracy is important for the choice of a particular method. However, because the small difference in accuracy when including six or ten wave classes, this performance criteria was not decisive. More decisive in choosing a particular acceleration method are the run times. For Mormerge, especially when including additional wave classes, the run times are much shorter (when enough computational capacity is available). Ease of use and applicability for a particular situation contribute only to a minor extent to the overall score, both in favour of Mormerge. Mormerge is thus more beneficial than morfac, especially when including additional wave classes (which in turn leads to a more accurate result). For the nearshore zone (water depth approximately < 6 m) no clear results in terms of accuracy of the acceleration method and the amount of wave classes to be included were obtained. For this zone additional research is recommended.

Samenvatting

De beschikbare rekenkracht van computers is tegenwoordig nog steeds de meest beperkte factor bij het simuleren van natuurlijke kust en zee systemen. Morfodynamische simulaties voor de langere termijn zijn tijdrovend en kosten veel rekenkracht. Om deze nadelige bijkomstigheid in te dammen kan een input reductie van meetsignalen in de tijd dan wel een versnelling van de morfologische veranderingen worden toegepast. Deze studie is een combinatie van beide opties. Voor de versnelling van de morfologische veranderingen zijn Morfac en Mormerge hedendaags het meest gebruikt. Deze methoden zijn gebaseerd op voortschrijdend inzicht in morfodynamisch modelleren. De prestatie van beide methoden en de voor- en nadelen voor een zandige kust met een vaargeul en haveningang, zijn het onderwerp van deze thesis.

Dit onderzoek zal allereerst twee introducerende vragen beantwoorden: welke input condities moeten combineert worden tot input scenario's om morfologische simulaties vergelijkbaar met de werkelijkheid te kunnen uitvoeren en hoe simuleren Morfac en Mormerge de langere termijn morfologie? Vervolgens, gebruik makende van een geschematiseerd Delft3D model in 2DH mode voor het kust- en offshore gebied van IJmuiden, is onderzocht hoe het getijsignaal kan worden gereduceerd, hoeveel golfklassen moeten worden meegenomen voor goede simulatieresultaten, welke acceleratiefactor is nog acceptabel om goede resultaten te behalen en wat de onderscheidende elementen zijn die bepalen welke methode het best gebruikt kan worden voor een bepaalde situatie? Alle simulaties zullen een tienjarige morfodynamische verwachting van het studiegebied simuleren door gebruik te maken van getij (en wanneer meegenomen, golven). De simulaties worden vergelijken met een referentiesituatie. Om de nauwkeurigheid van de simulaties te kwantificeren worden vier criteria berekend. Deze criteria zijn de Nash-Sutcliffe coëfficiënt (NS), Root Mean Square error (RMS), lineaire correlatiecoëfficiënt (R) en de helling van de lineaire regressielijn (B). Het nauwkeurigheidsniveau vereist voor een acceptabele simulatie wordt bereikt wanneer de NS coëfficiënt boven 0.95 is, de RMS lager dan 0.5, R hoger dan 0.99 en B lager dan 1.05. Een Multi-Criteria Analyse (MCA) vergelijkt de verschillen tussen de versnellingsmethoden, meegenomen golfklassen en versnellingsfactoren. De beoordelingscriteria van de MCA zijn: nauwkeurigheid, gebruiksgemak, toepasbaarheid (fysische verklaarbaarheid van wat er gebeurt) en rekentijd.

De referentiesituatie van deze studie wordt de brute-force simulatie genoemd. Deze brute-force simulatie maakt gebruikt van het reduceerde getijsignaal, een gemeten golfsignaal en een versnellingsfactor van tien om een tienjarige morfologische ontwikkeling te simuleren. Het gebruik van deze elementen in de brute-force simulatie is het meest tijd efficiënt en ligt het dichtst bij de realiteit voor de tijdslimiet van de studie.

Zowel Morfac als Mormerge versnellen de morfodynamiek door de berekende sedimenttransporten te vermenigvuldigen met een factor. Deze aanpak wordt legitiem geacht vanwege het verschil tussen de hydrodynamische en morfodynamische tijdsschalen. Het verschil tussen beide versnellingsmethoden zit in de berekening van verschillende condities (bijvoorbeeld variërende golfhoogtes of golfrichtingen). Morfac berekent deze condities achter elkaar. Iedere volgende conditie gebruikt de bodemsamenstelling berekend door de voorgaande conditie als input. De toegepaste versnellingsfactor wordt vermenigvuldigd met een gewicht. Dit gewicht is het percentage van voorkomen van die bepaalde conditie. De volgorde waarin de verschillende condities berekend worden, is willekeurig bepaald. Mormerge daarentegen berekent de verschillende condities parallel aan elkaar. De bodemsamenstelling wordt iedere flow tijdstap berekend door een gewogen gemiddelde van de bodemresultaten van alle condities te nemen. De gewichten in dit gewogen gemiddelde wordt eveneens bepaald door het percentage van voorkomen van een bepaalde conditie. Daarnaast wordt een vaste versnellingsfactor toegepast voor alle condities.

Voor de inputreductie van het model is een morfologisch getij afgeleid welke de morfologische verandering van een volledige springtij-doodtij cyclus zo nauwkeurig mogelijk nabootst. Deze nauwkeurigheid is gemeten door middel van de lineaire correlatiecoëfficiënt. Om schokken in het model te voorkomen (van het ene naar het andere getij) is het morfologisch getij harmonisch gemaakt. Dit harmonische morfologische getij bestaat uit vier getijdecomponenten te weten M_2, M_4, M_6 en M_8. Dit gereduceerde harmonische getij is eenvoudig te implementeren voor de lange termijn simulaties. In de validatie van het harmonische morfologische getij, vergeleken met waterstanden en stroomsnelheden, presteert dit getij erg goed vergeleken het getij van de springtij-doodtij cyclus. De Nash-Sutcliffe coëfficiënt gemiddeld over 41 observatiepunten in het domein van de waterstanden en de stroomsnelheden zijn 0.98 en 0.95 respectievelijk. De Brier Skill Score van de morfologische ontwikkeling veroorzaakt door het harmonische morfologische getij vergeleken met de morfologische ontwikkeling van de gesimuleerde springtij-doodtij cyclus is 0.96 (hierbij geeft een waarde van 1 een perfecte voorspelde ontwikkeling ten opzichte van een referentiesituatie aan). Voor de input reductie van de golven is het gemeten golvensignaal onderverdeeld in hoogte- en richtingsklassen. Voor elke combinatie van een hoogte- en richtingsklasse is een korte morfologische simulatie uitgevoerd. De resultaten van deze simulatie zijn gebruikt om de volgorde te bepalen van de mate waarin een specifieke conditie (combinatie van golfhoogte en richting) de totale morfologische ontwikkeling van het gemeten signaal nabootst. Deze volgorde is bepaald door de OPTI-routine methode en heeft geleidt tot vier verschillende golfklimaten (de golfklimaten bestaan uit één, twee, zes of tien golfklassen).

Alle uitgevoerde lange termijn simulaties laten duidelijk de formatie van kustnabije zandbanken, de migratie van de vaargeul, de ontwikkeling van de erosiekuilen en de sedimentatie direct voor de havendammen zien. In deze studie komt naar voren dat voor waterdieptes ongeveer groter dan 6 m de acceleratiefactor en methode niet bepalend zijn voor de nauwkeurigheid van het resultaat (t.o.v. de brute-force simulatie). In waterdiepten groter dan 6 meter is het sedimenttransportsysteem meer getij gedreven dan golf gedreven. Het model is hierbij versneld tot het maximum mogelijk wanneer men gebruikt maakt van deze inputreductie voor het getij; tenminste 1 harmonisch morfologisch getij moet gesimuleerd worden voor een valide resultaat. Geen significante verschillen in de resultaten konden worden geobserveerd. Het meenemen van extra golfklassen (bepaald door de OPTI-routine) resulteert wel in een verbeterde model prestatie. Tenminste zes golfklassen moeten worden meegenomen in de simulatie om een voldoende nauwkeurigheidsniveau te bereiken.

Een Multi-Criteria Analyse is uitgevoerd om te bepalen welke methode het meest geschikt is om te gebruiken en wat daarbij de onderscheidende elementen zijn voor de keuze van die methode. Elk criterium in de MCA (nauwkeurigheid, gebruiksgemak, toepasbaarheid en rekentijd) hebben een gewicht toegewezen gekregen. Alle criteria op hun beurt hebben een score van + + tot - - gekregen. De uitkomst van de MCA is daarom een gewogen gemiddelde van alle scores. Nauwkeurigheid is erg belangrijk in de keuze voor een bepaalde methode. Echter, vanwege de kleine verschillen in nauwkeurigheid wanneer zes of tien golfklassen worden gesimuleerd, is dit criterium niet bepalend. Meer bepalend voor de keuze van een bepaalde versnellingsmethode zijn de rekentijden. Vooral wanneer extra golfklassen worden meegenomen zijn de rekentijden gebruik makende van Mormerge vele malen korter (wanneer genoeg computer rekenkracht beschikbaar is). Gebruiksgemak en toepasbaarheid voor een bepaalde situatie genereren enkel kleine toevoegingen aan de totale MCA score, beide in het voordeel van Mormerge. Mormerge is dus in het voordeel vergeleken met Morfac, vooral wanneer extra golfklassen worden meegenomen (welke op hun beurt leiden tot een extra nauwkeurig resultaat). In de kustnabije zone (waterdiepten ongeveer kleiner dan 6 m) zijn geen eenduidige resultaten behaald met betrekking tot de versnellingsmethode en de hoeveelheid golfklassen mee te nemen. Voor deze zone is aanvullend onderzoek met betrekking tot het versnellen van lange termijn morfologische simulaties gewenst.

Preface

Five years ago, on the 30th of August 2010, my first lecture in Civil Engineering took place. The more I got into the field of Civil Engineering; it became clear that water is my subject. Choosing the track Water Engineering and Management, flooding, flood protection, flood risks, drought, water policy and standards, propagation of water and sediment, measurements and data analysis, physics, design and engineering, all subjects passed by. During the master phase, it also became clear that the understanding of water (and sediment/morphology) is still limited. Testing of hypotheses' and thoughts of how the natural system works costs a lot of effort. Increased computational capacities have eased this work. However, making a prediction of a very long time span for a system where the conditions are changing from second to second is still very difficult and very much restricted by the computational capacity available. I hope that this master thesis contributes to the knowledge, especially in engineering practice, about how and how fast the long term predictions for a morphodynamic system can be accelerated and what the advantages and disadvantages are. Understanding of the natural forces acting on the system to be simulated is essential to evaluate the results of the simulations.

Writing this thesis, a period of five years being a student is almost completed. These five years flew by very fast. Being a student offered a lot of opportunities to visit many projects in my field of interest. In addition, it offered several opportunities to visit places far away and experience different cultures. I would like to thank many people who made these five years very nice and pleasant (In Dutch there is a word for this: ''Gezellig''. However, no English translation exists that exactly means the same…..).

First of all, I would like to thank my family for the support and patience in the past five years. I would like to thank my friends for always being interested in my work, for the nice activities, nights out and for the trips we made. Hopefully many more will come. Besides, I would also like to thank my colleagues at ARCADIS River, Coast and Sea. They supported me, helped me out when I got stuck and inspired me for this research. Especially, Arjan Tuijnder for his supervision and providing feedback and Bart Grasmeijer for helping me out with the model, enthusiastic discussions about the topic, answering my always very simple questions and bringing me coffee!

At the university I would like to thank Jan Ribberink for his critical reviews and discussions of my work. A special thank goes to Pieter Roos. Using his network I got the opportunity to perform this master thesis at ARCADIS. He supervised this master thesis and provided very detailed feedback. With this feedback (also from Arjan, Bart & Jan) I was able to improve this thesis. Besides, Pieter, also thanks for being constructive and to think along with us to make it possible to follow a course when we were in South-America!

Rinse

Almelo, July 1th 2015

Contents

1 Introduction

1.1 RESEARCH BACKGROUND

Every day, many ships are entering and leaving the harbour of Rotterdam through the Euro-Maasgeul for all kinds of purposes. Ships with a maximum draft of 22.85 m are allowed to use the Euro-Maasgeul in the North Sea (Rijkswaterstaat, 2014). Behind the breakwaters of this waterway, at the coast, sandy beaches and dunes are present which protect the hinterland from flooding. Besides, they are of great touristic and economic value. The presence of this beach next to the nautical waterway means that the waterway incises the up-sloping sea bottom towards the coast.

Other examples in which the development of the (coastal) morphology to human activities is relevant are: cables and pipelines, offshore windfarms, oil platforms and other hydraulic structures, all founded on the bottom of a waterbody. These structures, including the nautical channels, are often present for several decades and are of great value for the world economy (e.g. internet cables). Because of the presence of highly economically valued items on the bottom of the sea, it is important to have a clear understanding of their complex behaviour. Morphodynamic models for the medium- and long-term are indispensable tools to understand this behaviour and to predict what will happen in the future.

The behaviour of the hydrodynamics and morphodynamics is affected by each other (Ranasinghe et al., 2010; Ribberink, 2011; Wijnberg, 1995). The hydrodynamics are changing the layout of the bottom through sediment transport and, in turn, the bottom layout changes the behaviour of the hydrodynamics, be it on different timescales. Modelling this mutual behaviour is difficult because of the interactive character of the hydro- and morphodynamics. In addition, the input conditions used for these models are changing in time, even from second to second. One can think of a varying wind speed and direction resulting in waves and currents that in turn interact with the tide and the morphology, thus changing the water levels and sediment transport. Also, not every grain on the sea bottom can be described individually with its particular shape and size. When all relevant physical processes would be included in a numerical model that simulates a couple of years of morphological changes, long run times of the simulation are needed because of the enormous number of calculations that have to be executed using the restricted computational capacity. Therefore, morphological modelling, especially in the vicinity of a coast, needs a form of process aggregation or information reduction (De Vriend, et al., 1993; Lesser, 2009).

According to De Vriend et al. (1993) three distinct approaches for medium- and long-term morphological modelling can be used:

- Input reduction. This is based on the idea that residual long-term effects can be described with models based on the description of small-scale processes forced with reduced representative inputs.
- Model reduction. The model itself can be reformulated at the scale of interest without describing the details of smaller-scale processes.

- Behaviour-oriented modelling. This approach only models the phenomenon of interest without understanding and describing the underlying processes.

This thesis employs a combination of the first two approaches: input reduction and model reduction to simulate the long-term morphological behaviour. Besides the input aggregation and a schematization of reality, often an acceleration of the morphological development is applied to reduce the computational effort and to obtain the results more quickly. For this model reduction, the acceleration factors (multipliers) are applied to the suspended and/or bed load sediment transport rates.

Amongst others, some very often and widely applied morphological medium- and long-term acceleration methods, for example applicable in Delft3D, are: Tide-averaging, Continuity-correction, Rapid Assessment of Morphology (RAM), Morfac and Mormerge (Roelvink & Reniers, 2012). These methods have been developed on the basis of progressive insight in morphodynamic modelling and the most efficient use of the available computational power. The most common and currently used methods to accelerate morphodynamic simulations are Morfac and Mormerge. These methods are more extensively described in section 3 of this thesis. Both methods include an acceleration factor for the morphological changes and are the subject of this thesis.

Several studies have shown good applicability of Morfac and Mormerge for modelling the medium- and long-term morphodynamics, e.g. Lesser et al. (2004); Lesser (2009); Van der Wegen & Roelvink (2008); Zimmerman et al. (2012). They can be implemented in various numerical models as Delft3D (Deltares), Mike21 (Danish Hydraulic Institute) and Telemac (Laboratoire Nationale d'Hydraulique, France). Example implementations of one of the morphological acceleration techniques in Delft3D, Mike 21 and Telemac can be found in the studies of Lesser et al. (2004), Jimenez & Mayerle (2010) and Knaapen & Joustra (2012) respectively. For this study, the numerical model Delft3D will be used (Open Source version 4168, in 2DH mode as will be explained in section 2).

1.2 PROBLEM DESCRIPTION & OBJECTIVE

In engineering practice several methods, as mentioned above, are nowadays used, e.g. in Delft3D, to simulate the medium- and long-term morphological behaviour of water bodies. The most common, recent and computationally efficient methods used are the Morfac and Mormerge. The focus in this thesis is on these two methods which are developed based on progressive insight in accelerated morphological modelling. The working procedures of these methods are explained in section 3.

Which of the two methods performs best under particular circumstances compared to a reference simulation (or reality), however, is not known. In practice several assumptions are made how to include the many different input conditions, their interaction and which morphological acceleration factor is still acceptable for a reasonable simulation. The choice as to which method will yield the best results is merely based on experience of the researcher and is the problem definition of this thesis.

1.2.1 RESEARCH OBJECTIVE

The objective of this thesis is to determine the performance of Morfac and Mormerge in simulating the long-term morphology of a schematized study area in Delft3D using several different input conditions compared to a reference situation, based on pre-defined criteria. The study area chosen in this study concerns the coastal and offshore area of IJmuiden, the Netherlands, to be explained in sub-section 1.3. For commercial purposes not only the accuracy of the results, but also the simplicity of use, the calculation

time and the applicability for a particular situation are important criteria for assessing the results of a certain method.

For this study, the emphasis is not on the calibration and validation of a morphological model for the study area. No specific attention will be paid to the influence of numerical parameters. The model built in this study will be used to address the influence of input reduction and of different acceleration methods compared with each other and to the situation without morphological acceleration and input reduction.

1.2.2 RESEARCH QUESTIONS

To achieve the above objective, several research questions are defined:

1. Which input conditions should be combined into 'input scenarios' to run morphological simulations that represent the reality?
2. How do Morfac and Mormerge simulate medium- and long term morphology?
   a. Which model equations are solved during the simulation and in what sequence?
   b. Which extra options are available in the execution?
   c. Which feedback loops between the morphodynamics and hydrodynamics are present and what are they doing?
   d. Are there any significant differences in the working procedures of the two methods resulting in significantly different results?
3. In what way can a real-time tidal signal be reduced to a representative tide that is able to simulate accurate hydrodynamic and morphodynamic results compared to a reference period?
4. How many wave classes resulting from the input reduction should be included in a simulation using Morfac and Mormerge to obtain accurate results compared to a reference simulation?
5. Which acceleration factor for the morphological changes is still acceptable to achieve accurate results compared to a reference simulation?
6. What are the distinguishing elements that decide which method is most appropriate for a certain simulation?

1.3 METHODOLOGY AND READING GUIDE

During this research, several steps based on the research questions will be performed to achieve the objective of this thesis. An overview of these steps is given in Figure 1. First, the study area for which a schematized model will be constructed is described (section 2). This description includes field data characteristics and reveals important hydrodynamic elements of the natural system. These elements should be included in the simulations to represent reality and will provide an answer for research question one.

A schematisation of the study area is chosen for simplicity. The schematized model should represent an existing situation for the practical application of the results. The study site chosen consists of the coastal and offshore area of IJmuiden, the Netherlands. Because of the relatively low fresh water discharge due to sluices and locks located at the canal entrance near the sea, on average only 95 m^3/s (Swinkels, Bijlsma, & Hommes, 2010), the salinity gradients outside the 2.5 km long harbour moles are neglected. Therefore, 3D modelling in the near shore is not necessary. If a very complex system was chosen where 3D modelling is necessary (e.g. when strong salinity gradients in the study area are present), computational times are very long and this is a risk to the time limit of the research. In addition, another very complex system has the risk that it cannot be pointed out which processes are responsible for certain changes. For example, an estuary or delta where many channels, shoals and tidal flats are present is less suitable for performing this study. A schematized model for the study area in Delft3D 2DH mode will be constructed (open source

version 4168). For this model, a so-called online approach in Delft3D is used. The online approach differs from an offline approach where the wave module uses the outcomes of the flow computations. In the online approach, the wave field in the flow module is updated periodicaly based on the most recent flow field results. The flow module in turn uses the most recently calculated wave field to compute a new flow field and sediment transport field (Deltares, 2014).

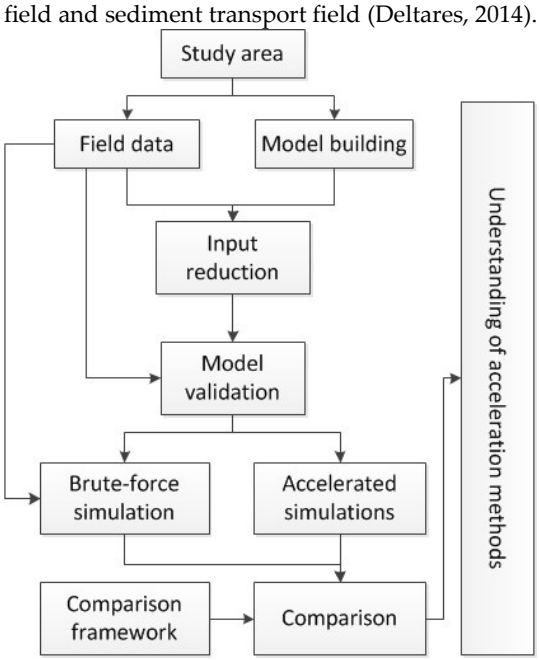

Figure 1 - Research approach visualised

To answer research question two, a thorough understanding of the morphological acceleration methods of interest is needed. In section 3, a detailed description of Morfac and Mormerge, and how these methods simulate the long-term morphology, is provided. This description includes information about the implementation of the acceleration methods in this study. In section 4, the schematized model will be set-up including grid building, bathymetry construction and definition of the boundary segments for the boundary conditions.

In section 5 the input reduction will be performed. Because of the continuously changing conditions of the system, a form of process aggregation is needed to avoid long run times of the simulations. The input reduction will be applied for the tide and the waves. These aggregated processes of tide and waves form the base of the long-term simulations. Several different scenarios will be built from simple (tide only) to more complex (tide – wave interactions and different wave heights/directions) which serve as input for the long-term simulations[1]. The various scenarios will in the end provide an answer for research question four.

[1] To speed-up the computations, the performed simulations are making use of a parallel computation on multiple cores of a computer. A script for this parallel computation has been provided by Arcadis. The script divides the computational grid in a user defined number of parts (6 in this case). Every part is computed by a different processor. These processors periodically exchange information to in the end calculate one final result for the complete computational grid. To check the influence of this parallel computation, a comparison is done with a simulation that has not been computed parallel. The results deviated only very locally (at some points at the connection of two parts of the computational grid). These differences were negligible. The parallel computation decreased the runtime approximately by a factor three.

For the input reduction of the tide, a so called ''morphological tide'' will be derived which should result in a morphological development as close as possible to a reference period. The reference period in this study is approximately a full spring-neap tidal cycle. By validating the morphodynamic results of the derived morphological tide with a simulation without input reduction (real-time data), research question 3 will be answered. The input reduction concerning the waves can be done in several ways. Because of the extensive information of wave characteristics available, the OPTI-routine is used (more detailed explained in section 5). The OPTI-routine determines the sequence of importance of the waves, including weights for a particular wave class, for the morphological development of the modelled study area.

The long-term simulations of both acceleration techniques will be compared to a reference simulation. This reference simulation, called the brute-force simulation, uses input reduction for the tide and a real-time measured signal for the waves, without an extra acceleration (because of the good applicability of this tide, see section 5.1). The brute-force simulation is performed for one year and will be compared to the same brute-force simulation, however accelerated with a factor ten to account for ten years (time span of long-term simulations). The comparison will be done when both brute-force simulations simulated one year of morphodynamic development. This comparison is done in order to check the performance of the ten year brute-force simulation compared to a non-accelerated simulation; this is the most time efficient way to simulate a ten year morphological development without losing much input data. The ten yearly morphodynamic development of the brute-force simulation will qualitatively be compared to field data to validate the applicability of the model. In engineering practice and consultancy, often a morphodynamic prediction of ten year is asked by clients. Therefore, a time span of ten years for the morphodynamic development is chosen in this study.

To answer research questions four and five, all simulations as listed in Table 1 will be performed. The number of tides simulated per year is related to the acceleration factor applied. To compare the bottom development of the many long-term simulations that will be performed, several cross sections will be defined which are of interest for this study. Looking at cross sections can reveal small differences between the bottom developments of the different simulations very easily. In addition, in making figures, many results for a particular cross section can be visualized in only one plot. Visualisation in this way of the performed simulations is much more efficient than comparing cumulative sedimentation and erosion patterns. For the defined cross sections, several performance indicators to quantify the accuracy will be calculated. These performance indicators are calculated with respect to the brute-force simulation of ten years and averaged over all cross sections for a quick comparison. The performance indicators include the NS coefficient, RMS, linear correlation coefficient and the slope of the linear regression line (B). An acceptable accurate result is obtained when the NS is above 0.95, the RMS lower than 0.5, R over 0.99 and B lower than 1.05. The performance indicator NS and the linear correlation coefficient (R) do have an upper limit of one (perfect match). The RMS has a lower limit of zero (perfect). These indicators are therefore easy to compare using colour scales. The optimal result for the slope of the linear regression line between the long-term accelerated simulations and the brute-force simulation of ten year is one. These results however can be both higher and lower. A colour scale is therefore not suitable. To make a colour scale possible, an upper or lower limit is needed. Therefore, an indicator for the slope of the linear regression line will be calculated. This indicator is defined as: ABS(average RMS – 1) +1. ABS means absolute value. Now the lower limit of the slope of the linear regression line is one (perfect) and a colour scale is applicable as well.

The long-term simulations will start using a sediment thickness of 25 m to avoid supply-limited sediment transport. In addition, a spin-up period of 1 day is used in the long-term simulations. For the long-term simulations, especially when accelerating, it revealed that the critical water depth for which the sediment calculation starts had to be increased to 0.3 m to avoid model instabilities at the coast (especially when

weighting the bottom development in Mormerge). Also the sedimentation and erosion of adjacent dry cells has been set to 25 % of the wet cells. These settings have been applied to all long-term simulations, including the brute-force simulations.

Table 1 - Long term simulations. For the tide-only case and the inclusion of one wave class, Morfac = Mormerge. The number of tides simulated per year in the table is related to acceleration factor applied.

Waves	0	1	2	6	10	2	6	10
Tides simulated per year			Mormerge			Morfac		
1								
2								
4								
6								
12								

All simulations listed in Table 1, including the brute-force simulations, will start directly after the validation of the input reduction. The results of the long-term simulations are presented in section 6. During the computation of the long-term simulations, the framework for comparing the acceleration methods with the brute-force simulation will be defined (section 7). By using this framework, the distinguishing elements that decide which acceleration method and factor are most appropriate for a particular simulation will become clear (research question seven). To compare the resulting bathymetries of all simulations, bottom changes as well as sediment transport rates can be used. In this study bottom changes will be used which will result in a higher correlation coefficient compared to a reference situation as pointed out by Van Rijn (2012).

The comparison of the (sub) variants will take place by means of a Multi-Criteria Analysis. The sub-variants are simulations in which parameters as the number of tides being simulated, which is related to the acceleration factor, are varied. In the analysis, both acceleration methods including the various input conditions are compared based on predefined criteria. The assessment criteria of the different acceleration methods are: accuracy, simulation time, ease of use and applicability for a particular situation (physical justification). In engineering practice and consultancy where a project has to be finished in time because of a deadline set by the client, a simulation time of 100 - 120 hours (± 5 days) still is acceptable. Ideally for long-term simulations, a simulation time of ± 60 hours is desired. When a computer needs 60 hours to compute the final model result, approximately three simulations a week can be performed and checked if the model simulated correctly. In consultation with the supervisors of this thesis a weighting for each criterion in the MCA will be determined. The outcomes of the MCA will determine which method is most suitable for a specific situation and which elements are relevant to obtain accurate results.

The research that will be performed as is described in this methodology should lead to answers for all research questions. In section 8, the conclusions of this research are presented including an extensive discussion of the results. Additionally, recommendations are made for further research.

2 Study area

2.1 INTRODUCTION

In this section, the study area and field data characteristics are described. As explained in the methodology sub-section (1.3), the coastal and offshore area of IJmuiden the Netherlands is chosen as the study site for this research. The description of the field data characteristics will reveal the hydrodynamic elements of the natural system that should be included in a model to simulate the area well. These important hydrodynamic elements will form the answer to research question one; which input conditions should be combined into 'input scenarios' to run morphological simulations that represent the reality.

2.2 STUDY AREA

The study site chosen consists of the area outside the harbour moles of the harbour of IJmuiden, the Netherlands; see Figure 2. This area will be implemented in a schematized way (section 4). The study site covers an area from the coast up to a water depth of 20 m w.r.t. NAP and tens of kilometres wide (North – South orientation).

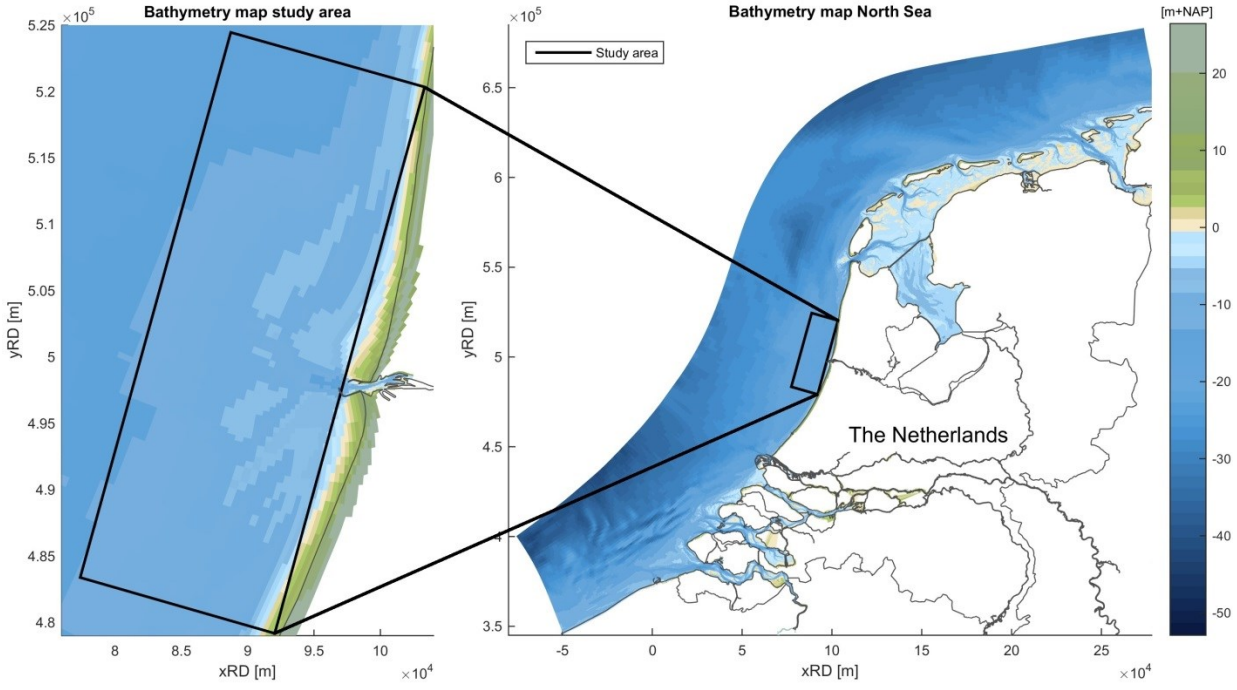

Figure 2 – Bathymetry study area and zoom-in. Colour map is the same for both figures. Data from: Vaklodingen 2000, Rijkswaterstaat. In the model a schematized bathymetry, based on field data, will be implemented (see section 4).

In the study area, the IJgeul is present which is a navigational channel in the North Sea. This navigational channel connects the offshore regions with the North Sea canal (Dutch: Noordzeekanaal) to reach the harbour of Amsterdam.

2.3 CHARACTERISTICS OF TIDE AND WAVES

The morphological development of the study area is mainly determined by waves (caused by wind) and the tide. These processes are necessary to derive input conditions for the morphodynamic development in this case study. Both processes are described more extensively in this section. Wind data is implicitly taken into account by the waves; the measured wave heights are caused by wind. In the model, no wind forcing is used to avoid wind driven currents. Field data of the tide and waves are obtained from live.waterbase.nl, the database of Rijkswaterstaat (Rijkswaterstaat, 2011). The most recent year with available validated data of all necessary measured variables is 2013. The data of the year 2013 are therefore used in this study. An example of measured data of the total water level, calculated tidal water level and measured wave height can be seen in Figure 3.

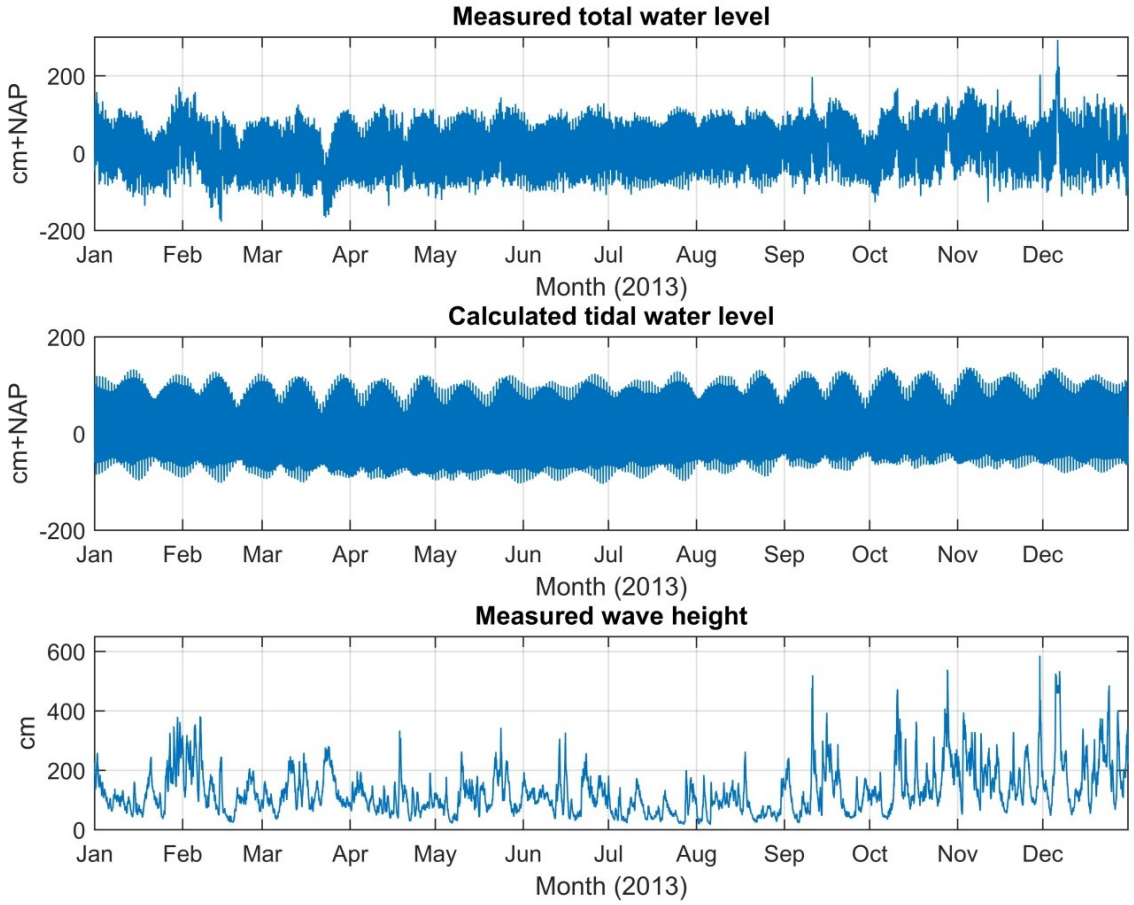

Figure 3 - Measured total water level (a) and calculated tidal water level (b) at station IJmuiden Buitenhaven. Measured wave height (c) at station IJmuiden Munitiestortplaats (Rijkswaterstaat, 2013).

2.3.1 TIDE

The tidal elevation in the North Sea is mainly caused by the Atlantic oscillation near Scotland. In combination with the Coriolis force, this results in a Kelvin wave in the North Sea. Due to the shape of the coasts around the North Sea, the propagation of the tide is deformed and causes a turning of the tide

around amphidromic points. The propagation of the tide near the Dutch coast is therefore from South to North. The further away from an amphidromic point, the higher the tidal range usually is. The interaction of constituents (M_2 and S_2) and the M_2 with higher harmonic M_4 respectively cause the spring-neap tidal cycle and the daily inequality of the tide in the North Sea.

For IJmuiden, the mean high vertical tide is around 1 m NAP, with spring tides up to 1.4 m NAP. The tidal range in the North is smaller than in the South, as shown in Figure 4. This difference in tidal range is caused by the position of the Netherlands with respect to the nearest amphidromic point. In addition, the tidal curve in the North Sea is asymmetrical. This is mainly caused by the distortion (phase differences) of the M_2 tidal constituent by the M_4 constituent, which results in a faster rise of the tide then fall (Elias, 2006).

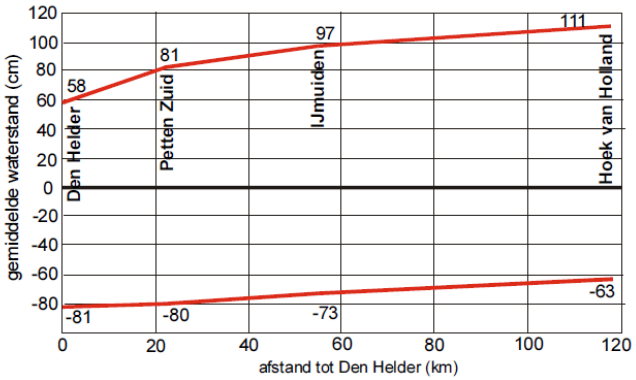

Figure 4 - Tidal range (in cm) along a part of the Dutch coast measured from Den Helder (0 km) (Van de Rest, 2004), data from (RIKZ, 2003). Red lines are indicating mean high water and mean low water for locations along the Dutch coast.

2.3.2 WAVES

Waves in the North Sea mainly result from local wind stress rather than swell (Van de Rest, 2004). These conditions vary from time to time (e.g. from day to day, as for example shown in Figure 3 c). In this figure, the seasonal variation of waves caused by the wind is clearly visible. In winter (October – February), the average wave height is more often higher than in summer (April – August). In addition, because of the geometry of the North Sea, waves originating from the Northwest or Southwest are occurring much more often with higher waves as can be seen in Figure 5. Waves originating from these directions can grow more in height because a longer fetch length of the wind. This causes a higher set-up (surge) of the water level because these waves are directed onshore. Easterly wave directions (waves originating from the East) do neither occur often nor result in high wave heights because of the vicinity of the coast (the waves originating from the East are causing a set-down of the water level, negative surge). Because of the orientation of the coast, waves from the North and South hardly result in high waves. These waves dissipate in the shallow water nearshore and are refracted towards the coast.

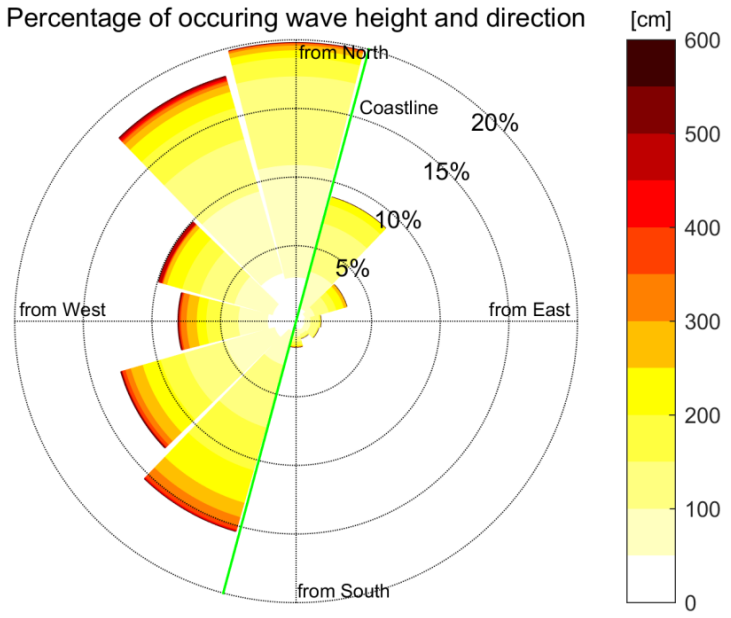

Figure 5 - Wave rose for wave climate measured at IJmuiden munitiestortplaats in 2013. The wave heights are obtained from the same signal as in Figure 3 (c). Data from: Rijkswaterstaat (2013)

3 Morphological acceleration techniques in numerical modelling

This section describes the morphological acceleration techniques Morfac and Mormerge. Besides input reduction, to be discussed in section 5, an acceleration of the morphological changes is an approach frequently applied to accelerate the morphodynamic long-term computations. In this section, first an introduction is provided in which a morphodynamic loop is shown and what in general the acceleration methods do. Next, the different acceleration methods will be discussed including the way they will be used in this study.

To compare the acceleration methods, a reference simulation will be performed. This reference simulation, called a brute-force simulation, uses a reduced tidal signal and a real-time wave signal without an extra acceleration of the morphological changes (because of the good applicability of this tide, see section 5.1). The brute-force simulation is performed for one year and will be compared to the same brute-force simulation, however accelerated with a factor ten to account for ten years (time span of long-term simulations). The comparison will be done when both brute-force simulations simulated one year of morphodynamic development. This comparison is done in order to check the performance of the ten year brute-force simulation compared to a non-accelerated simulation (further explained in section 6.1). In addition, various acceleration factors are tested in this case study. For both acceleration techniques, the acceleration factors applied are multiples of the number of harmonic morphological tides simulated per year (result of the input reduction as will be executed in section 5). Questions as: which equations are solved and in what sequence will be answered in this section. Also the implementation of the methods in Delft3D and the physical meaning of different elements will be provided. In the end, the similarities and differences between the acceleration methods and their implementation in Delft3D will become clear.

3.1 INTRODUCTION

Morphological models are indispensable tools for simulating the morphological behaviour of coastal areas, river- and sea bottoms. These models make use of a hydraulic-morphological system, or morphodynamic cycle, to calculate flow, sediment transport and bottom changes (Ribberink, 2011). The morphodynamic cycle can be tidally averaged, intra-tidal or by another user specified preferences be calculated. An example of a morphodynamic cycle is shown in Figure 6. Other, but similar examples of morphodynamic cycles can for instance be found in Ribberink (2011), Roelvink (2006) and Wijnberg (1995).

In the literature, several medium- and long-term morphological acceleration techniques in numerical modelling are known to accelerate the morphodynamic calculations. These techniques are making use of the morphodynamic cycle. The acceleration techniques (or methods) reduce the computational time, which is the crucial disadvantage when simulating longer time periods and large-scale applications (Jimenez & Mayerle, 2010; Lesser, 2009).

The morphological acceleration techniques accelerate the computation in various ways. The methods are developed on progressive insight in morphological modelling and computational power. Because of the progressive insight in morphodynamic accelerated modelling and the fact that all recently performed studies in this field use the Morfac or Mormerge method, the emphasis in this thesis is on these methods. The governing equations that are solved during the computation in Delft3D can be found in Appendix A: Delft3D model description.

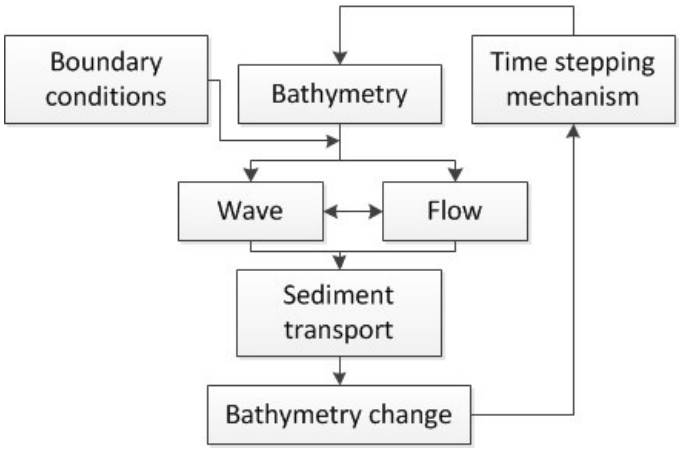

Figure 6 – Example of a morphodynamic loop, or cycle

3.2 MORFAC

Morfac is the first method that is characteristic for running flow, sediment transport and bottom updating all at the same small time steps. This contrasts previous methods for morphological acceleraction. Morfac is adapted from the elongated tide concept by Latteux (1995). The literature around this new method started around 2003 – 2004 when Lesser et al. (2004) proposed a three-dimensional morphological model with an morphological acceleration factor to accelerate the morphological changes for long-term modelling. The computation of the different components simultaneously and the two-way interaction of the flow and waves in which the sediment transport is calculated instantly, make it easy to include interactions between flow, sediment and morphology. This also reduces the storage of large amounts of data between the different processes (Roelvink, 2006).

The approach of running the flow, sediment transport and bottom updating at the same time does not take into account the difference between the morphodynamic and the hydrodynamic time-scales. To take advantage of this, a factor n is used to accelerate the morphological depth changes . In Delft3D, this multiplication is applied to the net sediment transports (bed load and/or suspended load) which are calculated every half time step (in water level points and half a time step later in the velocity points). The depth change based on the net sediment transports can be caluclated, if desired, every half a time step too. In order to avoid the violation of the continuity of sediment mass in the model, expressions are included that limit the erosion if the quantity of sediment at the bed approaches zero (Lesser et al., 2004). It is therefore important to check the thickness of the sediment layer in the model regularly.

For the complete model run this means that, for example after calculating the hydrodynamics of 10 tidal cycles and n = 10, a morphological simulation is done for 100 tidal cycles (which is comparable to 50 days). The flow diagram of Morfac can be seen in Figure 7.

A difference with previously used acceleration methods is that the bottom changes are computed in much smaller time steps. With a Morfac of 60, approximately one year of morphological change is simulated after 12 tidal cycles. If in a flow model, a time step of 5 minute is used, with a morfac of 60 the bathymetry is still updated every five hours. This results in a significant reduction of the computational time for Morfac. However, the short-term changes in reality due to varying wave and tide interactions put a limit on the morphological factor that is usable in simulations. A way to overcome this problem is to use a morphological factor that varies depending on the wave conditions. This is called variable Morfac. In this variant of Morfac, severe storms with a relatively low probability of occurrence would have a small Morfac and normal everyday conditions a high Morfac. The defined combinations of particular wave conditions with the tide, based on the input reduction as will be executed in this study, are simulated separately in a random sequence using the bottom layout of the previously executed class. All conditions are summed based on their percentage of occurrence or by changing the simulation times per condition (Lesser, 2009).

In this study, the time to be simulated is kept the same for all conditions. All conditions will be simulated for 10 years. Including a variable morfac (acceleration factor * percentage of occurrence of a particular wave condition) makes sure that every wave condition produces the right amount of morphological development, see Figure 8. The acceleration factors are choosen such that an integer number of harmonic morphological tides (result of the input reduction to be applied in section 5.1) are simulated per year as explained at the beginning of this section.

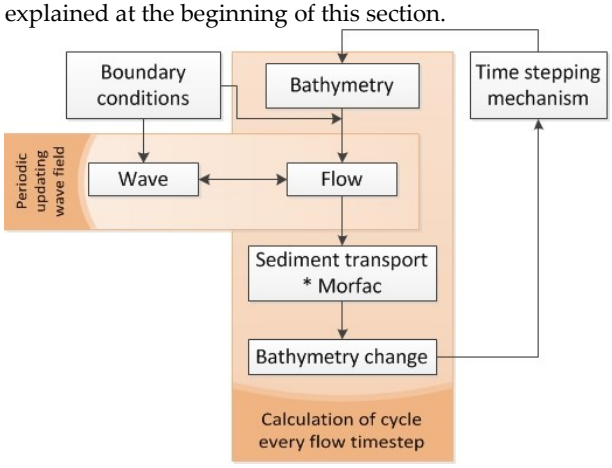

Figure 7 - Flow diagram of Morfac with an acceleration factor n

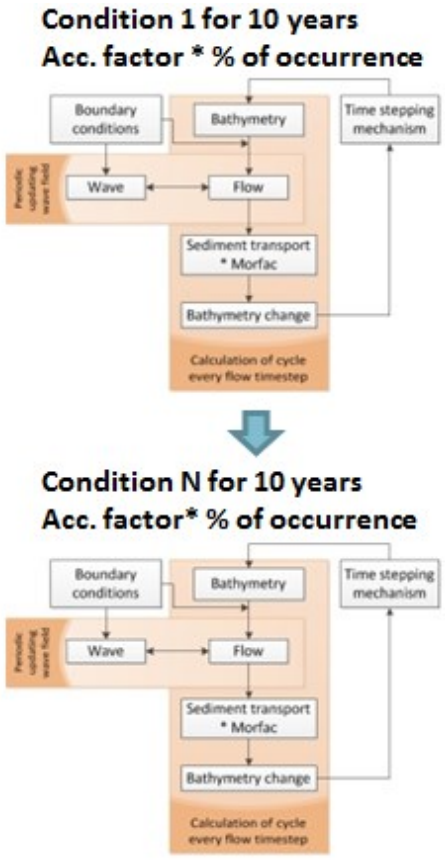

Figure 8 - Example of simulating different conditions using variable Morfac. The multiplication with the percentage of occurrence will not be applied if the morfac is fixed.

3.3 MORMERGE

Another method that has the stability and rate of accuracy of Morfac, but can perform the computations parallel, is Mormerge (Roelvink, 2006). In this approach it is assumed that the hydrodynamic conditions vary much more than the morphology. If the time interval in which all hydrodynamic conditions occur (ebb, flood, spring tide, neap tide, storms etc.) is small compared to the morphological time-scale, these processes can be run in parallel, using the same bathymetry and same acceleration factor for all conditions. This bathymetry is subsequently updated using a weighted average of the sediment transport rates for all hydrodynamic conditions based on the occurrence of the wave classes. The flow scheme of the method can be seen in Figure 9.

The various parallel processes for flow, wave and sediment transport can be defined based on different conditions that are present in a study area. These processes (input conditions) in this study are derived by applying input reduction (section 5). By computing the processes parallel, it is possible to include an instantaneously counteraction of conditions as is in reality. An example is that other tidal phases can be assigned to different wave conditions. This will lead to ebb and flood sediment transports counteracting each other at all times (as most times in reality) and can allow for the use of much higher morphological acceleration factors because of the reduced short-term amplitude changes (Roelvink, 2006). The tidal phase shift applied in this study is equally divided over the number of conditions included. A particular phase shift is randomly assigned to a wave class. For example, performing a Mormerge simulation which includes 10 wave classes, a phase shift per wave class of 36° (360°/10) is applied.

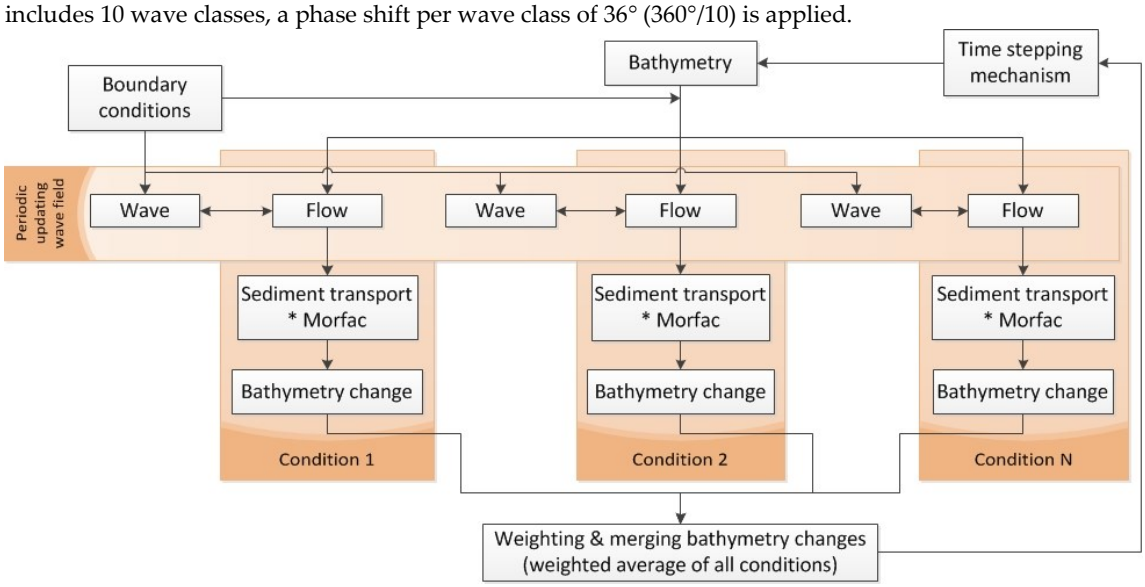

Figure 9 - Flow scheme of Mormerge with an acceleration factor included n included for all conditions.

For Mormerge, the bathymetric changes are weighted every flow time step. The weights in this study are a result of the input reduction for the waves as will be performed using the OPTI-routine. OPTI weights for the wave classes summed do not necessarily have to be equal to one. Because Mormerge automatically scales the OPTI weights to one, care should be taken to extract the correct output which represents a ten yearly morphodynamic development).

3.4 SIMILARITIES AND DIFFERENCES OF MORFAC AND MORMERGE

The acceleration methods Morfac and Mormerge are similar but have slight differences in calculating the bottom update. Both methods calculate the wave-flow interaction periodically and the sediment transport every flow time-step. The sediment transport and thus the related bottom changes are in turn multiplied

by an acceleration factor to determine the new bathymetry. This new bathymetry, computed every time-step, ensures that the hydrodynamic flow calculations (and waves) are always executed using the correct bottom layout.

The main difference between both methods is the way in which various conditions are computed. In Morfac, different conditions are computed after another, in a random sequence (or by a user defined sequence when information about this sequence is available) using the bathymetry of the previously computed condition. In Mormerge the conditions are computed parallel using the same bathymetry. Subsequently, the calculated bathymetric changes are merged based on a weighted average of the occurrence of particular conditions in reality. Mormerge can, in contrast to Morfac, also make use of different tidal phases for every condition. These phase differences can allow for the use of a much higher morphological acceleration factor as explained previously. In Delft3D, the different conditions are computed using a batch file to start a new computation for a particular condition. When a simulation does not include any wave condition or only one wave condition, Morfac equals Mormerge.

4 Model setup

4.1 DELFT3D PROCESS-BASED MODEL

To simulate the long-term morphology of the study area, the process-based model Delft3D is used (in 2DH mode, Open Source version 4168). This model describes waves, currents, sediment transport and bed level changes by a set of mathematical equations based on the conservation of mass, momentum, energy, etc. Delft3D consists of several modules of which two of them, the FLOW-module and the WAVE-module, are used in this thesis. The FLOW-module is the central module which communicates with the WAVE-module. A general overview of the equations solved in Delft3D and the solving scheme is given in Appendix A. This section describes the numerical input as the grid, initial bathymetry, physical parameters and other settings, boundary conditions and initial conditions.

4.2 GRID

The grid used in this study is an orthogonal curvilinear staggered grid. This grid is constructed using the RGFGRID feature of Delft3D. When constructing a grid, attention should be paid to the features that have to be modelled. Important areas and processes need to have sufficient grid cells to represent that particular item well. Furthermore, some general guidelines for constructing a grid are determined by Arcadis (Grasmeijer, Adema, & Jellema, 2014). These guidelines are restricting the maximum smoothness in both directions, the orthogonality and the aspect ratio. The smoothness is the ratio between the lengths of adjacent grid cells in a certain direction. The orthogonality determines the perpendicularity of a cell and the aspect ratio is the ratio between the length and the width of a grid cell.

In this research, a schematized study area of the coast of IJmuiden is chosen (see section 2, Study area). The schematization of the study area compared to the reality can be seen in Figure 10. The grid approximately is 15 * 42 km (M*N direction, see Figure 10). The other important characteristics of the grid and the grid criteria for a Delft3D computation are listed in Table 2.

Table 2 - Grid characteristics

	Grid	Criterion (Grasmeijer, Adema, & Jellema, 2014)
Total number of cells	21624	-
M number of cells	106	-
N number of cells	204	-
M –smoothness	1.13	< 1.2
N – smoothness	1.19	< 1.2
Orthogonality	0.006	< 0.04
Aspect ratio	1 (inner area)	< 2

To model the nearshore processes and the behaviour of the nautical channel accurately, the grid has been refined in these areas of interest. The coarsest grid cells at the boundaries are 450 * 300 m (M*N direction). The finest grid cells in- and around the nautical channel and the coast are 30 * 15 m (M * N direction).

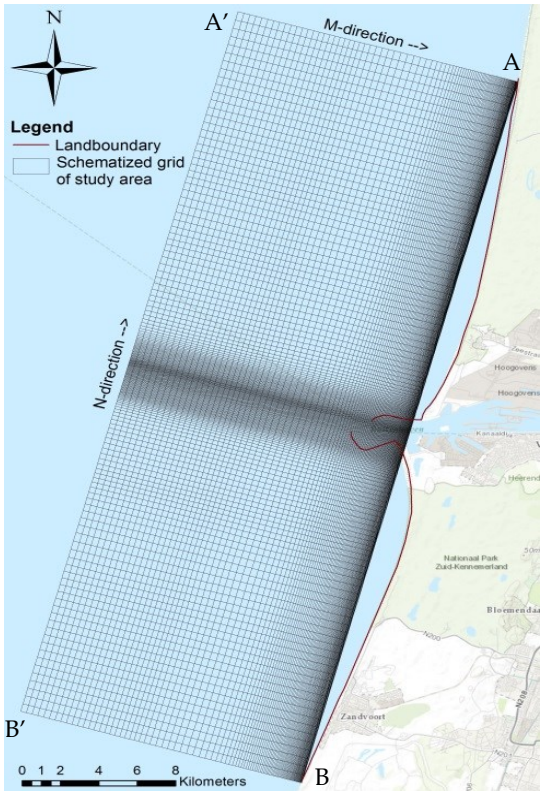

Figure 10 - Grid study site, coastal area IJmuiden. With real land boundary (red) and schematization (black)

4.3 NUMERICAL PARAMETERS

4.3.1 INITIAL BATHYMETRY

The initial bathymetry used in this study is constructed with the Quickin feature of Delft3D. This initial bathymetry is derived from JARKUS Raaien profiles in the area of interest. The Raaien 4800, 5000, 6000 and 6200 are assumed to represent an average uniform coastal profile around the harbour moles of IJmuiden, see Figure 11. From these profiles, the average coastal profile of IJmuiden has been derived. The average profile for the initial bathymetry starts at +5 m NAP to make sure that under the tidal elevation and wave height, no reflective numerical processes at the coastal boundary will occur in Delft3D. The average coastal profile has been extended with an exponential slope to -20 m NAP at 15 km offshore the coast, see Figure 11.

In the study area grid and initial bathymetry, the IJgeul is present (a nautical channel) that is around 20 m deep. This nautical channel is enclosed by harbour moles in the nearshore. The harbour moles are represented by thin dams in Delft3D that reach up to approximately 1200 m offshore where the water depth approximately 9 m is. Thin dams are chosen because these features are much smaller than the grid cell size. The bathymetry including the harbour moles and the nautical channel is shown in Figure 12. The bathymetry is very similar (but more schematized) to the bathymetry used in a study to reduce the sedimentation between the harbour moles (Bijlsma, Mol, & Winterterp, 2007).

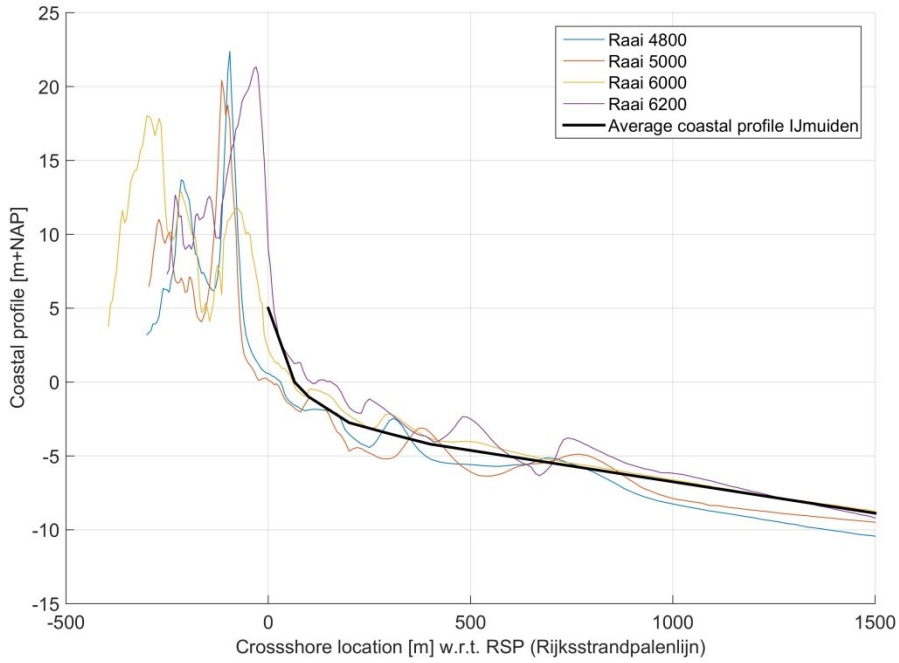

Figure 11 - JARKUS profiles of Raaien 4800, 5000, 6000 and 6200 in 2013 (Rijkswaterstaat, 2013).

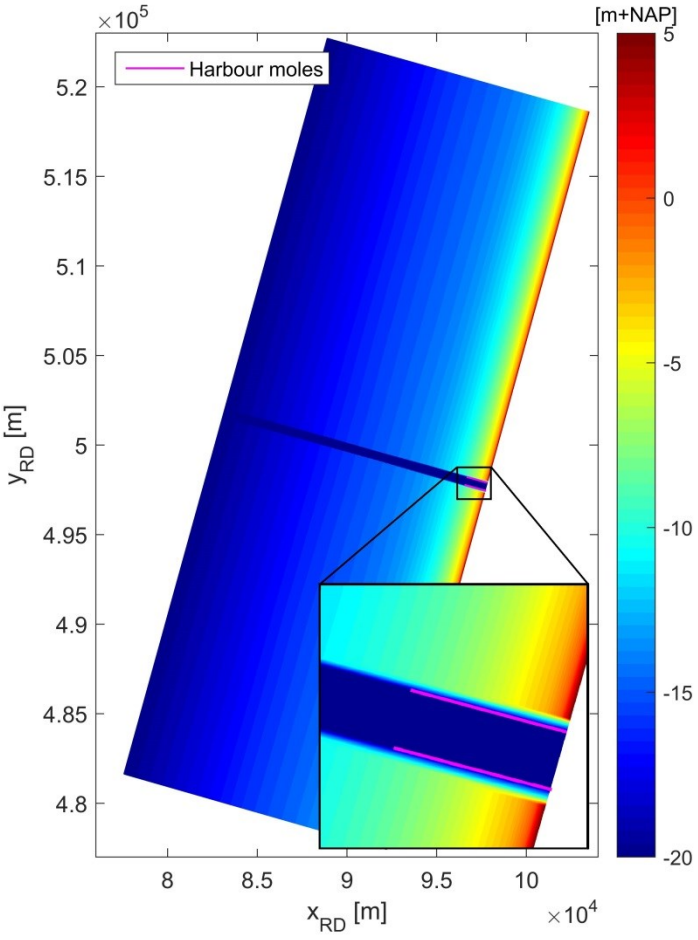

Figure 12 - Schematized bathymetry based on the average coastal profiles near IJmuiden. In this map, the IJgeul, harbour moles, bathymetry and a close-up of the beach area near the harbour moles are present.

4.3.2 BOUNDARY CONDITIONS

The numerical model Delft3D used in this study can solve the hydrodynamic and morphodynamic calculations with various boundary conditions. Which type of boundary conditions is most suitable, depends on the phenomena to be studied and the information available in the study area (Deltares, 2014).

For this study, several measuring locations are present in, or nearby the study area. To convert data from these stations to the exact location of the boundary conditions, interpolation of data from at least three stations is needed. To avoid this cumbersome interpolation of all boundary segments of the model, the model has been nested into an overall model, the Kuststrookfijn Astro model (abbreviated as Kustfijn) developed by Arcadis[2] (Alkyon, 2001b). The Kustfijn model has been validated to reproduce water levels at the Dutch coast. An example of the model domain of the Kustfijn model including the study area of this thesis is shown in Figure 13.

The open boundaries (North, West and South) of the nested model are divided into segments. The East boundary (the coast) is a closed boundary. This closed boundary is an upsloping beach to 5 m + NAP which can flood and dry. The start and end points of the open boundary segments are extracted from the overall model. To match the boundaries of the nested model as closely possible with the overall model, a maximum of 5 grid cells per segment is applied. This makes that the North and South boundaries are both divided into 21 segments and the West boundary into 41 segments. Between the start and end point of the segments where the water level is extracted from the overall model, the intermediate points are linearly interpolated. For the WAVE module, the same boundary locations are applied except that these boundaries are uniform (no subdivision into segments). The imposed wave conditions are the same for all boundaries and are uniformly applied over the boundaries. The wave boundaries nearshore are left out to avoid unrealistically high waves at the coast (H = 0 up to approximately 10 m water depth).

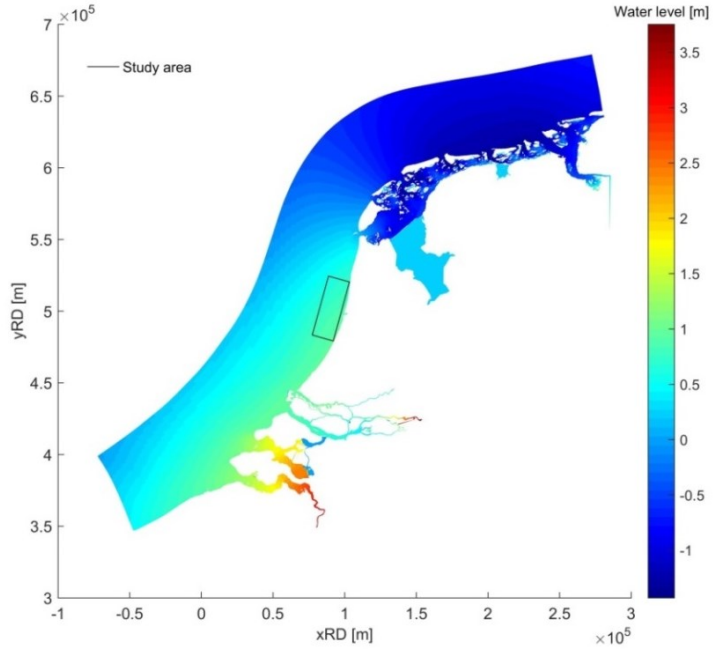

Figure 13 - Model domain Kustfijn model including the enclosure of the study area

Because of the validated water levels of the Kustfijn model, a water level boundary condition has been chosen for the Western boundary of the study area. It is however not desirable to include all boundaries of

[2] The Kuststrook models have been developed by Alkyon Hydraulics. This company was acquired by Arcadis in 2007.

the type water level. A small error in the water levels will result in continuity problems. These continuity problems can only be compensated for in a large response of the velocity components (Deltares, 2014). Therefore, at the cross-shore boundaries (North and South) a Neumann type of boundary condition is applied. This type of boundary condition specifies the normal water level gradient. In combination with the Western water level boundary, the solution of the mathematical boundary problem is well-posed. The Neumann boundary conditions at the cross-shore boundaries can handle various different processes acting on a boundary where the exact water level or velocity is not known beforehand, as is desired in this study. Using this type of boundary, the model determines the correct solution for the Neumann boundary segments by applying the imposed normal water level gradient (Roelvink & Walstra, 2004).

To avoid the model making an artificial boundary layer along the boundary, the advective terms containing the normal gradients of the open boundaries are switched off. In addition, the water level boundary is made less reflective. The reduced reflection makes sure that short wave disturbances propagating towards the boundary from inside the model are not fully being reflected back into the domain as is the case when this parameter is set to zero.

4.3.3 OTHER PARAMETERS AND SETTINGS

The sediment concentration used in this study contains only one fraction. The D_{50} of this fraction is 200 µm with a specific density of 2650 kg/m^3 and a dry bed density of 1600 kg/m^3. This D_{50} value is found representative for the study area (Van Alphen, 1987; Wijnberg, 1995). A uniform Chézy roughness coefficient of 65 m$^{1/2}$/s and a horizontal eddy viscosity of 1 m^2/s are used in the model (default Delft3D). The water density has been set to 1020 kg/m^3. In the model, no salinity or temperature gradients are included.

To calculate the flow, a hydrodynamic time-step has to be specified which fulfils the Courant number criteria. This criterion provides an indication of the accuracy and numerical stability of the model and should generally not exceed a value of ten. For an implicit scheme where stability is not an issue (as is used in this study), the Courant number criterion is mainly important for the accuracy of the model. The Courant (Friedrich-Lewy) number (CFL) criterion for Delft3D is defined as (Deltares, 2014):

$$CFL = \frac{\Delta t \sqrt{gH}}{\min\{\Delta x, \Delta y\}} < 10 \qquad \rightarrow \qquad \Delta t < \frac{10 * \min\{\Delta x, \Delta y\}}{\sqrt{gH}} = \frac{10 * 15}{\sqrt{9.81 * 20}} = 10.7\ s \qquad 1$$

In which Δt is the time step (in seconds), g the acceleration of gravity (m/s^2), H the maximum water depth (m) and $min\{\Delta x, \Delta y\}$ is the minimum of the smallest grid sizes (m). For this study, the minimum of the grid cells is approximately 15 m and the maximum water depth is 20 m in the nautical channel. This results in a maximum time step of 10.7 sec. Because of the relatively simple geometry of the model, a time step of 12 seconds (0.20 minutes) is applied. This small violation of the CFL criterion does not result in a decreased performance in terms of accuracy (section 5.3). The frequency of the communication between the FLOW and WAVE modules in Delft3D is set to 60 minutes. The measurement interval of the wave climate used is also 60 minutes. A complete list of all parameters used in the model can be found in Appendix A.6.

4.3.4 INITIAL CONDITIONS

To reduce the spin-up time of the model as much as possible, first a model run of a full spring-neap tidal cycle has been performed without bed update to calculate the correct water level, velocity, sediment concentration and the active layer of sediment thickness in Delft3D. These conditions are then used at the start of a model run.

5 Input reduction

In simulating the medium- and long-term morphodynamic behaviour of a study area, input reduction is desirable to avoid unnecessary time consuming computations with real-time data (Latteux, 1995). This input reduction will be applied to the tide and wave boundary conditions. Afterwards, the simulation results of the reduced input conditions are validated based with a simulation using real-time data (no input reduction). This section will provide an answer to research question three in what way a tidal signal can be reduced to a representative tide for an accurate long-term simulation.

5.1 TIDE SCHEMATIZATION

For the schematization of the tide, a so called 'morphological tide' will be derived. This morphological tide is a harmonic tide of two consecutive tidal cycles that should result in the same morphological development as a daily average of the astronomical tide for approximately a full spring-neap tidal cycle. The morphological tide will be chosen such to match the change in the morphology for an entire spring-neap cycle in reality as closely as possible. Because of the daily inequality of the tidal water levels in the study area, a double morphological tide (or two consecutive tides) will be derived.

In this study the method of Roelvink & Reniers (2012) is used which is in principle the same as Latteux (1995). Roelvink & Reniers (2012), however, recommend to only calculate one spring-neap tidal cycle instead of a full year of morphological behaviour to derive the morphological tide. The method is easy to apply and uses a scaling factor directly derived from linear regression instead of a calibration of parameters such as in the method of Lesser (2009). The following procedure should be executed to derive the morphological tide according to Roelvink & Reniers (2012):

- First, a simulation of flow and sediment transport including bottom changes over approximately a full spring-neap tidal cycle should be performed as a reference situation (simulation without waves).
- The next steps has to be performed for each consecutive tide (double tide in this study):

1. Calculate the correlation between the tide-averaged transport rates or bottom changes in all grid points for the full spring-neap tidal cycle and all consecutive double tides separately. The linear correlation coefficient is defined as:

$$r = \frac{cov(x,y)}{\sigma(x) * \sigma(y)} \qquad 2$$

Where a value r = 1 indicates a perfect match of the shapes of both datasets. $cov(x,y)$ is the covariance of datasets x and y. $\sigma(x)$ and $\sigma(y)$ are the standard deviations of both datasets. The linear correlation coefficient indicates the correctness of the shape of the bottom changes; the correlation represents the rate of linearity between these bottom changes (McClave, Benson, & Sincich, 2010). A correlation of 1 means that the bottom changes of both periods (double consecutive tide and full spring-neap tidal cycle) is fully linear and positive. A correlation of zero means no linearity at all between the two datasets.

2. Together with the correlation coefficient, the slope of the linear regression line between the bottom changes of the full spring-neap tidal cycle and each double tide has to be calculated. This slope parameter indicates the correctness of the magnitude of the bottom changes; a slope equal to the number of double tides simulated is a perfect match. This slope parameter is used as a time-scale factor. The computed bottom changes should be multiplied with this factor to obtain the actual bottom changes for a full spring-neap tidal cycle.

Both parameters, the correlation coefficient and the slope of the linear regression line combined provide quantitative information of the shape and magnitude of all double consecutive tides in which they represent the shape and magnitude of bottom changes of the simulated spring-neap tidal cycle. Ideally, a double tide should be chosen with a correlation coefficient closest to one and a slope parameter closest to the number of double tides simulated.

For this study, the following parameters are calculated for the approximately simulated spring-neap tidal cycle (2/4/2013 to 30/4/2013, 28.45 days), see Figure 14 (here only the best fit of all tides is shown, the results of the other double tides can be found in Appendix B.1). From the full series, the tide with the highest correlation and the most adequate slope parameter is no. 20 (Figure 14). This tide has a correlation coefficient of 0.9993 and a slope parameter of 20.342. This tide is visualized in Figure 15. The tide period is from 11 April 2013 06.50 h to 12 April 2013 07.40 h and is chosen as the morphological tide for this study. The morphological development (cumulative sedimentation and erosion pattern) of this full spring-neap tidal cycle can be seen in Appendix B.2.

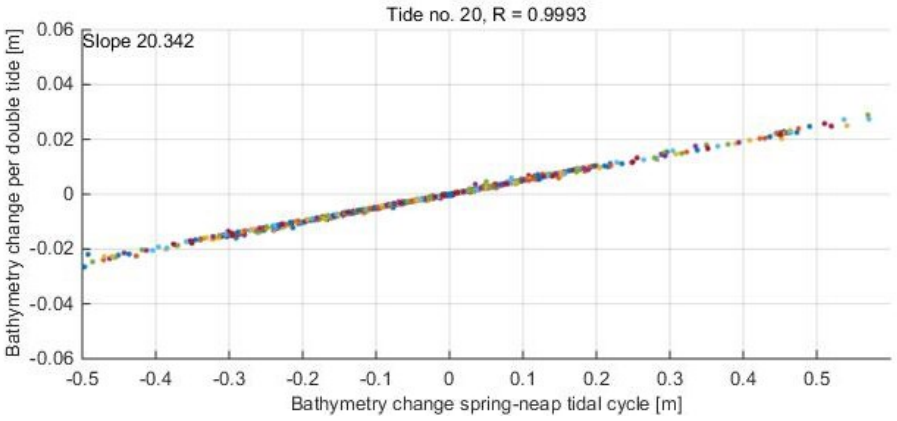

Figure 14 - Correlation and slope parameter of morphological tide

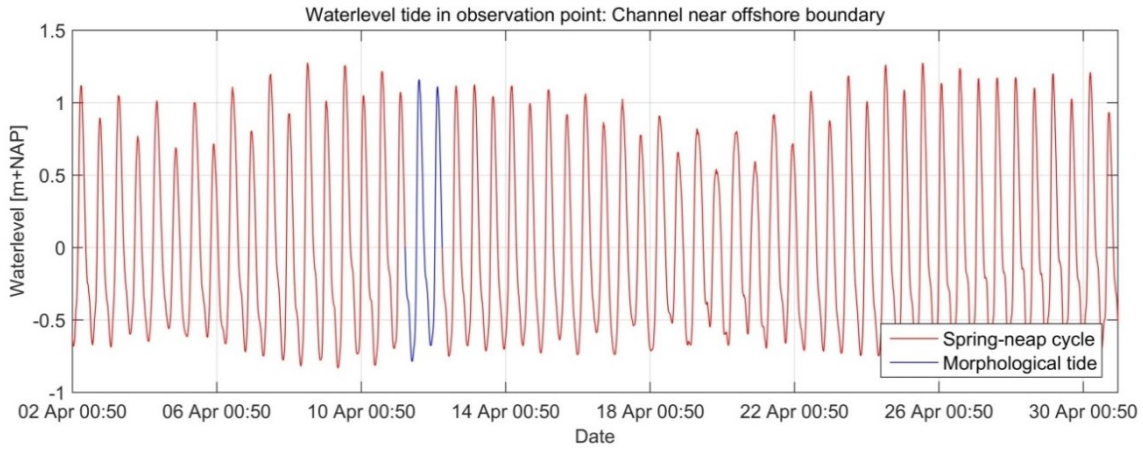

Figure 15 - Morphological tide (blue) derived from full spring-neap tidal cycle (red)

To make the selected tide a perfectly periodic boundary condition with a base frequency equal to the M_2 tidal constituent frequency, a harmonic analysis of the selected time series is performed. For this harmonic analysis, the selected morphological tide is repeated several times to be able to extract various harmonic constituents from this signal. The main tidal constituents derived from this signal are the M_2 and higher harmonics M_4, M_6 and M_8 tidal constituents. Amplitudes and phases values of the harmonic tidal constituents for the grid corner points northwest and southwest are listed in Table 3. The choice for only incorporating these four constituents is supported by the tidal form factor F which is defined as (Pugh, 2004):

$$F = \frac{\hat{\zeta}K1 + \hat{\zeta}O1}{\hat{\zeta}M2 + \hat{\zeta}S2} = 0.14 \qquad 3$$

This value of 0.14 means that the tide is semidiurnal and thus mainly determined by the M_2 constituent distorted by the higher harmonics. The derived harmonic morphological tide is shown in Figure 16. The derived harmonic morphological tide shows the characteristics of the increasing tidal amplitude towards the South and towards the coast as expected by the explanation of the characteristics of the tide in the North Sea (section 2.3.1).

Table 3 - Harmonic tide conditions

Location	Constituent	Amplitude (m)	Phase (°)
Northwest	M_2	0.6624	142.90
	M_4	0.2213	178.27
	M_6	0.1115	239.92
	M_8	0.0613	303.66
Maximum total amplitude		1.0565	
Southwest	M_2	0.7138	99.53
	M_4	0.2804	151.84
	M_6	0.0477	214.41
	M_8	0.0546	212.15
Maximum total amplitude		1.0965	

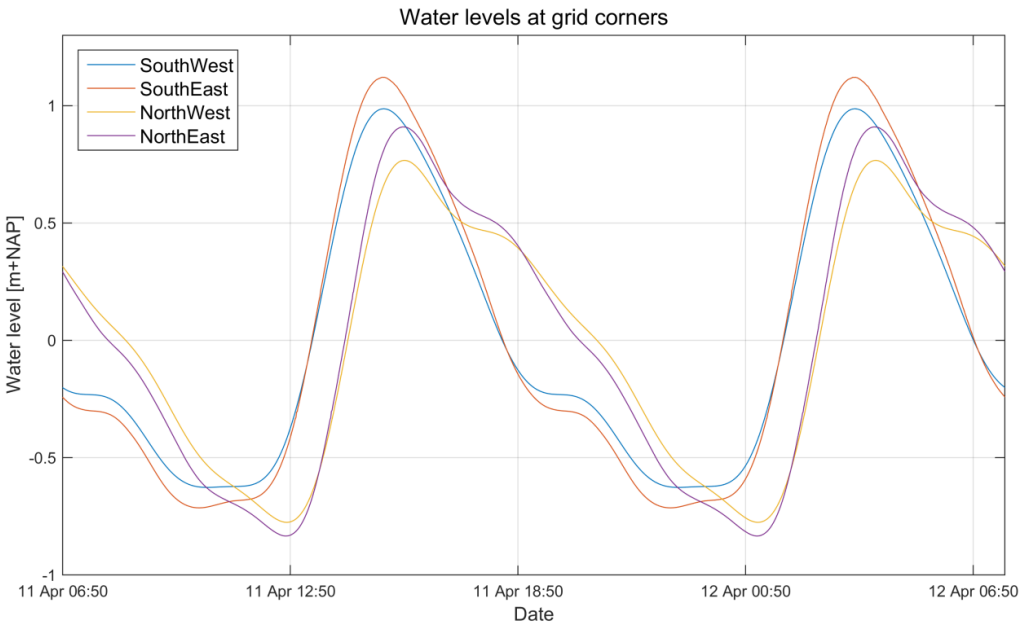

Figure 16 - Water levels of the harmonic boundary conditions at grid corners

5.2 WAVE SCHEMATIZATION

A full wave climate is the state of the waves at a certain location over a period of time. These conditions depend on meteorological conditions and can vary from time to time (even from second to second). In practice, it is impossible to include all these short variations. Therefore, a schematization of the wave climate is necessary. Regarding the schematization of a full wave climate, as for example shown in Figure 3c, the goal is to reduce the wave classes as much as possible without losing much accuracy in the morphological development of these waves compared to the full wave time series.

The schematization of the wave climate will be done for the characteristics of the waves measured at the ''IJmuiden munitiestortplaats'' measurement location. It is located around 30 km offshore in front of IJmuiden where the water depth is around 20 m (Van de Rest, 2004), equal to the water depth at the seaward open boundary of the model used in this study. The measured wave characteristics are therefore assumed to give representative values at the boundaries of the model used in this study.

To schematize the wave climate, the time series of the year 2013 is used to take the hourly, daily, weekly and even seasonal variations into account. These wave conditions in turn are classified into directional and magnitudinal classes, as can be seen in Figure 5. The full wave climate is divided into 12 directional and 12 magnitudinal classes and thus into 144 different combinations of wave height and direction. However, because of the location of the measurement station (far offshore), the waves occurring from 15° to 195° w.r.t. North (measured clockwise), are not realistic in this study. These waves would then originate from the land. Leaving out these waves leaves 72 combinations. In addition, not every combination of wave height and wave direction is present (see Figure 5). This results in 62 combinations of wave height and wave direction for this study area. All combinations are listed in Table 12, Appendix B.3).

The full wave climate divided into 62 distinct classes will now be reduced to scenarios with 0, 1, 2, 6 and 10 different wave classes to compare the morphological acceleration methods. All those scenarios should reproduce the full wave climate as closely as possible. To select the best combinations of classes, two frequently used approaches exist (Van Rijn, 2012):

- The first approach is to manually determine the wave classes based on the wave height, direction and morphological impact. The morphological impact is assumed to be proportional to the wave height to some power and is derived from the CERC formula for alongshore sediment transport at a uniform coastline.
- The second approach uses a target dataset. This target dataset is created by short morphological simulations of all wave height-direction combinations and are weighted afterwards based on their percentage of occurrence. After the weighting, this target dataset is assumed to be representative for the morphological development of the full wave climate. The approach can be further divided into the so called ''optimum selection'' (OPTI-method), or for example the method of correlation. The OPTI-method is more suited when several wave classes have to be determined. In addition, as pointed out by Van Rijn (2012), the method of correlation (even for the selection of one wave class) did not improve the results in terms of the correlation coefficient and the Root Mean Square error (RMS) in that study.

Because of the extensive information available of wave heights, direction and the combination of the two, the second approach is chosen to perform the wave schematization. To determine the wave climates, the OPTI-method is used (Mol, 2007). The procedure of the OPTI-method is visualised in Figure 17.

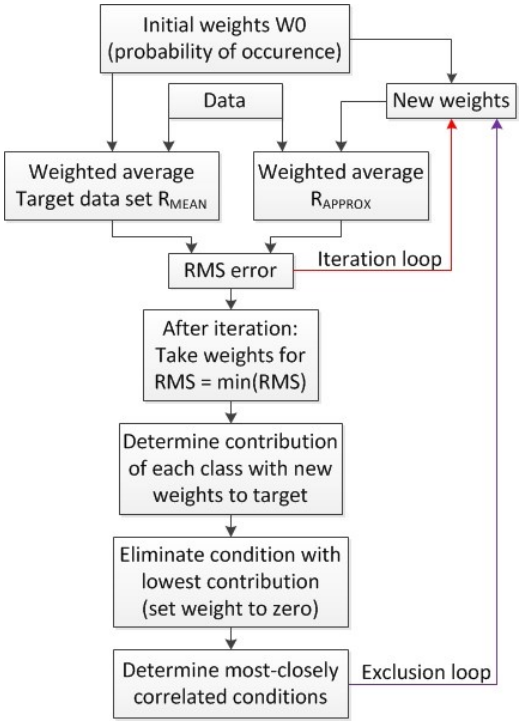

Figure 17 - Overview of OPTI-method procedure, modified from Van Rijn (2012)

After the calculation of the target dataset as explained previously (R_{MEAN}), the OPTI-method determines which wave class has the smallest relative contribution to e.g. the bottom change of the target data set. This wave class will be dropped out (its weight will be set to zero). After the first exclusion, an iteration loop starts in which all remaining classes are assigned a new individual weight factor. With these new weights, a new average result (R_{APPROX}) is determined and compared to the target data set. The accuracy of the new reduced set of wave classes is described by the RMS. The RMS is defined as:

$$RMS = \sqrt{\frac{1}{n}\sum_{i=1}^{n}(x_i - y_i)^2} \qquad 4$$

In which x is the bottom change of the target data set, y is the bottom change of a particular wave class and n the number of wave classes.

The new weight factors assigned to the wave classes is a product of the original weight multiplied by a value in the range from 0 – 2 (uniformly distributed with an expected value of 1). This multiplication is assumed as a random allocation of new weights. When a large number of iterations is made, the new weight of a certain class will be multiplied with a value close to one; it is therefore very similar to the original weight. All R_{APPROX} results of the determined weight based on the user defined amount of iterations are compared with the target dataset. One of the results with its particular weights for the wave classes will reproduce the target data set the best in terms of the RMS. In this combination of wave classes and weights, the class with the smallest contribution to achieve the target dataset is dropped (weight set to zero). Next, the following exclusion step is started, following the same procedure. The process continues until only one wave class with a certain weight factor is left.

In Figure 18 the development when leaving more and more classes out on the correlation and the RMS is shown for a number of iterations. As can be seen in Figure 18, a higher number of iterations does not necessarily lead to a better approximation of the target dataset. The method, per exclusion step, determines the best combination of wave classes and weights for the target dataset. Once chosen, the least contributing wave class will be dropped out. At the following exclusion step, a different combination of

the remaining wave classes and weights is chosen. This combination, in some cases, could perform better when the already dropped wave class would be included again. However, once a wave class is dropped out, it cannot contribute anymore to any other combination of wave classes and assigned weights. This certainly holds for situation where only a small number of wave classes is left.

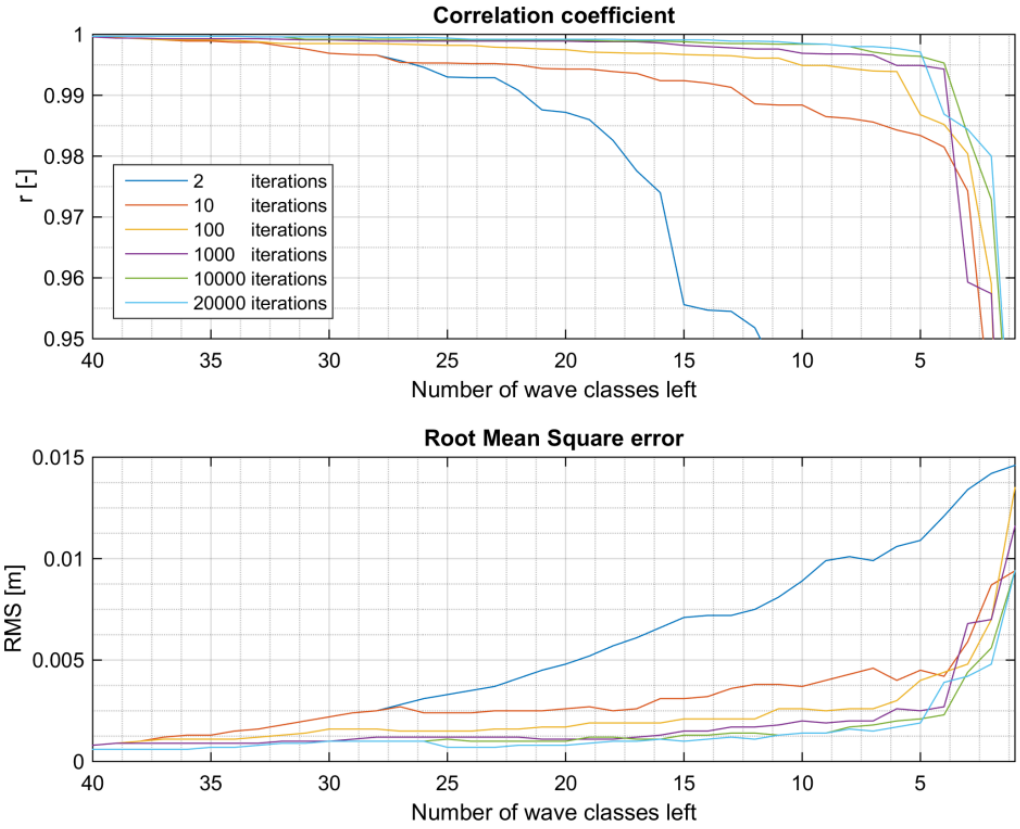

Figure 18 - Development of correlation coefficient and the RMS when excluding wave classes. For clarity of the plots, the exclusion of the first 12 wave classes is left out (the x-axis should start at 62)

The correlation coefficient of the bottom changes between the inclusion of 10 and 62 wave classes is 0.9985 using 20000 iterations and leads to an RMS of 1.4 mm between the inclusion of 10 wave classes and the full wave climate (Figure 18). The derived wave scenarios are listed in Table 13, Appendix B.4 and visualised in Figure 19. For the wave period, the average value of all measured values in that particular wave height and direction class has been taken.

As can be seen in Figure 19, waves from the Northwest and southwest are the most important for the morphological development of the study area. These waves are assigned the highest weights. In addition, the incoming wave directed exactly 45° to the coast, propagating in the same direction as the tide (to the North) is assigned as the wave for which the morphological development is the most important (largest weight). This is the resulted wave class determined by the OPTI-method when only 1 wave will be included in the simulations.

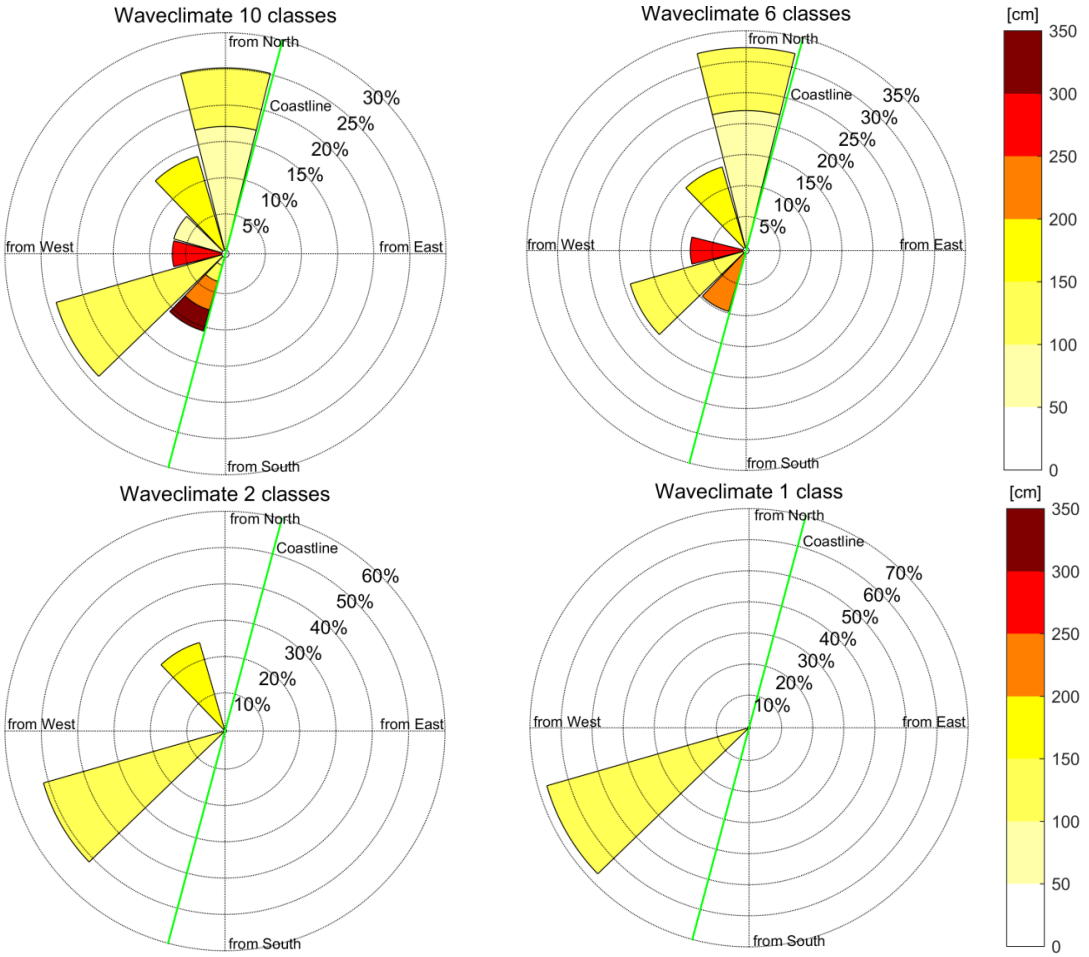

Figure 19 - Derived wave climates, determined by OPTI method. Weights are calculated by the OPTI method and are slightly different from the original weights (percentage of occurrence).

5.3 VALIDATION OF INPUT REDUCTION

5.3.1 FRAMEWORK

To check the model performance of the reduced input conditions, these reduced input conditions are validated based on the comparison with the situation in which no input reduction is applied. The validation is done in two ways; hydrodynamic only and morphodynamic. The hydrodynamic only validation uses a fixed bottom after which the water levels and the flow velocities will be compared to the situation with the non-reduced input conditions. The morphodynamic validation will compare the bathymetric changes using the reduced and non-reduced input conditions. To give an indication of the model skill, the Nash-Sutcliffe coefficient is used for the hydrodynamic validation (Nash & Sutcliffe, 1970). The Nash-Sutcliffe coefficient (NS) is commonly applied for expressing the accuracy of hydrodynamic conditions as for example in Horstman et al. (2015). The NS coefficient is defined as:

$$NS = 1 - \frac{\sum(X - Y)^2}{\sum(X - \bar{X})^2} \quad 5$$

In which Y is the simulated result (prediction) and X is the reference situation (simulation with field data). The overbar means that the average has to be taken. In this validation, 41 observation points (in time) distributed over the study area of the water levels and flow velocities will be compared. A temporal

average of the observation points is used in this research. An NS coefficient of one indicates a perfect match between the reference situation and the simulated result. A value smaller than zero means that the model has no predictive capabilities.

For the morphodynamic simulation, the correlation coefficient (r) and the Brier Skill Score (BSS) will be used (spatially). The morphodynamic simulation will be performed with bed level updates enabled. The BSS is a commonly applied method to evaluate coastal morphodynamic models which make use of continuous data (Sutherland, et al., 2004). The Brier Skill Score for morphological models is defined as:

$$BSS = 1 - \frac{\overline{(Y-X)^2}}{\overline{(B-X)^2}} \quad 6$$

In this formula Y is a prediction, X is an observation (the definition of X and Y is the same for the BSS and the NS) and B is a baseline situation. The overbar means that the average has to be taken (spatially). The BSS provides a quantification of the skill of a model in which skill means accuracy in relation to a baseline prediction. A BSS of 1 indicates a perfect match between the prediction and observation. There is no lower limit in this method. A value of zero means that the model prediction is the same as the baseline situation. To determine the origin of a particular error (phase, amplitude or mean error), the Brier Skill Score can be decomposed in terms of deviations in predictions and measurements as proposed by Murphy & Epstein (1989). The decomposed variant (which results in the same BSS) is expressed as:

$$BSS = \frac{\alpha - \beta - \gamma + \epsilon}{1 + \epsilon} \quad 7$$

With the terms:

$\alpha = r^2_{Y'X'}$ 8 is a measure of phase error in space (when the sediment is moved to the wrong position). A value of one indicates perfect modelling of phase.

$\beta = \left(r_{Y'X'} - \frac{\sigma_{Y'}}{\sigma_{X'}}\right)^2$ 9 is a measure of the amplitude error (when the wrong volume of sediment is moved). A value of zero indicates perfect modelling of amount of sediment moved.

$\gamma = \left(\frac{<Y'> - <X'>}{\sigma_{X'}}\right)^2$ 10 is a measure of the mean map error (when predicted average bed level deviates from the measured bed level). A value of zero indicates perfect modelling of the mean.

$\epsilon = \left(\frac{<X'>}{\sigma_{X'}}\right)^2$ 11 is a normalization term which is only affected by measured changes from the baseline prediction.

And:

$Y' = Y - B$ 12 Modelled anomalies

$X' = X - B$ 13 Measured anomalies

$r_{Y'X'} = \frac{<Y'X'>}{\sigma_{Y'}\sigma_{X'}}$ 14 Anomaly correlation coefficient (Sutherland, et al., 2004)

To give an indication of the qualification of the model, Van Rijn et al. (2003) proposed the following classification for the morphology using the Brier Skill Score (Table 4):

Table 4 - Qualification of model skill according to the Brier Skill Score (Van Rijn et al., 2003)

Qualification	BSS
Excellent	1.0 – 0.8
Good	0.8 – 0.6
Reasonable/fair	0.6 – 0.3
Poor	0.3 – 0
Bad	< 0

5.3.2 RESULTS

The model is validated using the reduced input conditions (harmonic morphological tide) compared to the model run with the field data (water levels of the Kustfijn model) for a simulation of 24 h 50 min (plus a spin-up period of 24 h 50 min). The water levels of the harmonic morphological tide compared to the tide which has been chosen as the representative tide for the full spring-neap tidal cycle (morphological tide), can be seen in Figure 20. The NS coefficient for the water levels of the harmonic morphological tide compared the morphological tide, averaged of 41 observation points distributed over the model domain, is 0.98. The standard deviation of this averaged NS value is 0.0004. For the flow velocities, the NS coefficient averaged over all observation points is 0.95 with a standard deviation of 0.043. An example of the spatially varying water levels at a particular moment in time can be seen in Figure 21. The corresponding water levels of both simulations used for Figure 21 can be found in Appendix B.5.

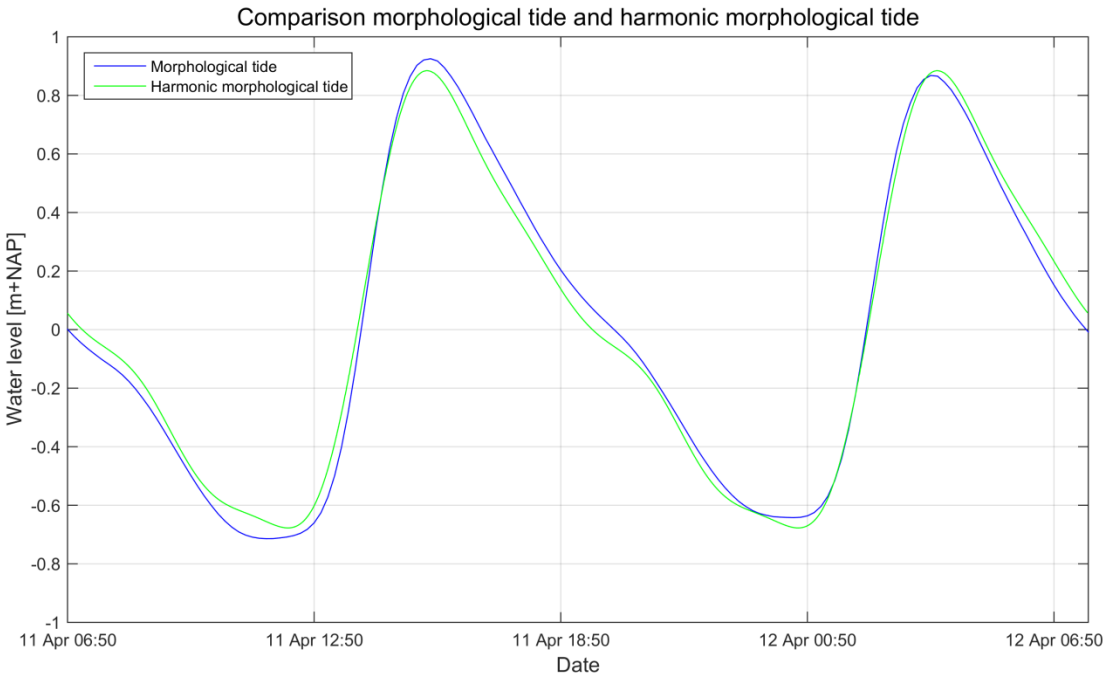

Figure 20 – Comparison of morphological tide and harmonic morphological tide for the observation point in the nautical channel near the western boundary.

The morphodynamic validation is performed using the bathymetric changes of the full spring-neap tidal cycle simulated and the harmonic morphological tide (multiplied with the slope of the linear regression line to compare an equal simulated time span). The slope of the linear regression line of the harmonic morphological tide compared to the full spring-neap tidal cycle is 20.9312 (which is, as expected, very similar to the slope of the linear regression line of the morphological tide, see section 5.1). The linear correlation coefficient of the bottom changes (spatially calculated over all grid cells) of the harmonic morphological tide is 0.9783. The Brier Skill Score of the resulting bathymetry of the harmonic

morphological tide simulation compared to the resulting bathymetry of the spring-neap tidal cycle and initial bathymetry is 0.958. This BSS is composed of the following components:

$\alpha = 0.957$	(Phase error)
$\beta = 0$	(Amplitude error)
$\gamma = 0$	(Mean map error)
$\epsilon = 0.00005$	(Normalization term)

This means that the harmonic morphological tide simulated compared to the full spring-neap tidal cycle simulation only results in a small phase error (the sediment is moved into the wrong position). The differences in bathymetries are visualised in Figure 22. In Appendix B.5 the bathymetric changes of both simulations are shown.

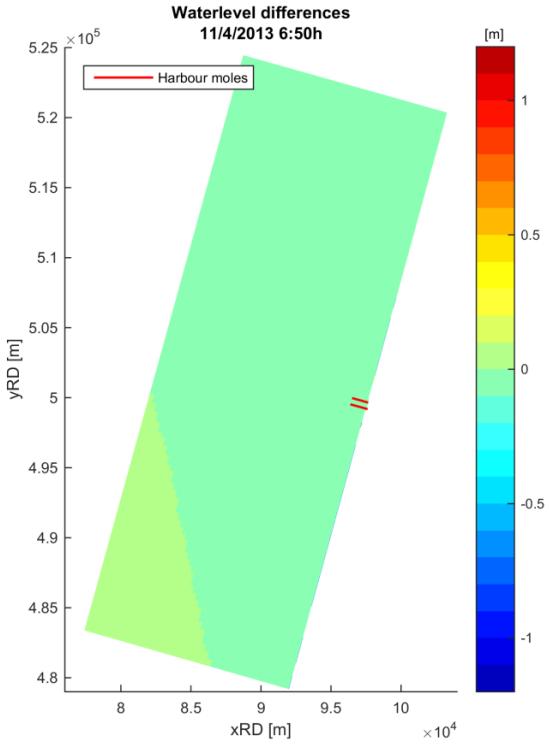

Figure 21 - Water level difference between simulation with derived field data boundary conditions and harmonic morphological tide boundary conditions

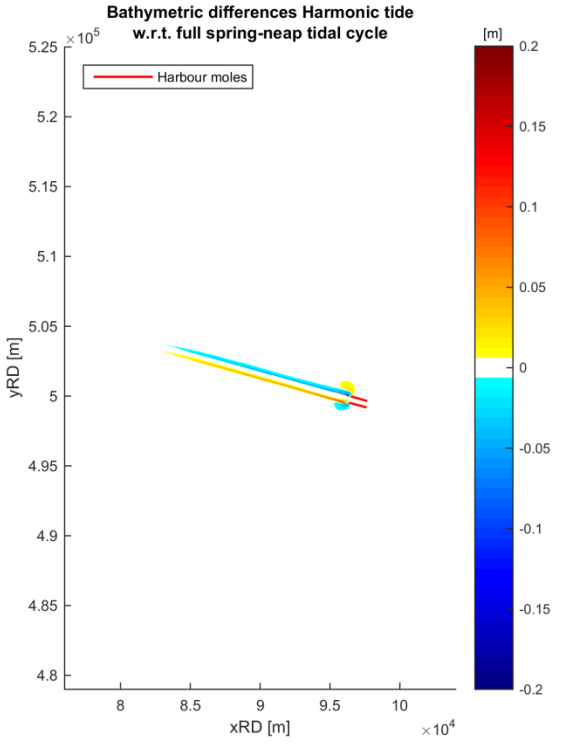

Figure 22 - Differences in bathymetries (the bathymetry change of the harmonic morphological tide is multiplied with the slope of the linear regression line)

5.4 SUMMARY INPUT REDUCTION

In reducing computational times and accelerating morphodynamic simulations, real-time data have been converted to distinct classes (waves) and/or a representative signal (harmonic morphological tide). This simplification of measured real-time data has, as discussed above, several consequences in terms of loss of accuracy of the observed features present in reality. After validation of the input reduction for the tide, it became clear that the loss of accuracy when using a harmonic morphological tide is very limited. The advantage of reducing the time needed to simulate the morphodynamics therefore overrules the disadvantage of a loss of accuracy and features that are present in the morphodynamic modelling using reduced input conditions. In addition, the harmonic morphological tide is easy to apply in long-term modelling and avoids shocks of the model from one tide to another.

6 Results long-term morphological modelling

In this section, the results of the long-term simulations are presented. First a short introduction is provided about the cross sections defined for the comparison. In section 6.1 the accelerated brute-force simulation of ten years will be validated by a comparison with the non-accelerated brute-force at t = 1 year and after ten years qualitatively based on field data. Section 6.2 shows the results of the accelerated simulations. Section 6.3 provides the results in terms of accuracy of the performance indicators resulting from the defined cross sections. For all cross sections, four performance indicators are calculated to quantify the accuracy and these are averaged over all seven cross sections (see section 1.3 methodology). In the end this section provides an answer to research questions four and five about how many wave classes should be included and which acceleration factor is still acceptable to achieve accurate results with respect to the reference simulation. Sedimentation and erosion maps of all results are shown in Appendix C.

The cross sections that are of interest for the bottom development in this study are shown in Figure 23. Cross sections 1 and 2 are alongshore cross sections that will reveal information about the migration of the nautical channel directly in front of the harbour moles and further offshore. Cross sections 3 and 4 are located in line with the harbour moles on the bottom of the nautical channel in the initial bathymetry and cross section five is in the middle of the nautical channel. These cross sections will provide quantitative information about the development of the nautical channel both in the alongshore and cross-shore direction. Two cross sections, North and South of the harbour moles, (no. 5 & 7) are included to see cross-shore variations in the morphological development of the beaches towards deep water

6.1 VALIDATION BRUTE-FORCE SIMULATION

To compare the accelerated long-term simulations, a brute-force simulation has been performed as a reference. As mentioned previously, this brute-force simulation makes use of the harmonic morphological tide. The bottom development of the harmonic morphological tide compared to the daily averaged bottom development of the spring-neap tidal cycle simulated is higher. The harmonic morphological tide produces a morphological development of 1.36 days per day simulated (28.45 / 20.9312). Therefore, only 20.9312/28.45 * 365 = 268.5 days have to be simulated to account for 1 year and is computationally more efficient. The real-time wave signal measurements for the full wave climate of 2013 now must be adapted as well (from 60 min measurement intervals to 60 * 20.9312/28.45 = 44.142 min measurement intervals).

The model only runs this simulation for one year because of computational times. To account for ten years of morphological development, this brute-force simulation is performed once more with an acceleration factor of ten. To check the validity of the acceleration with a factor ten, both simulations (accelerated and non-accelerated) are compared at t = 1 year. The morphological development of both brute-force

simulations can be seen in Figure 24. After one year of simulation, hardly any differences can be observed between the accelerated simulation and the non-accelerated simulation.

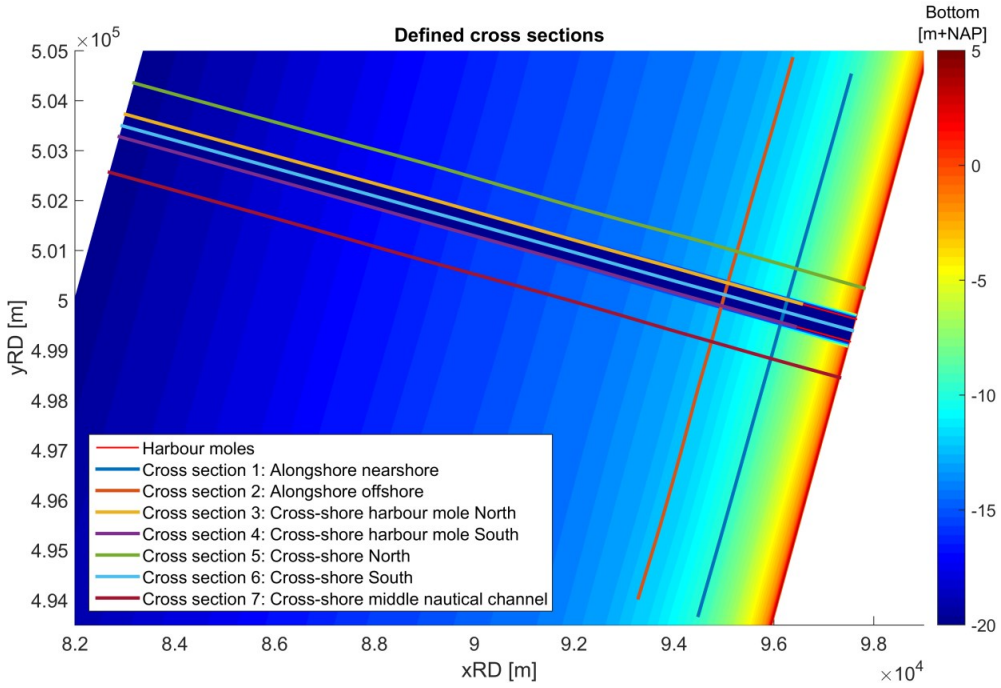

Figure 23 - Defined cross sections for comparison of long-term accelerated simulations

In terms of performance indicators, the accelerated simulation with respect to the non-accelerated simulation is shown in Table 5. The first row in Table 5 is the non-accelerated brute-force simulation with respect to itself and shows the optimal performance coefficients. The accelerated brute-force simulation performs very well in terms of the performance indicators. Therefore, the brute-force simulation accelerated with a factor 10 provides a good prediction of the morphological development for ten years.

Table 5 – Accuracy performance accelerated brute-force simulation after one year morphological development with respect to the non-accelerated brute-force simulation.

	Average NS	Average RMS	Average R	Average B	Indicator B
BF 1 y	1.0000	0.0000	1.0000	1.0000	1.0000
BF 1 y accelerated	0.9518	0.1532	0.9938	0.9449	1.0551

The resulting bathymetry and the sedimentation and erosion pattern are shown in Figure 25 and Figure 26. In Figure 26, it is visible that in the long-term simulation, some boundary effects are present near the coast at the northern and southern boundaries. These effects are outside the area of interest and are neglected in the comparison of the results.

The ten yearly morphological development of the brute-force simulation shows similarities with the morphological development observed after 1968 when the harbour moles of IJmuiden were extended from the beach only, into the sea. The observed sedimentation and erosion 8 years after the extension of the harbour moles is shown in Figure 27 (a map of exactly 10 years after the extension of the harbour moles was not available). The model simulation shows the formation of nearshore bars (Figure 26) as is qualitatively in agreement with the observed data (Figure 27). Very similar is the development of the 8 m deep scour hole directly in front of the southern harbour mole (Figure 26 right). This scour hole however covers a smaller area in the model, probably caused by the different layout of the southern harbour mole. In the model, the flow convergence is more abrupt compared to reality where the flow converges smoother around this harbour mole. The smoother flow convergence in reality can cause a larger length of

the scour hole (and area as well). The development of the scour hole is in agreement with the expected value. As a rule of thumb, the expected depth of a scour hole in front of a harbour mole with respect to the surrounding sea bottom is approximately equal to the water depth at that location (Van Rijn, 2005).

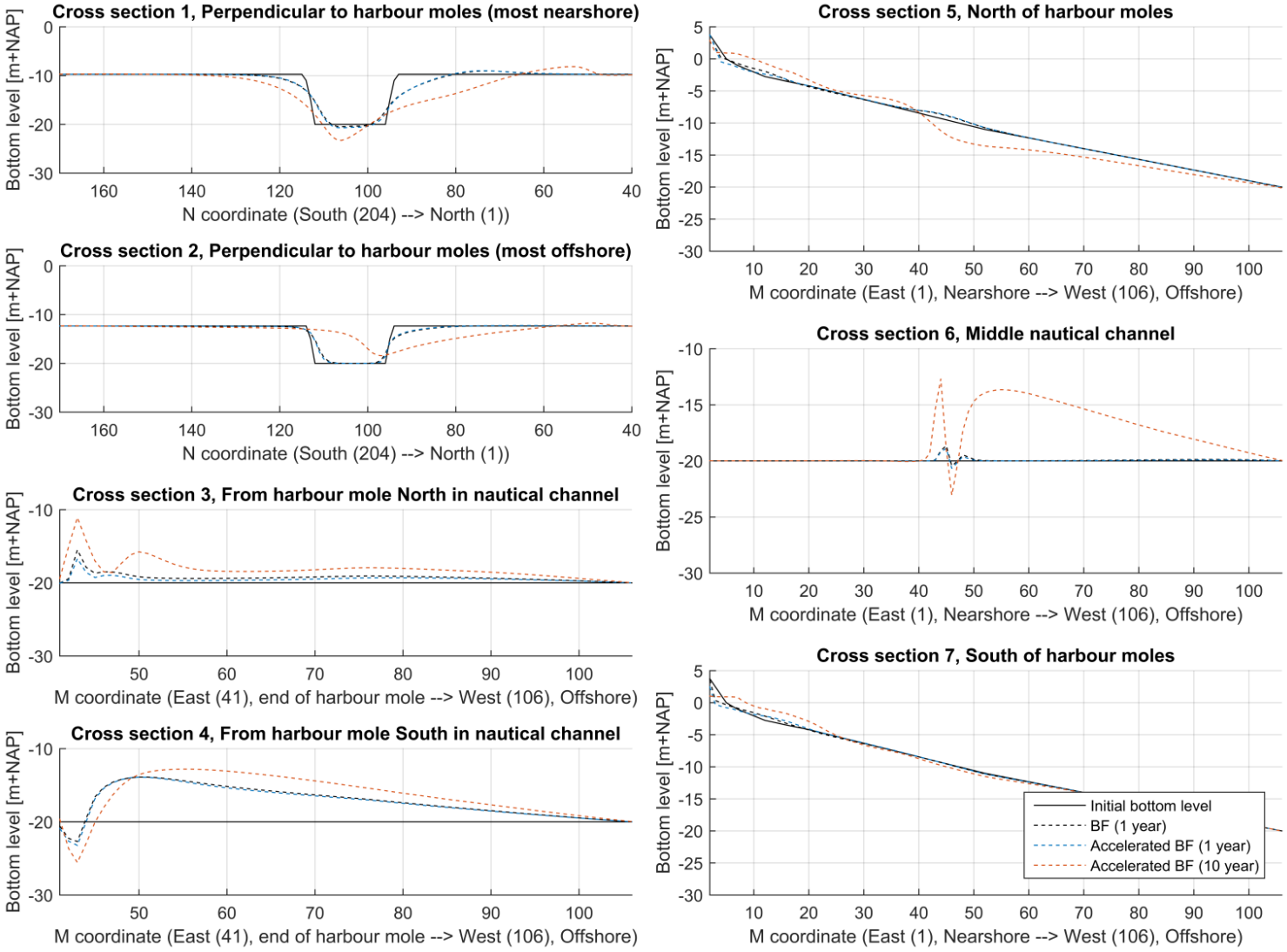

Figure 24 - Results per cross-sections for the brute-force simulations. Results are plotted for the one year morphological development (accelerated as well as not accelerated) and the ten year morphological development.

The aggregation of the beaches north and south of the harbour moles is around 500 m in ten years as shown in Figure 25. These beaches accrete (sedimentation takes place) because they are located in a sheltered area for flow due the flow convergence around the harbour moles. These areas act as a kind of sediment trap. This pattern, qualitatively, is also observed in reality as can be seen in Figure 27. In addition, an eddy develops around the southern harbour mole which causes sedimentation just in front of both harbour moles. This eddy and sedimentation pattern are also observed in studies to the bottom development of the coastal area of IJmuiden (Boutmy, 1998; Hendrickx, 1988; Verhagen & Van Rossum, 1990), however more located between the harbour moles. Because of a back basin being present in reality, the water can flow into and out of this basin resulting in larger flow velocities between the harbour moles than in the model. This presumably causes the difference in location of the sediment hump being in front of the harbour moles in the model and between the harbour moles in reality.

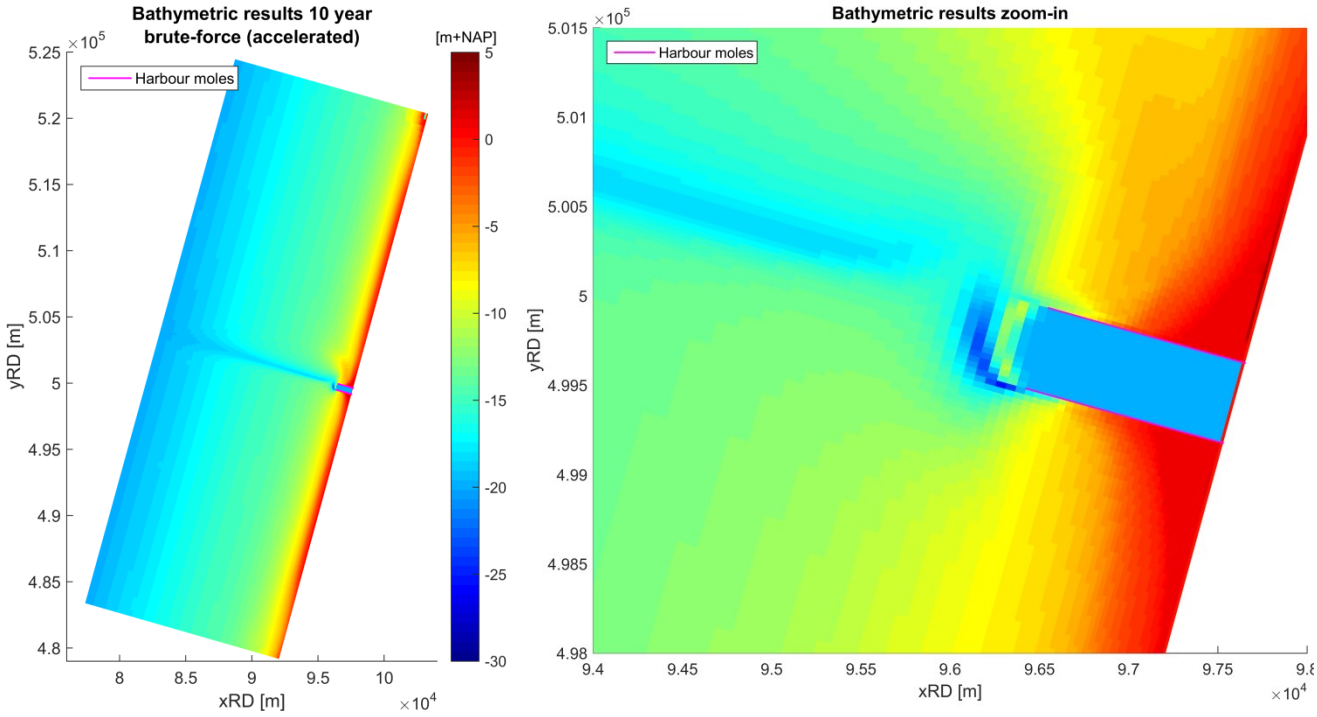

Figure 25 - Bathymetric map accelerated brute-force simulation (left) of ten year and zoom-in of interest area (right)

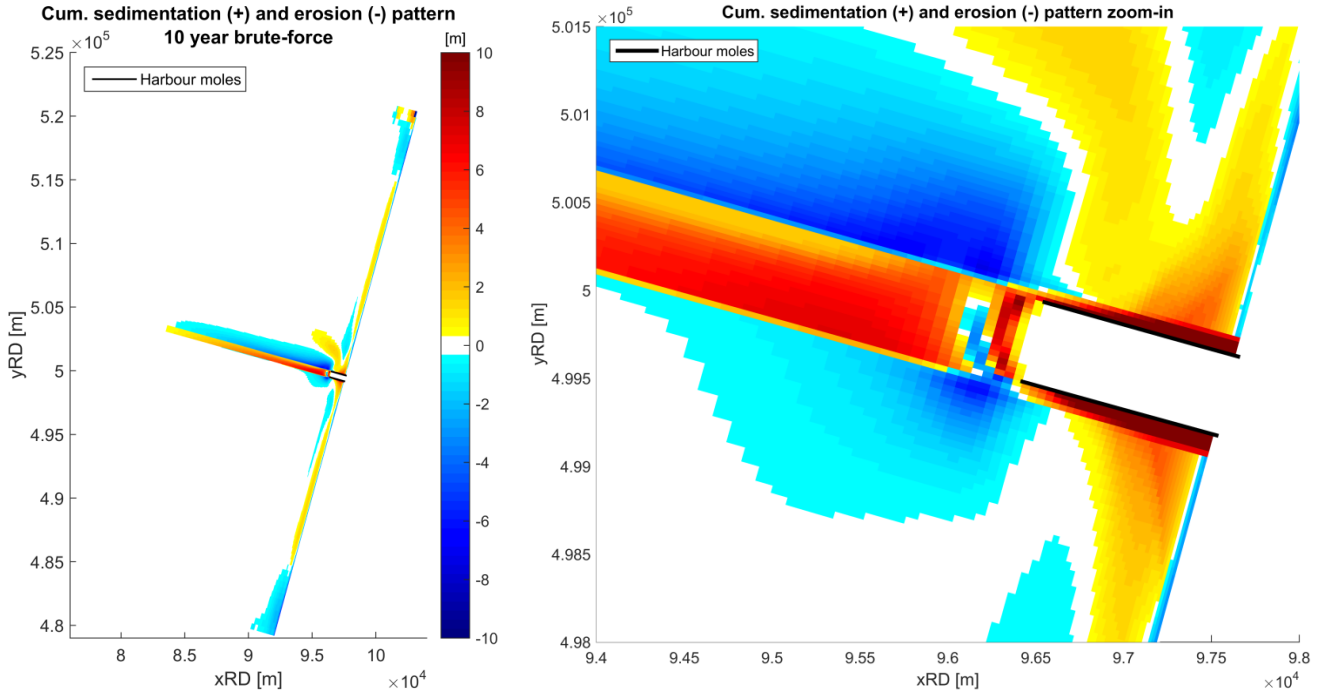

Figure 26 - Cumulative sedimentation (+) and erosion (-) pattern ten yearly morphodynamic development accelerated brute-force simulation (left) and zoom-in of interest area (right)

Less pronounced in the studies of the field data is the migration of the nautical channel to the North (in the direction of the net sediment transport). This migration is clearly visible in the model (cross sections 2 & 6, Figure 24 and Figure 25). The migration of the nautical channel is around 20 m per year (200 m in ten years). In reality however, this migration rate is only about 2 – 4 m per year (Ribberink, 1989). The propagating behaviour of the nautical channel to the North in the model is much stronger nearshore than further offshore (Figure 26) because of the larger flow velocity differences. The water depth in the nautical

channel relative to the surrounding water depth is much larger nearshore than offshore, causing larger flow velocity differences nearshore. Because of the sediment transport during flood to the North and at ebb to the South, the net sediment transport rate is directed northerly. Therefore, sedimentation takes place at the southern side of the nautical channel and erosion takes place at the northern side, as for example explained in Hoogewoning & Boers (2003).

Possible explanations for this propagating behaviour of the nautical channel not present in reality is a calibration of the sediment transport rate in the model, different sediment characteristics at these offshore locations, or that the nautical channel is kept in place by dredging in reality. Dredging is not included in the model. The amount of sediment dredged in the nautical channel is ± 1.3 Mm^3 per year (Boutmy, 1998; Van Heijst et al, 2005). After ten years in the brute-force simulation, approximately 17.4 Mm^3 of sand has to be dredged to keep the nautical channel in place and at the desired depth. The quantity of sediment that should be removed is in the same order of magnitude as in the natural system.

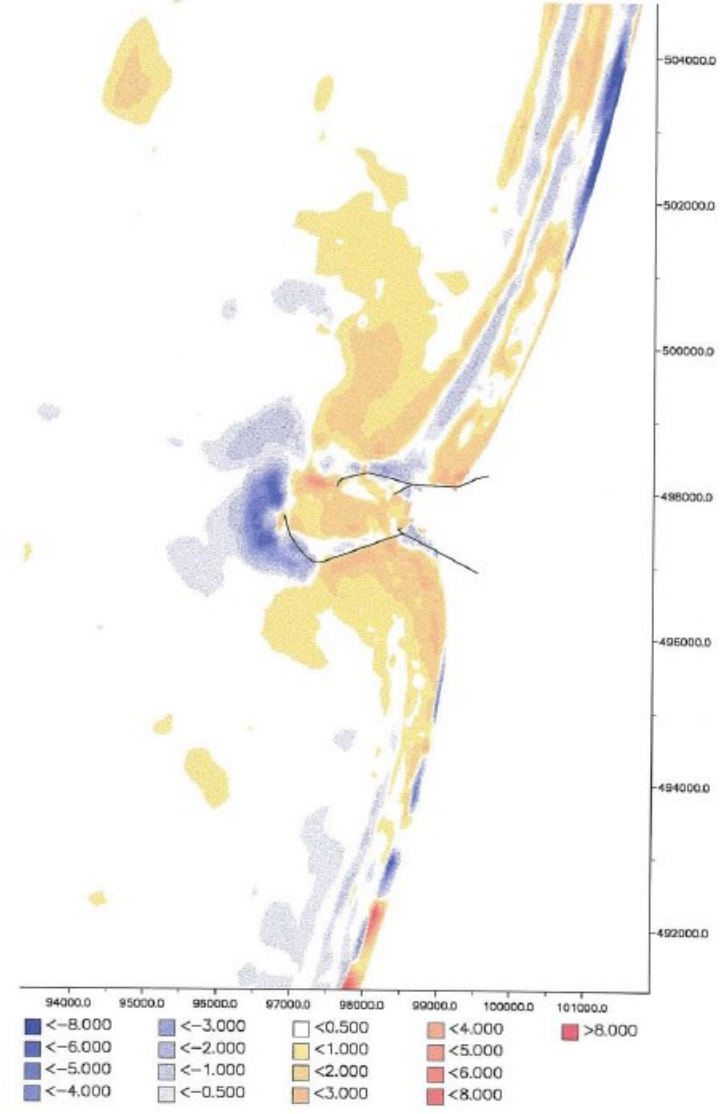

Figure 27 - Difference plot observed bathymetry IJmuiden in 1976 relative to 1968 in m (Boutmy, 1998)

6.2 RESULTS OF THE ACCELERATED SIMULATIONS

In this section, the results (differences and similarities) of the accelerated simulations with respect to the ten year accelerated brute-force simulation are presented. This is done by means of some example results. The cross section plots for all acceleration factors are shown in Appendix C.1, for the inclusion of different wave classes in Appendix C.2 and cumulative sedimentation and erosion maps for all simulations are shown in Appendix C.3.

The acceleration factors for the tide only case as a result of the input reduction (and also for Mormerge) are shown in Table 6. To accelerate the long-term simulations using Morfac, the calculated acceleration factors above have to be multiplied by the weight of the wave class (Table 13, Appendix B.4). In figures and maps, the number of harmonic morphological tides per year simulated, which is related to the acceleration factor applied, is abbreviated as TPY.

Table 6 - Acceleration factors for a ten year simulation using different numbers of tides per year simulated (TPY)

Harmonic tide(s) simulated * acceleration factor is an one yearly morphodynamic development	Calculation	Acceleration factor
1 tide per year (TPY)	$20.9312 * \frac{365}{28.45} * 1$	268.537
2 tides per year (TPY)	$20.9312 * \frac{365}{28.45} * \frac{1}{2}$	134.269
4 tides per year (TPY)	$20.9312 * \frac{365}{28.45} * \frac{1}{4}$	67.1343
6 tides per year (TPY)	$20.9312 * \frac{365}{28.45} * \frac{1}{6}$	44.756
12 tides per year (TPY)	$20.9312 * \frac{365}{28.45} * \frac{1}{12}$	22.378

When comparing the long-term simulations, a remarkable result is the absence of dependency of the morphological acceleration factor on the accuracy of the results. For both acceleration techniques, different morphological acceleration factors do not result in significantly deviating results in terms of accuracy with respect to the brute-force simulation, as for example can be seen in Figure 28 and Figure 29. The results when different numbers of tides per year have been simulated (inherent to the acceleration factor) are all in line with each other. Only small deviations are visible. These deviations are presumably more a result of the model schematization (model artefacts as grid sizes and numerical uncertainty) than the acceleration factors.

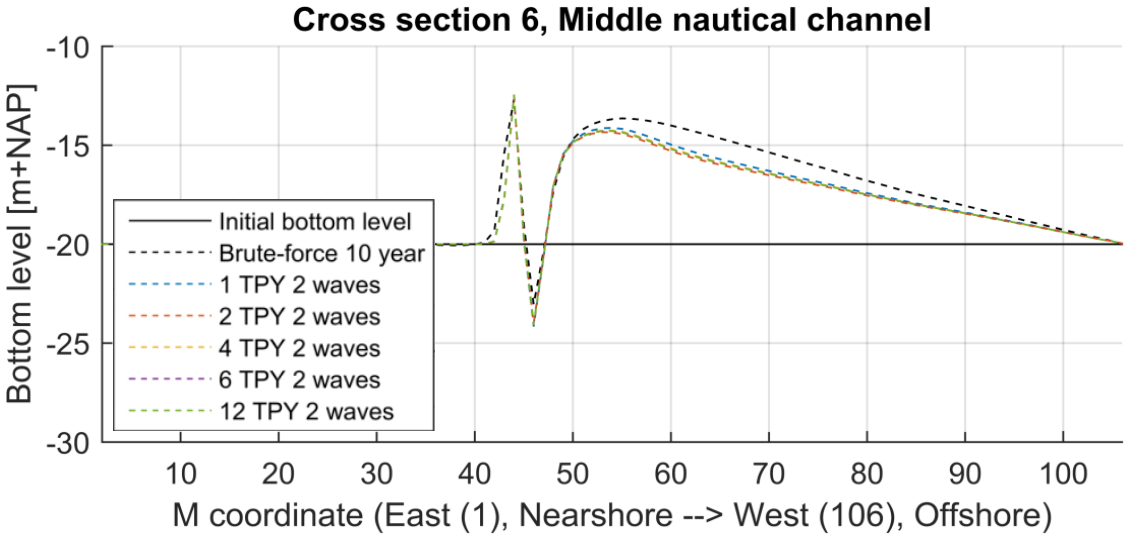

Figure 28 - Results Cross section 6 Morfac simulation including two wave classes

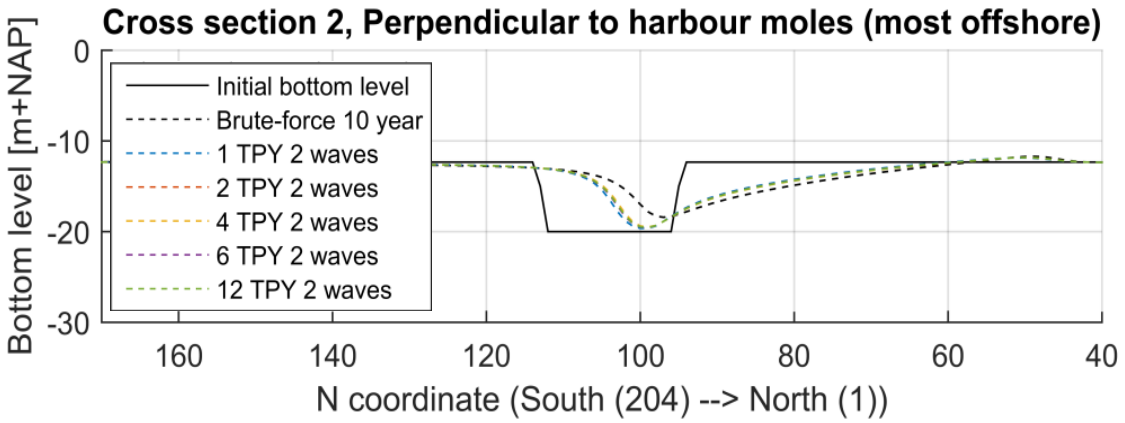

Figure 29 - Results Cross section 2 Mormerge simulation including two wave classes.

Because of the lack of dependency of the acceleration factors applied on the accuracy of the results, the model has been accelerated even more. In Figure 30 and Figure 31, two cross sections are shown including a simulation accelerated with a factor 1074.2 (simulates one tide per four years, orange line) and a simulation accelerated with a factor 2685 (simulates one tide per ten years, yellow line). For these simulations, the water depth from which a sediment calculation in Delft3D will be applied had to be increased to 1.5 m to avoid model instabilities at the coast (too large changes occurred for Delft3D). To see the effect of the wave conditions included, a result of the tide-only simulations has been included as well.

In Figure 30 and Figure 31 it is shown that when the water depth is approximately over 6 m, acceleration factors even up to 2685 can be used to simulate the bottom development accurately with respect to the reference simulation. The acceleration factor of 2685 is the largest possible using the input reduction technique as is applied in this study; at least one harmonic morphological tide has to be simulated for the results to be valid. The morphological effects caused by the ten wave conditions applied are made clear due to the inclusion of a tide-only simulation. The ten wave classes included are, even with these high acceleration factors, simulating the morphology accurately. Inclusion of waves in the model results in significantly deviating results compared to the tide-only simulation. From these figures it revealed that only one harmonic morphological is able to simulate a ten yearly morphological development at water depths over 6 m.

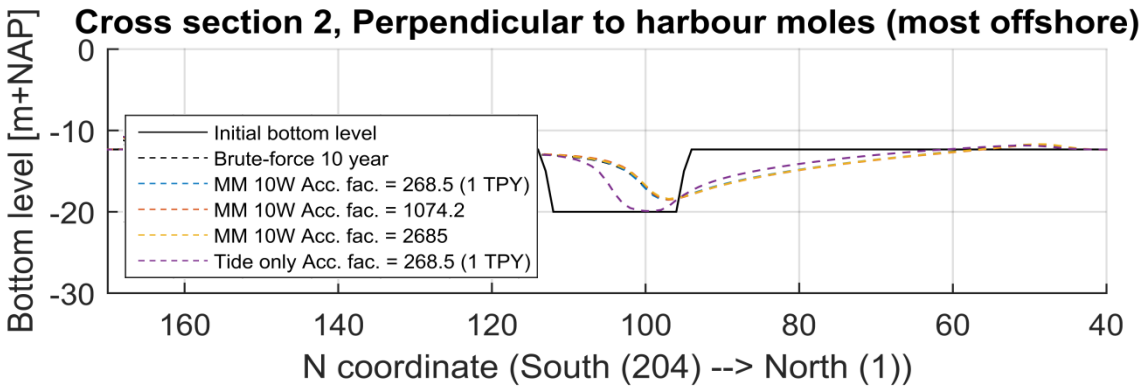

Figure 30 - Results Cross section 2 Mormerge with ten waves, different acceleration factors and a tide only simulation

In addition, both acceleration techniques showed that when including additional wave classes, the results become more accurate with respect to the brute-force simulation where a full wave climate has been simulated, as can be seen Figure 32 and Figure 33. This pattern is also clearly visible when comparing area maps to the brute-force simulation. In Figure 34 an example is shown for which no wave condition has

been included in the simulation. Next to Figure 34, in Figure 35, an example is shown were ten wave classes are included. The differences between these figures clearly illustrate the effects of the waves on the morphology. This effect is much stronger nearshore (in shallow water) than offshore.

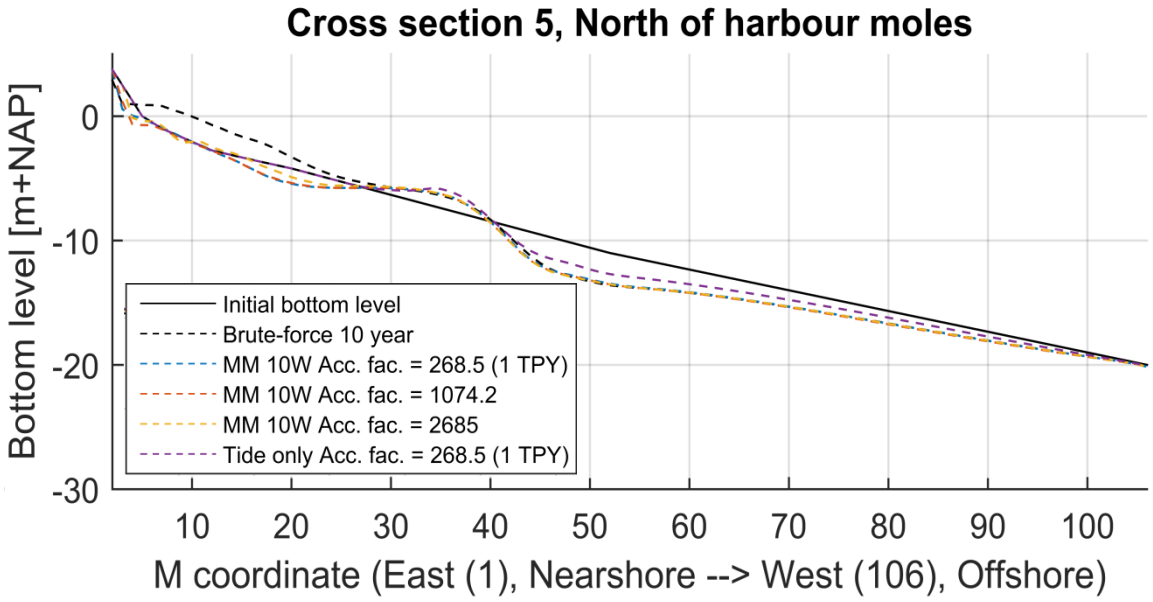

Figure 31 - Results Cross section 5 Mormerge with ten waves, different acceleration factors and a tide only simulation

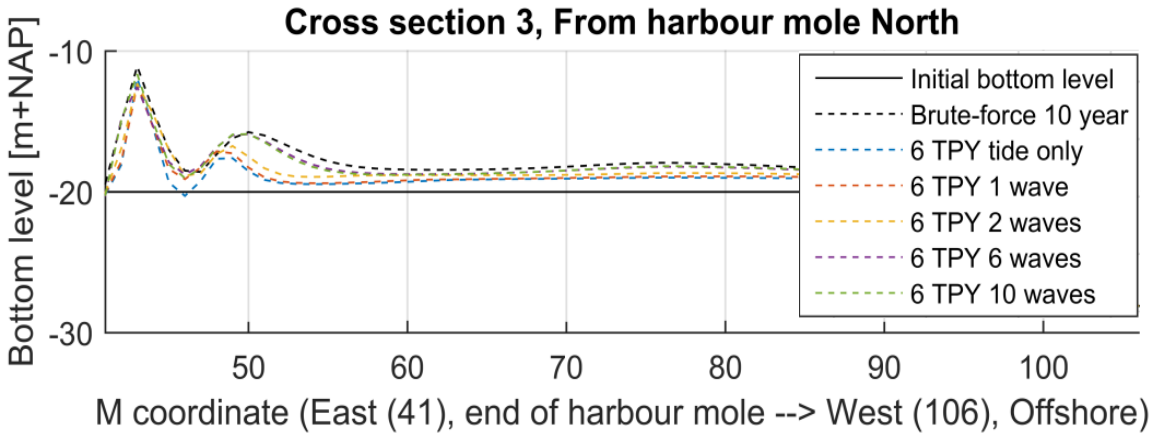

Figure 32 - Results Cross section 3 Morfac simulation, 6 TPY all waves

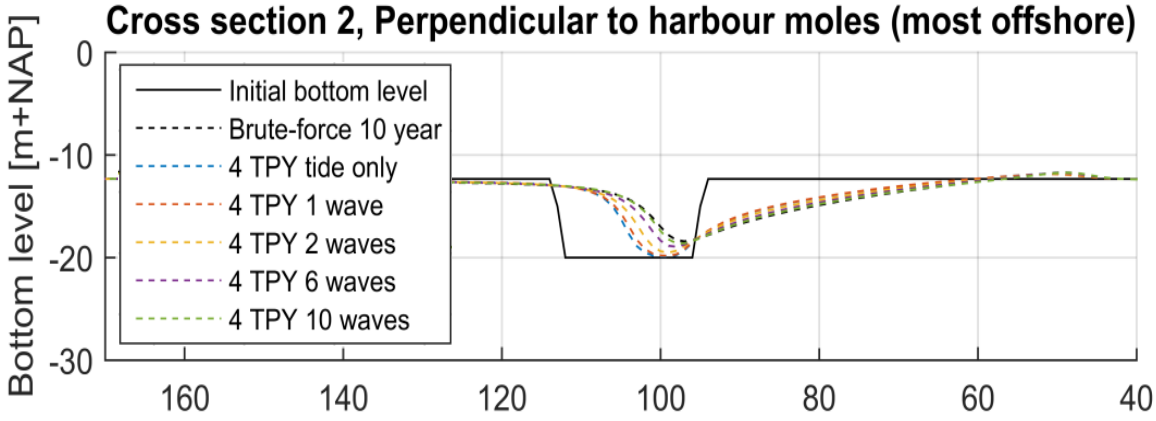

Figure 33 - Results Cross section 3 Mormerge simulation, 4 TPY all waves

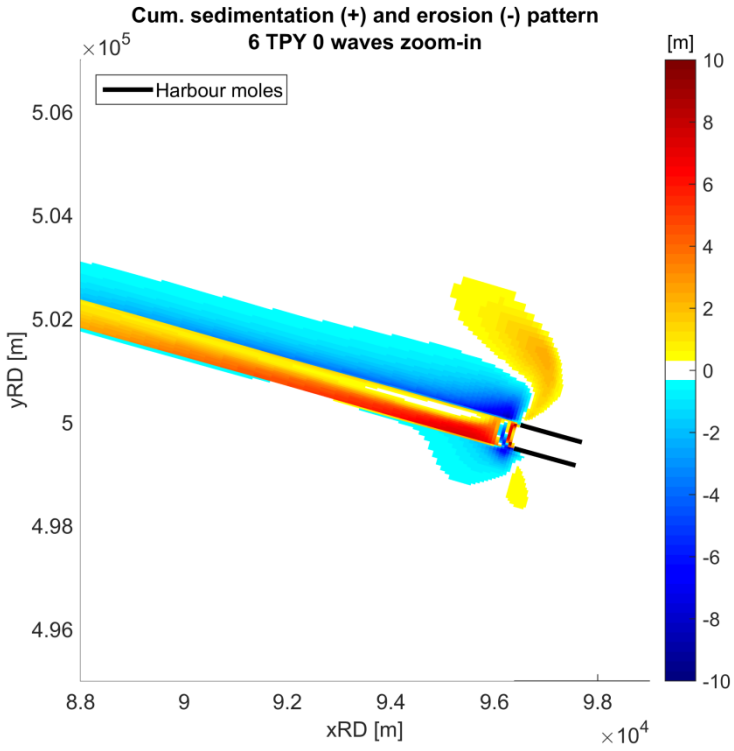

Figure 34 - Zoom-in of cumulative sedimentation and erosion pattern tide only, 6 TPY simulation

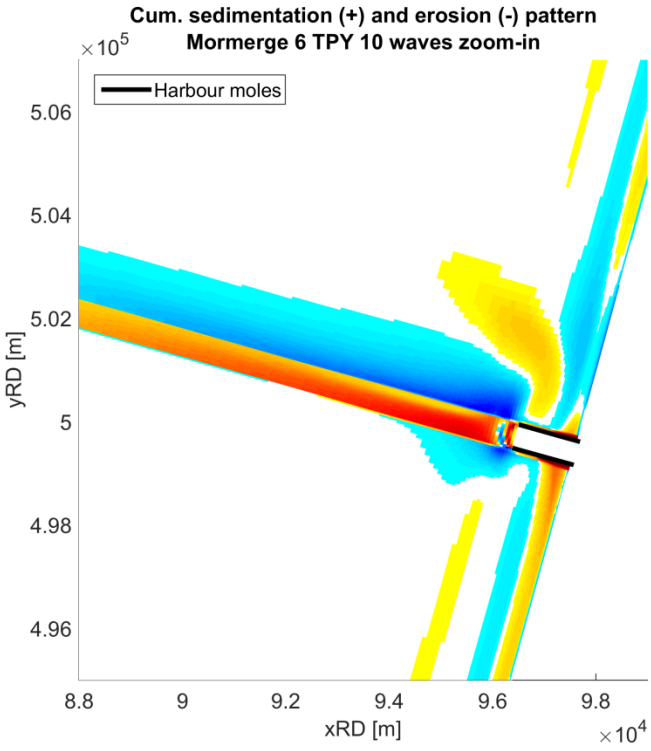

Figure 35 - Zoom-in of cumulative sedimentation and erosion pattern Mormerge 10 waves, 6 TPY simulation

As a result of including additional wave classes, also higher waves are included (see Table 13 for the wave classes included in each scenario). These waves cause an increased rate of sediment stirring which leads to more bottom development. The critical depths for which wave driven sediment transport becomes negligibly small can be calculated using the wave driven orbital velocity near the bed $\overline{U}$ and the critical shields parameter θ_{crit}. The critical shields parameter, which determines if sediment transport will take place, can in turn be calculated by for example using the dimensionless grain diameter of Van Rijn (1993). The dimensionless grain diameter is defined as:

$$D_* = (\frac{\Delta g}{\nu^2})^{1/3} * D = 5.01 \quad 15$$

In which:

D_* dimensionless grain diameter (-)

g gravitational acceleration (9.81 m/s^2)

ν viscosity of water (1*10^{-6} m^2/s)

D sediment diameter (2*10^{-4} m)

Δ $(\rho_s - \rho)/\rho$. ρ_s is the specific density of the sediment (2650 kg/m^3) and ρ is the density of water (1020 kg/m^3)

Given the dimensionless grain diameter for this study is in the range of 4 – 10, the critical shields parameter can be calculated using (De Vriend, 2005):

$$\theta_{crit} = \frac{0.14}{D_*^{0.64}} = 0.05 \quad 16$$

The shield stresses caused by the waves depends on the bed shear stress τ_b. The relation of the shields stress and the bed shear stress can be defined as follows:

$$\theta = \frac{\tau_b}{(\rho_s - \rho) * g * D} \quad 17$$

To initiate sediment transport, $\theta > \theta_{crit}$ (neglecting sediment transport by bottom slope gradients effects) and thus $\tau_b > 0.16$ N/m². The linear dispersion relationship (Equation 18) determines the peak wave orbital velocities near the bottom (water depth h) given particular wave parameters (wave height H_s (m), wave period T_P (s) and wave number k).

$$\overline{U} = \frac{\pi * H_s}{T_p * \sinh(kh)} \quad 18$$

Using this relationship, the bed shear stress can be calculated as follows:

$$\tau_b = \rho g \frac{\overline{U}^2}{C^2} \quad 19$$

In which C is the Chézy coefficient (65 $m^{1/2}/s$). Now, the critical water depths for the derived wave classes where the shields stress exceeds critical shields parameter can be found in Table 7:

Table 7 – Critical water depths (plus related wave height and period) for wave driven sediment transport. The critical bottom levels for wave driven sediment transport also are dependent on the tidal variation (± 1.1 m in this study).

Wave climate	Wave height H_s (m)	Wave period T_P (s)	Depth (m)
1 wave	1.25	4.26	8.65 m
2 waves	1.75	5.11	13.45 m
6 waves	2.75	5.65	19.35 m
10 waves	3.25	5.66	20.85 m

Figure 32 and Figure 33 are showing as well that the large migration rate of the nautical channel in the brute-force simulation can only be reached when six or ten wave classes are included in the model. These wave scenarios are able to stir up the sediment also at large water depths as in the nautical channel. Inclusion of at least six wave classes for an accurate result is in accordance with the study of Van Rijn (2012) who concluded that at least five wave classes should be incorporated for an accurate morphologic development of the Western Scheldt. The quantified performace in terms of accuracy when including six or ten wave classes and between the slight differences using Morfac or Mormerge, will be discussed in section 6.3.

Near the harbour moles, in the zone where hardly any flow takes place, qualitatively all simulations showed sedimentation, albeit to a different extent for each simulation. An item in which no clear preferred wave climate or acceleration method can be determined is the development of the beaches in the nearshore zone (breaker, surf and swash zone) further away from the harbour moles (cross sections 5 and 7). The nearshore behaviour of the various long-term simulations is highly variable (water depths smaller than 6 m approximately). No clear pattern can be extracted. In general, clear nearshore bank formation is observable in all simulations (Cross section 5, Appendices C.1 & C.2). The magnitude of this bank formation is similar for all simulations.

6.3 COMPARISON OF PERFORMANCE PARAMETERS LONG-TERM SIMULATIONS

To give an overview of the performance of all long-term simulations compared to the accelerated brute-force simulation, a table is provided (Table 8) in which the performance indicators are averaged over all seven cross sections. The performance indicators include the Nash-Sutcliffe coefficient (NS), linear correlation coefficient (R), the Root Mean Square error (RMS) and an indicator for the slope of the linear regression line (B). A colour scheme has been added for clarity; the greener the better (see section 1.3 methodology).

Table 8 reveals that inclusion of more waves leads to more accurate results for the cross sections. The effect of the different acceleration factors on the performance parameters is very small and is more caused by model artefacts as grid size. In addition, the differences in simulated results for Morfac and Mormerge are

very small. Morfac performs slightly better for the climates with two and six waves included. Mormerge performs slightly better when ten waves are included. These trends are similar for all parameters listed.

Table 8 - Performance parameters compared to the Brute-Force ten yearly morphodynamic development (BF 10 Y). The first row presents the optimal result (reference situation). A colour scale has been added for clarity (from green, best result, to red, the worst result).

Wave Climate	Acceleration factor	Performance Criteria				
		Average NS	Average RMS	Average R	Average B	Indicator B
BF 10 Y		1.0000	0.0000	1.0000	1.0000	1.0000
0 Waves	1 TPY	0.7962	0.9268	0.9523	0.9623	1.0377
	2 TPY	0.8070	0.9053	0.9549	0.9735	1.0265
	4 TPY	0.8029	0.9157	0.9536	0.9676	1.0324
	6 TPY	0.8047	0.9121	0.9540	0.9696	1.0304
	12 TPY	0.8051	0.9117	0.9541	0.9695	1.0305
1 Wave	1 TPY	0.8399	0.8060	0.9602	0.9404	1.0596
	2 TPY	0.8508	0.7774	0.9627	0.9507	1.0493
	4 TPY	0.8465	0.7964	0.9615	0.9454	1.0546
	6 TPY	0.8484	0.7801	0.9620	0.9463	1.0537
	12 TPY	0.8490	0.7814	0.9622	0.9471	1.0529
		Morfac				
2 Waves	1 TPY	0.9019	0.7790	0.9752	0.9744	1.0256
	2 TPY	0.8942	0.8087	0.9729	0.9598	1.0402
	4 TPY	0.8988	0.8004	0.9743	0.9651	1.0349
	6 TPY	0.8979	0.8012	0.9740	0.9638	1.0362
	12 TPY	0.8982	0.8008	0.9740	0.9644	1.0356
6 Waves	1 TPY	0.9788	0.4219	0.9940	0.9520	1.0480
	2 TPY	0.9777	0.4449	0.9936	0.9486	1.0514
	4 TPY	0.9771	0.4489	0.9934	0.9482	1.0518
	6 TPY	0.9766	0.4529	0.9933	0.9476	1.0524
	12 TPY	0.9765	0.4520	0.9933	0.9478	1.0522
10 Waves	1 TPY	0.9832	0.3576	0.9954	0.9829	1.0171
	2 TPY	0.9830	0.3690	0.9953	0.9816	1.0184
	4 TPY	0.9820	0.3802	0.9951	0.9799	1.0201
	6 TPY	0.9818	0.3802	0.9950	0.9796	1.0204
	12 TPY	0.9818	0.3793	0.9951	0.9802	1.0198
		Mormerge				
2 Waves	1 TPY	0.8946	0.6727	0.9734	0.9457	1.0543
	2 TPY	0.9116	0.6247	0.9780	0.9582	1.0418
	4 TPY	0.9203	0.6058	0.9804	0.9659	1.0341
	6 TPY	0.9112	0.6354	0.9779	0.9571	1.0429
	12 TPY	0.9139	0.6292	0.9786	0.9594	1.0406
6 Waves	1 TPY	0.9670	0.4254	0.9911	0.9757	1.0243
	2 TPY	0.9798	0.3713	0.9945	0.9881	1.0119
	4 TPY	0.9738	0.3955	0.9930	0.9824	1.0176
	6 TPY	0.9758	0.3878	0.9935	0.9842	1.0158
	12 TPY	0.9737	0.3942	0.9929	0.9821	1.0179
10 Waves	1 TPY	0.9873	0.3619	0.9963	1.0027	1.0027
	2 TPY	0.9815	0.3858	0.9952	0.9951	1.0049
	4 TPY	0.9852	0.3703	0.9960	0.9991	1.0009
	6 TPY	0.9844	0.3706	0.9958	0.9985	1.0015
	12 TPY	0.9849	0.3675	0.9959	0.9995	1.0005

6.4 SUMMARY

The brute-force simulation accelerated for ten years using the harmonic morphological tide and the full wave climate of 2013 did not result in deviating results at t = 1 year with respect to the non-accelerated brute-force simulation. In addition, the ten yearly development of the brute-force simulation qualitatively compared with field data of the study area showed a lot of similarities. The brute-force simulation chosen as a reference for this research is able to qualitatively simulate a ten yearly morphodynamic development of the schematized study area very well.

The long-term simulations using different acceleration factors and different acceleration techniques revealed that the acceleration factor applied is not of importance for the accuracy. The input conditions applied in this study are accelerated to its maximum (acceleration factor of 2685) for the use of the derived harmonic morphological tide. No significantly deviating results were obtained using various acceleration factors. Also, the differences between the acceleration techniques are only minor. In the nearshore zone further away from the harbour moles, the deviations between the simulations are more pronounced. There can however not be pointed out which simulation technique yield the best results at these locations, no clear trend is present.

The largest differences between the results of the long-term simulations are in the inclusion of extra wave classes. Including additional wave classes in Mormerge is smoother towards the brute-force simulation than in Morfac. In general, it is clear that when including additional wave classes, the results are more accurate with respect to the brute-force simulation. At least six wave classes should be included to achieve acceptable results in terms of accuracy.

7 Multi-Criteria Analysis

7.1 FRAMEWORK

To compare the long-term accelerated simulations for engineering practice, not only the accuracy in terms of performance indicators (section 6.3) is important. Also criteria as simulation time, ease of use and applicability for a particular situation are relevant. This Multi-Criteria Analysis (MCA) will provide an answer for research question six about what the distinguishing elements are that decide which method is most appropriate for a certain simulation. The most important parameter in the comparison of the results is accuracy. Therefore, only five simulations in which the most accurate results were obtained (section 6.3) are included in this MCA. Because of the importance of the accuracy, a weight of 5 is applied for this criterion. The weights for each criterion are determined in consultation with the supervisors of this thesis. All criteria are ranked from + + (best) to - - (worst) to make a quick overview of the MCA possible. The weightings are multiplied with the rankings in which + + equals 5 and - - equals 1.

The simulation time of all long-term simulations is shown in Table 9. These simulation times are only indicative. The time needed to perform a simulation is also dependent on the computer (and number of cores) available. The simulation time can run up while computing when several simulations are performed at the same time on a particular computer. This increase of simulation time happens if the number of cores needed for the flow/wave simulations exceeds the number of cores available on the computer at that moment. In the MCA, the simulations times will be ranked from the fastest (+ +) to the slowest (- -) simulation. A weight of 4 is applied for this criterion because the rate of accuracy still overrules the simulation time. In engineering practice and consultancy where a project has to be finished in time because of a deadline set by the client, a simulation time of 100 - 120 hours (± 5 days) still is acceptable. Ideally for long-term simulations, a simulation time of ± 60 hours is desired. When a computer needs 60 hours to compute the final model result, approximately three simulations a week can be performed and checked if the model simulated correctly.

Table 9 - Simulation time (hours) of long-term simulations

Waves	0	1	2	6	10	2	6	10
Tides			Mormerge			Morfac		
1	0.9	4.7	9	13	15	13	29	42
2	1.8	10	16	22	32	26	47	66
4	3.5	20	38	34	62	36	78	147
6	5.5	29	53	73	106	60	142	345
12	14	55	150	157	213	134	329	684

For the criteria ease of use (how fast and easy it is to build and start-up a simulation) and applicability for a particular simulation (how well does this acceleration method represents what is happening in reality) also a ranking from (+ +) very good to (- -) very bad is applied. The weights for these criteria are 1 and 0.5 respectively. The results of the Multi-Criteria Analysis are shown in Table 10.

7.2 RESULTS OF THE MULTI-CRITERIA ANALYSIS

In determining scores for a particular simulation, it is important to consider the results relative to each other and to the reference situation. For the criteria ease of use, Mormerge is more favourable than Morfac (when using Matlab to create the input files). Also for applicability Mormerge is favourable (closer to reality, more variable in time). Another point of importance for this MCA is to choose simulations which computed faster than the accelerated brute-force simulation (acceleration factor of ten, run time is approximately 156 hours). If the computational times are longer, the brute-force simulation is in advantage. In addition, as mentioned in section 1.3, a result is accurate when the NS-coefficient is above 0.95, the linear correlation coefficient is over 0.99, the Root Mean Square error is less than 0.5 and the indicator of the linear regression line is under 1.05. Therefore, the simulations with 0, 1 or 2 wave conditions included are not sufficient in terms of accuracy. Considering these preconditions, the MCA is defined as follows:

Table 10 - Results Multi-Criteria Analysis. Tides PY: Tides simulated per year (related to the acceleration factor applied)

		Simulation	1	2	3	4	5
Criterion	Weight	Simulation includes:	6 Tides PY 10 Waves Mormerge	1 Tides PY 10 Waves Mormerge	1 Tides PY 10 Waves Morfac	1 Tides PY 6 Waves Mormerge	1 Tides PY 6 Waves Morfac
Accuracy	5		++	++	++	+/-	+/-
Run time	4		--	+	-	++	+/-
Ease of use	1		+	+	+/-	+	+/-
Applicability	0.5		+	+	+/-	+	+/-
Total (weighted)			35	47	37.5	41	31.5

Although accuracy is one of the most important parameters for the choice of a particular acceleration factor and technique, this is only to a lesser extent determinative for the final scores. Because of the very minor deviations in accuracy between the simulations (Table 8), the choice for including six or ten wave classes does not make a large difference in the MCA scores. The run times of different simulations are however more determinative in choosing a particular acceleration factor, technique and wave climate. There is a trade-off between the accuracy the results and the computational time needed. In terms of accuracy, the difference in performance criteria for the inclusion of six or ten wave classes is small. For the computational times, the inclusion of ten wave classes takes approximately 25 % more time to compute compared to the inclusion of six wave classes (Table 9). The choice for a particular wave climate is therefore depending on the situation (time available and normal run time of the simulation). Ease of use and applicability only add small contributions to the MCA scores.

Taking into account the MCA criteria and the previously mentioned preconditions, the MCA reveals that Morfac can only be favourable when using the highest acceleration factors. When accelerating with a smaller factor, the computational times are increasing too much. Mormerge is thus more beneficial. The run times in Mormerge are significantly lower for the inclusion of multiple wave classes. This effect, the favourability of Mormerge compared to Morfac, becomes larger when including additional wave classes. An important side effect is that the result becomes also more accurate when including more wave classes.

The choice for a particular acceleration technique is mostly determined by computational capacity available and run times. For Mormerge, more computational capacity needs to be available at one moment in time. To reduce the run times, a choice should be made how many conditions should be included in the model to achieve sufficient accuracy and which acceleration factor is still applicable to avoid an unstable model. When accelerating less, the run time will approximately increase linearly.

8 Discussion and Conclusions

The acceleration of long-term morphodynamic simulations is recommendable to avoid long run times. In this study, Morfac and Mormerge have been compared to each other and to a brute-force simulation using a Delft3D 2DH model. For the long-term simulations which made use of these acceleration methods, still a lot of options were possible. In this study it is chosen to fix all parameters and time periods for both acceleration methods. The acceleration factor and the number of wave conditions were varied to check additional questions concerning the input reduction and the usability in engineering practice. This section includes a discussion of the results (section 8.1), answer to the research questions in the conclusions (section 8.2) and recommendations for further research (section 8.3). The discussion of the model used and the obtained results is subdivided into a part for the input reduction and a separate part for the long-term simulations.

8.1 DISCUSSION

The results of this study are obtained by the use of a numerical model. The numerical model used is Delft3D in 2DH mode. The grid for the schematized study site has been refined at the areas of interest. The finest grid cells are 30 * 15 m in a total study area of 42 * 15 km. The choice for this grid size is a balance between the features that the model should be able to calculate accurately and the run time. Because of this grid size, nearshore processes are not modelled accurately. In addition, no specific attention is paid to processes at transition from wet to dry.

8.1.1 INPUT REDUCTION

The input reduction performed in this study is a first step in accelerating the long-term morphodynamic simulations. These reduced input conditions are derived by comparing very short simulations with respect to the time span for which the morphology will be simulated in the long term. The deviations already observed between the simulated results of the reduced input conditions and the field data can therefore be further exaggerated, stay in the same order, or can converge to a kind of equilibrium of the system. In addition, reducing the input conditions will result in a loss of real-time information. By taking a spring-neap tidal cycle as a reference for which the input reduction will be performed, it is attempted to reduce this loss of information in the output of the model. In performing the input reduction however, both time spans (the one of the reference situation and the situation for the reduced input conditions) have to be simulated. Taking only one spring-neap tidal cycle is a trade-off with respect to the computational effort.

Another item of discussion is the reduction and inclusion of wave effects. The water level boundary conditions derived to simulate the full spring-neap tidal cycle are extracted from the Kustfijn Astro model which has been validated with water level measurement at different measurement locations offshore and nearshore the Dutch coast. This signal however, included no wave measurements. The wave conditions are derived from a separately measured (real-time) signal. This signal is converted into directional and

magnitudinal bins for which short morphodynamic simulations have been performed including their rate of occurrence. These simulations have been performed for a very short period (morphodynamic only 24 hours and 50 min). This short period is not enough for the waves by changing the bottom layout to have a significant effect on the hydrodynamics. The wave schematisation using the OPTI-routine is thus based on initial changes. It is assumed that the sequence of occurrence of different wave conditions did not influence the morphological development and no irreversible development, caused by a particular wave class, took place. This assumption is also made when performing long-term simulations using Morfac with at least two wave conditions included in the model. To test the validity of the model based on the assumptions mentioned above, a real-time simulation should be executed for a much longer time scale. This benchmark simulation using real-time data however would cost a lot of time (all wave classes should run for a long time span) and was not feasible in the time limit of this thesis.

Further reduction of this real-time signal to conditions which are important for the morphological development resulted in several different scenarios with particular wave conditions. These scenarios could however not be validated because of the schematized model used in this study (no measured bathymetric data is used which could validate these scenarios). Although this is important for hindcasting and predicting morphological development in reality, this was not the purpose of this thesis. Here it is assumed that the derived wave scenarios are indeed the most important ones for the long-term morphological development.

After the derivation of different wave scenarios, it was remarkable that most high wave classes are left out. These waves, mostly occurring during storms, are not important for the long-term morphological behaviour (as is represented by this full wave climate of one year). This long-term morphodynamic wave impact behaviour can also be observed in the study of Dastgheib (2012) to long-term morphological modelling of large tidal basins. In addition, in determining new weights for the individual wave classes, waves originating from the Northwest and Southwest were overall assigned most severely.

8.1.2 LONG-TERM ACCELERATED SIMULATIONS

The brute-force simulation used in this study for a ten year morphodynamic development is chosen such that it can be computed within acceptable time limits (see problem definition, section 1.2). To achieve this ten yearly morphodynamic development, the harmonic morphological tide and a real-time wave signal were used and accelerated by a factor ten. This means that the results are expected to show a behaviour that is similar to the accelerated simulations. A comparison of the results after one year between this brute-force simulation and a non-accelerated brute-force simulation hardly showed deviating results. It is therefore assumed that this trend (no significantly deviating results between the accelerated and non-accelerated brute-force simulation) will continue and that the accelerated brute-force simulation is representative for a ten yearly morphodynamic development.

Comparing the morphodynamic development after ten years of the brute-force simulation to field data showed many similarities. The scour hole and sedimentation just in front of the harbour moles as well as the formation of nearshore banks is present and in the right order of magnitude. The brute-force simulation however seems to have an enlarged tide-induced sediment transport compared to the field data. The migration rate of the nautical channel in the zone where the flow is not disturbed by the harbour moles is too high. A calibration of the sediment transport rates or sediment characteristics could solve this mismatch. Because the goal of this thesis was not to calibrate and validate a numerical model for the study area, the constructed model is applicable for this study; it simulates qualitatively realistic behaviour.

In comparing the acceleration methods, all parameters were fixed. One item that was not the same between Morfac and Mormerge is the tidal phase for a particular wave condition. Because of the physical justification of this phase shift (an instantaneously counteracting sediment transport in time because of different tidal phases of each condition) this phase shift has been applied in Mormerge. Implementing the phase shift for the derived harmonic morphological tide in Delft3D is cumbersome; care should be taken for each boundary segment. The tidal phases at the begin and end of a boundary should not exceed the transition from 360° to 1°. Delft3D will interpolate this as a phase of around 180°. To avoid this, some manual adjustments had to be made which can result in a slightly distorted tide for this condition. In addition, to create a complete shifted harmonic morphological tide, every tidal constituent has to be shifted individually. If all tidal constituents would be shifted by the same number of degrees, a tidal mirror image will be created.

For the comparison of the results of both acceleration methods, care had to be taken which map result of the simulation needed to be extracted. For Morfac, the last map represents a ten yearly morphodynamic development. Using Mormerge however, the determined weights by the OPTI-routine method (which added up do not necessarily have to be equal to one) are scaled back to one again (automatically by Mormerge). Therefore, an additional scaling has been applied for which map result in Delft3D should be extracted for a particular wave scenario. This scaling makes it possible to compare the ten yearly morphodynamic development of both acceleration techniques. The scaling sometimes did not result in an integer map number result, in that case rounding was applied. This rounding can lead to slight deviations of the map result being exactly the ten yearly morphodynamic development. This effect is more pronounced when higher acceleration factors are applied (these simulations produced less map results and can deviate therefore more). The effects of the scaling and rounding applied are not pronounced in the comparison of both acceleration methods. In addition, the small deviations in the results of the long-term simulations between the acceleration techniques (order 30 m horizontally, one grid cell) are presumably more a result of model artefacts and numerical uncertainties rather than differences between the acceleration techniques.

8.2 CONCLUSIONS

In section 1.2 (problem description and objective) the research questions for this thesis are stated. In this section these questions will be answered. The answers will form the conclusions of this research.

1. *Which input conditions should be combined into ''input scenarios'' to run morphological simulations that represent the reality?*

Based on the field data characteristics for the study site chosen, at least the tidal forcing and forcing by wave characteristics should be taken into account when a schematized model will be constructed to represent this area.

2. *How do Morfac and Mormerge simulate the medium- and long term morphology?*

Morfac and Mormerge both simulate the medium- and long-term morphology using the morphodynamic cycle. In the morphodynamic cycle, based on an initial bathymetry, the flow (and optionally wave) fields are solved using boundary conditions. Next the sediment transport is calculated by the resulting flow velocity field and the bed will be updated. In the next time step, the updated bed is fed back as an initial condition. This morphodynamic system, for example in Delft3D, is solved using a coupled discretized system of differential equations. Optionally, the flow and wave can interact with each other periodically. In this communication between the wave and flow computations, both flow and wave can use and extend variables of another to simulate as accurate as possible (feedback between wave and flow). Also many

extra parameters/variables for the sediment calculations, drying and flooding, morphological update (bed update) and the numerical solving scheme are available.

For the acceleration methods Morfac and Mormerge, the main difference is in the sequence of computations for the different input conditions (as varying wave conditions). Morfac performs this computation one after another. Every condition is computed for the complete time span which has to be simulated. In this computation, the morphological acceleration factor is multiplied by the percentage of occurrence of that particular wave class. The bathymetric result of a particular wave class is used as the initial bathymetry for the following wave class to be simulated. Mormerge in turn executes these computations parallel. All wave conditions are started at the same moment and simulated for the full time span of the simulation. The bed is updated every flow time step and weighted by the percentage of occurrence of every wave class. The weighted bed update is then used for the hydrodynamic computations in the next time step. The morphological acceleration factor is kept constant in Mormerge.

3. *In what way can a real-time tidal signal be reduced to a representative tide that is able to simulate accurate hydrodynamic and morphodynamic results compared to a reference period?*

To reduce the tidal input signal for the model, a double consecutive tide out of a full spring-neap tidal cycle (reference period) was chosen which represented the morphodynamic development the best in terms of the linear correlation coefficient compared to this a full spring-neap tidal cycle (measured water level signal). The linear correlation coefficient of the bottom development of this double consecutive tide (morphological tide) with respect to the bottom development of spring-neap tidal cycle simulated is over 0.99. A correction factor was applied to match the magnitude of the bottom development as well (slope of the linear regression line). This morphological tide has been made harmonic (using tidal constituents) to make it useful to simulate an endless period without any shocks in the model.

The validation of the input reduction of the tide showed that the loss of accuracy by the derivation of a harmonic morphological tide is very limited. The morphological development of the study area using the harmonic morphological tide matched the morphological development of the simulation using a complete full spring-neap tidal cycle as input very well. The Brier Skill score of this comparison was 0.96.

4. *How many wave classes resulting from the input reduction should be included in a simulation using Morfac and Mormerge to obtain accurate results compared to a reference simulation?*

The input reduction of the waves is performed using the OPTI-routine. This method results in the determination of the wave classes (and corresponding weights) which are most important for the morphodynamic development of the study area. Out of the OPTI-routine method results, four wave scenarios are chosen with one, two, six and ten wave classes respectively for simulating the long-term morphodynamic development. It became clear that when including additional wave classes, the morphodynamic development results are more accurate with respect to the brute-force simulation (reference simulation). After the long-term accelerated simulations using Morfac and Mormerge, it was revealed that at least six wave classes should be included to represent the accelerated ten yearly brute-force simulation accurately. The difference in terms of accuracy for the inclusion of six or ten wave classes is very small.

5. *Which acceleration factor for the morphological changes is still acceptable to achieve accurate results compared to a reference simulation?*

The long-term simulations using different acceleration factors in this case study showed that the acceleration factor is not of importance for the accuracy. No significantly deviating results were obtained. The input conditions applied are accelerated to the maximum achievable for the use of the derived harmonic morphological tide (acceleration factor of 2685 which is the simulation of one harmonic

morphological tide for ten years). Using the input reduction technique for the input conditions as applied in this study, at least one harmonic morphological tide needs to be simulated for the results to be valid.

6. *What are the distinguishing elements that decide which method is most appropriate for a certain simulation?*

The long-term simulations showed that the acceleration factor in both acceleration techniques is not of importance for the accuracy of the results. Also the choice for a particular acceleration method does not result in significantly deviating results. The inclusion of additional wave classes is more determinative in terms of accuracy, but only to a minor extent when including six or ten wave classes. The choice for a particular acceleration method and factor can however be decisive in engineering practice when looking at run times. Mormerge can compute much faster when enough computational capacity is available at once, especially when a larger amount of wave classes is included. Morfac is only in favour when the highest acceleration factors are applied and only a few wave classes are included. Especially the latter reason, inclusion of only a small number of wave classes (zero, one or two), will result in a significantly lower model performance in terms of accuracy. This model performance was not considered acceptable.

Mormerge is therefore generally more suited for long-term morphodynamic simulations in tide and wave driven environments (if enough computational capacity is available). The chance for irreversible bathymetric changes to happen, when for example one extreme wave condition is simulated for its complete time span causing a large bathymetric change, is smaller because of the instantaneously counteracting sediment transports when applying a phase shift for the tide in each wave condition. Mormerge is thus physically more justified. In addition, Mormerge is easier to set up and implement and has the advantage that numerical parameters can be adjusted individually per wave condition, if desired.

In general, the model is applicable for long-term morphodynamic simulations in deeper water. The distortion of the flow by the harbour moles is simulated accurately. A qualitative comparison with bathymetric field data revealed that the long-term morphodynamic behaviour is modelled well. A calibration of the tide-induced sediment transport or sediment characteristics at deeper water should however be performed to simulate the correct nautical channel migration. In the nearshore zone, no preferred acceleration technique or acceleration factor could be determined.

8.3 RECOMMENDATIONS

An item for which this study could not provide a clear answer is the applicability of the acceleration techniques in the nearshore zone. It is recommended to do additional research with a model that is more suited for shallow water zones, wave breaking and the transition from wet to dry. For such a study, a finer grid resolution should be implemented. From JARKUS data, it is easy to test this case and check the applicability of the different acceleration techniques compared to field data.

Because the waves only cause stirring of the sediment in this model, it is recommended to first calibrate the tide-induced sediment transport rate and sediment characteristics for the long-term. This calibration can solve the issue concerning the large migration rate of the nautical channel. In addition, when setting up a model, it is recommendable to analyse the wave signal, convert this into directional plus magnitudinal bins and perform an OPTI-routine to extract the sequence of importance of the waves for the morphodynamic development. After the OPTI-routine, a quick calculation should be performed which will determine if a particular wave type will have effect on the morphodynamic development at a particular depth.

Bibliography

Alkyon. (2001b). *Herstel 1:3 koppeling binnen modellentrein, Fase 2 - modelbouw en afregeling, rapport A705R3, Oktober 2001.*

Bijlsma, A.C., Mol, A.C.S., & Winterterp, J.C. (2007). *Numeriek modelonderzoek naar de reductie van neer in de monding van de voorhaven van IJmuiden. WL | Delft Hydraulics report: H4926.* RWS Rijksinstituut voor Kust en Zee.

Boutmy, A.E.G. (1998). *Morphological impact of IJmuiden harbour. Validation of Delft3D/Delft3D-RAM 1968 - 1996.* Delft: WL | Delft Hydraulics & TU Delft.

Dastgheib, A. (2012). *Long-term process-based morphological modeling of large tidal basins. PHD Thesis*. Delft: TU Delft / UNESCO-IHE.

De Vriend, H.J. (2005). *River Engineering. Reader Ct3340.* TU Delft, Faculty of Civil Engineering and Geosciences. Section Hydraulic and Offshore Engineering.

De Vriend, H.J., Capobianco, M., Chesher, T., de Swart, H.E., Latteux, B., & Stive, M.J.F. (1993). Approaches to long-term modelling of coastal morphology: a review. *Coastal Engineering, vol. 21,* pag. 225 - 269. doi:10.1016/0378-3839(93)90051-9.

Deltares. (2014). *Delft3D-FLOW user manual.* Delft: Deltares.

Deltares. (2014). *Delft3D-WAVE user manual.* Delft: Deltares.

Elias, E. (2006). *Morphodynamics of Texel Inlet. PHD Thesis.* Amsterdam: IOS Press, Delft University Press.

Grasmeijer, B.T, Adema, J., & Jellema, K.T. (2014). *Arcadis coastal modelling guidelines; confidential.* Zwolle: ARCADIS Nederland bv.

Hendrickx, P. (1988). *Scour near harbour of IJmuiden (in Dutch). Report H460.* Delft: Delft Hydraulics.

Hoogewoning, S.E., & Boers, M. (2003). *Fysische effecten van zeezandwinning. Rapport RIKZ/2001.050.* Den Haag: Rijksinstituut voor Kust en Zee/RIKZ.

Horstman, E.M., Dohmen-Janssen, C.M., Bouma, T.J., & Hulscher, S.J.M.H. (2015). Tidal-scale flow routing and sedimentation in mangrove forests: Combining field data and numerical modelling. *Geomorphology, vol. 228*, pag. 244 - 262. doi:10.1016/j.geomorph.2014.08.011.

Jimenez, N., & Mayerle, R. (2010). A methodology to simulate medium term morphological changes in a practical computing time. *Proceedings of the International Conference on Coastal Engineering; No 32,* Shanghai.

Knaapen, M.A.F., & Joustra, R. (2012). Morphological acceleration factor: usability, accuracy and run time reductions. *XIXth TELEMAC-MASCARET User Conference.* Oxford, UK: HR Wallingford.

Latteux, B. (1995). Techniques for long-term morphological simulation onder tidal action. *Marine Geology vol. 126,*pag. 129 - 141.

Lesser, G.R. (2009). *An approach to medium-term coastal morphological modelling. PHD Thesis.* Delft: TU Delft / Unesco-IHE.

Lesser, G.R., Roelvink, J.A., Van Kester, J.A.T.M., & Stelling, G.S. (2004). Development and validation of a three-dimensional morphological model. *Coastal Engineering. Vol 51, 883 - 915.* doi:10.1016/j.coastaleng.2004.07.014.

McClave, Benson, & Sincich. (2010*). Statistiek; een inleiding voor het hoger onderwijs.* Amsterdam: Pearson Education Benelux.

Mol A.C.S. (2007*). R&D Kustwaterbouw Reductie Golfrandvoorwaarden OPTI Manual. Research report H4959.10.* WL|Delft Hydraulics, the Netherlands.

Murphy, A.H., & Epstein, E.S. (1989). Skill Scores and correlation coefficients in model verification. *Monthly weather review, vol. 117*, pag. 572 - 582. doi: http://dx.doi.org/10.1175/1520-0493(1989)117<0572:SSACCI>2.0.CO;2.

Nash, J.E., & Sutcliffe, J.V. (1970). River flow forecasting through conceptual models. Part 1-A Discussion of principles. *Journal of Hydrology, vol. 10*, Pag. 282 - 290.

Pugh, D. (2004*). Changing Sea Levels: Effects of Tides, Wheather and Climate.* Cambridge: University Press.

Ranasinghe, R., Swinkels, I.C.S., Luijendijk, A.P., Bosboom, J., Roelvink, J.A., Stive, M.J.F., & Walstra, D.J.R. (2010). Morphodynamic upscaling with the Morfac approach. *Coastal Engineering. Vol 58*, 806 - 811. doi:10.1016/j.coastaleng.2011.03.010.

Ribberink, J.S. (1989). *Zeezandwinning. Onderbouwende notitie, Rapport WL, H825.* Delft: Delft Hydraulics.

Ribberink, J.S. (2011). *River Dynamics 2: Transport Processes and Morphology.* Enschede: University of Twente.

Rijkswaterstaat. (2011, 8 25). *Watergegevens*. Retrieved from Rijkswaterstaat: http://www.rijkswaterstaat.nl/water/waterdata_waterberichtgeving/watergegevens/index.aspx#v2

Rijkswaterstaat. (2013). *Servicedesk Data*. Retrieved from Rijkswaterstaat.

Rijkswaterstaat. (2014, 12 27). *Noordzee.* Retrieved from Rijkswaterstaat: http://www.rijkswaterstaat.nl/water/feiten_en_cijfers/vaarwegenoverzicht/noordzee/index.aspx

RIKZ. (2003*). Getijtafels voor Nederland 2004*. Den Haag. ISBN 90-12-09919-6: Rijksinstituut voor Kust en Zee, afdeling informatiesystemen.

Roelvink, J.A., & Reniers, A.J.H.M. (2012). *A guide to modelling coastal morphology*. Singapore: World Scientific Publishing Co. Pte. Ltd.

Roelvink, J.A., & Walstra, D.J.R. (2004). Keeping it simple by using complex models. *Advances in Hydro Science and - Engineering, Vol. 6*.

Roelvink, J.A. (2006). Coastal morphodynamic evolution techniques. *Coastal Engineering. Vol. 53*, 277 - 287. doi:10.1016/j.coastaleng.2005.10.015.

Sutherland, J., Peet, A.H., & Soulsby, R.L. (2004). Evaluating the performance of morphological models. *Coastal Engineering, vol. 51*, pag. 917 - 939. doi:10.1016/j.coastaleng.2004.07.015.

Swinkels, I.C.S., Bijlsma, A.C., & Hommes, S. (2010). *Blue Energy Noordzeekanaal*. Delft: Deltares.

van Alphen, J. (1987). *De morfologie en lithologie van de brandingszone tussen Terheijde en Egmond aan Zee*. Utrecht: Rijkswaterstaat, directie Noordzee. Report NZ-N-87.28, 22p.

Van de Rest, P. (2004). *Morfodynamica en hydrodynamica van de Hollandse kust. MSc Thesis.* Delft: TU Delft.

Van der Wegen, M., & Roelvink, J.A. (2008). Long-term morphodynamic evolution of a tidal embayment using a two-dimensional, process-based model. *Journal of Geophysical Research. Vol. 113*, C03016, doi:10.1029/2006JC003983.

Van Heijst, M.W.I.M., Cleveringa, J., De Kok, J.M. (2005). *Vaargeulenonderhoud, zandwinning & kustlijnzorg: risico's en perspectieven voor Rijkswaterstaat.* Rijkswaterstaat, Dienst Weg- en Waterbouwkunde Rapport DWW-2005-050. -5 Publicatiereeks grondstoffen 2005/04; Rapport RIKZ 2005-25, 72 p.

Van Rijn, B.W.F. (2012). *Influence of wave climate schematisation on the simulated morphological development of the Western Scheldt entrance.* Delft: Arcadis & TU Delft.

Van Rijn, L.C. (1993). *Principles of sediment transport in rivers, estuaries and coastal seas*. Amsterdam: AQUA Publications.

Van Rijn, L.C. (2005). *Principles of sedimentation and erosion engineering in rivers, estuaries and coastal seas*. Amsterdam: Aqua Publications. ISBN 90-800356-6-1.

Van Rijn, L.C., Roelvink, J.A., & Ter Horst, W. (2001). *Approximation formulae for sand transport by currents and waves implementation in Delft-MOR*. Report no. Z3054.20/40. Delft: Delft Hydraulics.

Van Rijn, L.C., Walstra, D.J.R., Grasmeijer, B.T., Sutherland, J., Pan, S., & Sierra, J.P. (2003). The predictability of cross-shore bed evolution of sandy beaches at the time scale of storms and seasons using process-based profile models. *Coastal Engineering, vol. 47*, pag. 295 - 327.

Verhagen, H.J., & Van Rossum, H. (1990). *TR-13. Grote Civiele Werken. Invloed op kustgedrag*. Ministerie van Verkeer en Waterstaat; Rijkswaterstaat.

Wijnberg, K.M. (1995). *Morphologic behaviour of a barred coast over a period of decades. PhD Thesis.* Utrecht: Universiteit Utrecht. ISBN 90-6266-125-4.

Zimmerman, N., Trouw, K., Wang, L., Mathys, M., Delgado, R., & Verwaest, T. (2012). Longshore transport and sedimentation in a navigation channel at Blankenberge (Belgium*). International Conference on Coastal Engineering (ICCE 2012),* (pp. book of papers. pp. 1 - 16). Santander, Spain.

List of Figures

List of Tables

Appendices

A. DELFT3D MODEL DESCRIPTION

The model used in this study is a 2DH Delft3D model which solves the unsteady shallow-water equations in two dimensions, depth averaged, based on the Navier-Stokes equations. The model solves the equations based on finite differences and consists of several different components which can interact with each other. These components, amongst others, are the FLOW-module and the WAVE-module. The DELFT3D-FLOW module consists of the hydrodynamics, sediment transport and the morphodynamics. These components will be described differently here as well as the wave module, grid and boundary conditions.

A.1. HYDRODYNAMICS

The horizontal momentum equations that are solved in the calculations are based on the assumption that the fluid is incompressible and a non-varying water density is present in the x-y direction. The vertical momentum is reduced to the hydrostatic pressure relation because the vertical accelerations are assumed to be small compared to the gravitational acceleration. In addition, the $k-\epsilon$ turbulence closure model is present.

$$\frac{\partial \bar{u}}{\partial t} + \bar{u}\frac{\partial \bar{u}}{\partial x} + \bar{v}\frac{\partial \bar{u}}{\partial y} + g\frac{\delta \zeta}{\delta x} = f\bar{v} + v_h\left(\frac{\partial^2 \bar{u}}{\partial x^2} + \frac{\partial^2 \bar{u}}{\partial y^2}\right) + \frac{g\bar{u}|\sqrt{\bar{u}^2 + \bar{v}^2}|}{hC^2} + \frac{\rho_{air} C_d W_x \sqrt{W_x^2 + W_y^2}}{\rho_0 h} \quad (20)$$

$$\frac{\partial \bar{v}}{\partial t} + \bar{u}\frac{\partial \bar{v}}{\partial x} + v\frac{\partial \bar{v}}{\partial y} + g\frac{\delta \zeta}{\delta y} = f\bar{u} + v_h\left(\frac{\partial^2 \bar{v}}{\partial x^2} + \frac{\partial^2 \bar{v}}{\partial y^2}\right) + \frac{g\bar{v}|\sqrt{\bar{u}^2 + \bar{v}^2}|}{hC^2} + \frac{\rho_{air} C_d W_y \sqrt{W_x^2 + W_y^2}}{\rho_0 h} \quad (21)$$

| 1 | 2 | 3 | 4 | 5 | 6 | 7 |

The terms in the horizontal momentum equations represent: 1 Inertia, 2 Advection, 3 Horizontal pressure gradient, 4 Coriolis force, 5 Horizontal viscosity, 6 friction term and 7 Wind forcing (not used in this study).

And the depth-averaged continuity equation reads (evaporation, precipitation and discharge are neglected):

$$\frac{\partial \zeta}{\partial t} + \frac{\partial [h\bar{u}]}{\partial x} + \frac{\partial [h\bar{v}]}{\partial y} = 0 \quad (22)$$

Where:

ζ Water level according to reference level (m)
d Depth towards reference level (m)
h Total water depth (m)

$\bar{u}, \bar{v}$ depth averaged flow velocity in x- and y-direction respectively (m/s)
W_x,W_y Wind speed in x- and y-direction respectively (m/s)
f Coriolis parameter (1/s)
g Gravity acceleration (m/s^2)
C Chézy coefficient (m$^{1/2}$/s)
C_d Wind shear stress coefficient
ρ_0 Density of water (kg/m^3)
ρ_{air} Density of air (kg/m^3)
v_h Horizontal eddy viscosity (m^2/s)

More information about the derivation of terms in the momentum equation, for example the horizontal viscosity term or the horizontal pressure term, can be found in: Lesser et al. (2004) and Deltares (2011).

A.2. SEDIMENT TRANSPORT AND MORPHOLOGY

The transport of sediment in DELFT3D is modelled with the sediment continuity equation to determine the bed level changes. The bed is updated every time-step based on the calculated bed level changes. The bed update can be multiplied with a morphological acceleration factor.

$$\frac{\partial z_b}{\partial x} + \frac{\delta(s_{b,x} + S_{s,x})}{\partial x} + \frac{\delta(s_{b,y} + S_{s,y})}{\partial x} = 0 \qquad 23$$

Where:
$S_{s,x \text{ or } y}$ Suspended sediment transport in x- or y-direction (kgm^{-1}s^{-1})
$S_{b,x \text{ or } y}$ Bed load sediment transport in x- or y-direction (kgm^{-1}s^{-1})

The sediment transport and morphology (sub) module in Delft3D supports both bed load transport and suspended load transport of non-cohesive sediments. For the sediment transport formulas in Delft3D, TRANSPOR1993 is used. TRANSPOR1993 follows the principles of Van Rijn (1993) using a reference height. Below the reference height, the bed load is calculated. Above this reference height, the suspended load is used to calculate the transport. The suspended sediment is computed by solving an advection diffusion equation (Elias, 2006). The bed load is calculated by the transport formula of Van Rijn (1993). The sediment exchange with the bed is calculated by sink and source terms as specified by the Van Rijn (1993) approach.

In the TRANSPOR 1993 module, four different sediment transport classes are distinguished:
Current-related suspended transport $S_{s,c}$
Wave-related suspended transport $S_{s,w}$
Current-related bed load transport $S_{b,c}$
Wave-related bed load transport $S_{b,w}$

Where:

$$S_s = S_{s,c} + S_{s,w} \qquad 24$$

$$S_b = S_{b,c} + S_{b,w} \qquad 25$$

More information about the computation of the different sediment transport classes can be found in for example: Elias (2006 and Van Rijn (1993).

A.3. WAVE MODULE

Wind-generated waves in DELFT3D are simulated by the WAVE-module. Two options to calculate the waves are included in DELFT3D-WAVE, the third generation SWAN (Simulating Waves Near shore) model and the stationary second-generation HISWA model. SWAN is the successor of the HISWA model and overcomes several limitations of the HISWA model. In addition, SWAN is unconditionally stable and has a perfect coupling with the FLOW-module. Therefore, the SWAN third generation model is used in the graduation project. It computes the wave generation by wind, wave propagation, non-linear wave-wave interactions and wave energy dissipation for a given topography, wind field, water level and current field (Deltares, 2014).

The SWAN model describes the waves with a two-dimensional wave action density spectrum. The spectrum considered is the action density spectrum N(σ,θ) which is equal to the energy density divided by the relative frequency: $N(\sigma,\theta) = \frac{E(\sigma,\theta)}{\sigma}$, with σ the relative frequency and θ the wave direction. The evolution of the wave spectrum in SWAN is described by the spectral action balance (Deltares, 2014):

$$\frac{\delta}{\delta t}N + \frac{\delta}{\delta x}c_x N + \frac{\delta}{\delta y}c_y N + \frac{\delta}{\delta \sigma}c_\sigma N + \frac{\delta}{\delta \theta}c_\theta N = \frac{S}{\sigma} \text{ (for a Cartesian coordinate system)} \quad (26)$$

| 1 | 2 | 3 | 4 | 5 |

In which the terms represent: 1 local rate of change of action of density in time, 2 propagation of action in space with velocities $c_{x \text{ or } y}$, 3 shifting of the relative frequency due to variations in depth and currents, 4 depth-induced and current-induced refraction and term 5 S is the source term of energy density representing the effects of generation, dissipation and non-linear wave-wave interactions.

A.4. GRID & BOUNDARY CONDITIONS

The Delft3D model performs the computations on a grid. Various types of grids like rectangular, curvilinear or spherical grids are possible which are assumed well-structured and orthogonal. These grids can also be nested in other, larger grids. In this thesis, for simplicity, one grid will be used with coarse grid sizes at the boundaries and a finer resolution towards the areas of interest in the study site. The numerical grid in this study is an orthogonal, curvilinear staggered grid. The principle of a staggered grid is shown in Figure 36 where the thick lines are the boundaries (enclosure) and within the boundaries the numerical grid (black rectangle).

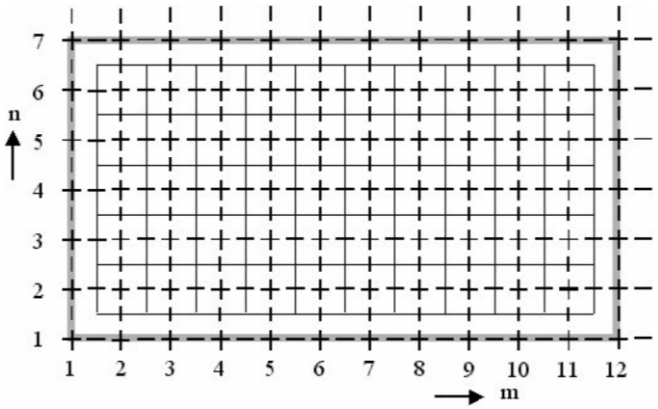

Figure 36 - Staggered grid (Deltares, 2014) with + the water level points, - the horizontal velocity points and | the vertical velocity points. The depth is specified at the grid corners.

In Delft3D, several boundary conditions can be applied for the open boundaries. These include: water level boundaries, velocity boundaries, flux or discharge boundaries, Neumann (water level gradient)

boundaries and Riemann (weakly reflective) boundaries. The choice for a particular boundary condition depends on the situation to be studied (Deltares, 2014).

A.5. SOLUTION PROCEDURE

The solution procedure of Delft3D is based on finite differences. The variables are arranged in a so-called Arakawa C-grid. Here, the water level points are defined in the grid centre and the velocity points are perpendicular to the grid cell faces (Deltares, 2014). An example of a solution procedure is shown in Figure 37. Figure 37 shows a cyclic solving procedure as is used in this study.

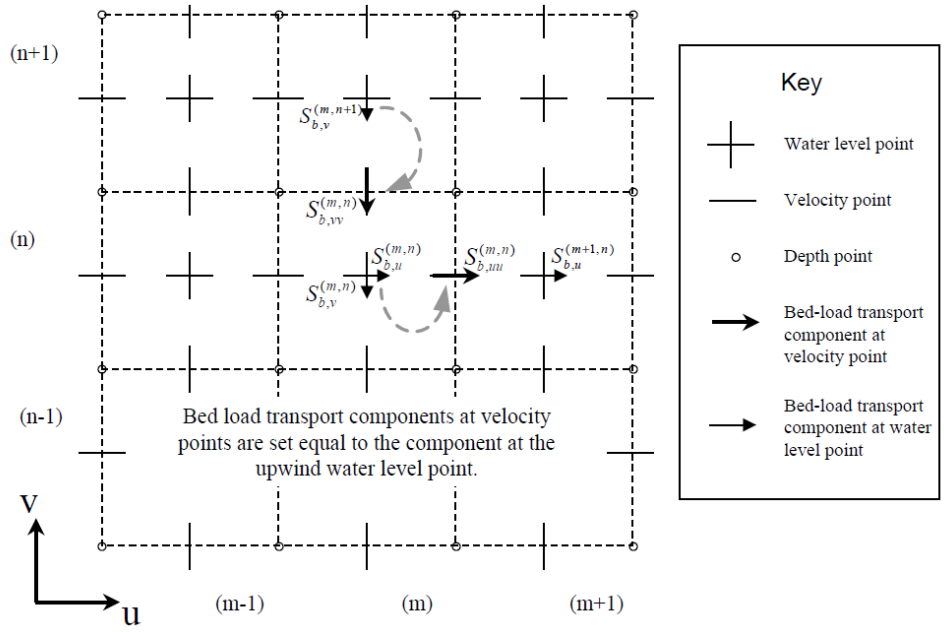

Figure 37 - Delft3D solution procedure showing the upwind method of setting bed-load sediment transport components at velocity points (Lesser, 2009).

A.6. NUMERICAL PARAMETERS DELFT3D MODEL

Table 11 - Numerical parameters Delft3D model as used in this study. Description obtained from FLOW and WAVE manuals Delft3D

	Parameter	Value	Description
FLOW	Δt	0.2	Flow time step (min)
	Ag	9.81	Gravitational acceleration (m/s^{-2})
	ρw	1020	Water density (kg/m^3)
	Tzone	1	GMT time zone
	Rettis	180	Thatcher-Harleman return time surface (min)
	Rettib	180	Thatcher-Harleman return time bottom (min)
	Betac	0.5	Parameter spiral motion
	Roumet	C (Chezy)	Roughness formulation
	Ccofu	65	Chezy coefficient U direction ($m^{1/2}/s$)
	Ccofv	65	Chezy coefficient V direction ($m^{1/2}/s$)
	Dicouv	10	Horizontal eddy diffusivity (m^2/s)
	CSTbnd	YES	Advection term with normal gradients switched off
	Irov	0	Flag to activate partial slip condition
	Iter	2	Number of iterations in continuity equation
	Dryflp	YES	Flag for extra drying and flooding

	Dpsopt	MAX	Option for check at water level points
	Dpuopt	MOR	Option for check at velocity points
	Dryflc	0.1	Treshold depth drying and flooding (m)
	Dco	-999	Marginal depth in shallow area's (m)
	Tlfsmo	0	Time interval to smooth the hydrodynamic boundary conditions (min)
	Trasol	Cyclic-method	Numerical method for advective terms
	Momsol	Cyclic	Numerical method for momentum terms
MOR	EpsPar	False	Vertical mixing distribution according to Van Rijn
	IopKCW	1	Flag for determination ks and kw
	RDC	0.01	Current related roughness height (m)
	RDW	0.02	Wave related roughness height (m)
	MorStt	1440	Spin-up interval from Tstart till start of morphological changes (min)
	Tresh	0.05	Treshold sediment thickness for reducing sediment exchange (m)
	MorUpd	True	Update bathymetry during FLOW simulation
	EqmBc	True	Equilibrium sand concentration profile at inflow boundaries
	DensIn	False	Include effect of sediment concentration on fluid density
	AksFac	1	Van Rijn's reference height
	RWave	2	Wave related roughness
	AlfaBs	1	Streamwise bed gradient factor for bed load transport
	AlfaBn	1.5	Transverse bed gradient factor for bed load transport
	Sus	1	Multiplication factor for suspended sediment reference concentration
	Bed	1	Multiplication factor for bed-load transport vector magnitude
	Susw	1	Wave-related suspended sediment transport factor
	Bedw	1	Wave-related bed-load sediment transport factor
	SedThr	0.3	Minimum water depth for sediment computations (m)
	ThetSD	0.25	Factor for erosion of adjacent dry cells
	HMaxTH	1.5	Max depth for variable THETSD
	FWFac	1	Vertical mixing distribution according to Van Rijn
SED	RhoSol	2650	Specific density (kg/m^3)
	SedDia	200	Median sediment diameter (D50) (μm)
	CDryB	1600	Dry bed density (kg/m^3)
	IniSedThick		From restart file (m), or 5 m
	FacDSS	1	Initial suspended sediment diameter
WAVE	Windspeed	0	(m/s)
	Windir	0	Wind direction (°)
	Waterlevelcorrection	0	(m)
	Northdir	90	Direction of North relative to x axis (°)
	Genmodephys	3	Third generation
	Breaking	True	Include wave breaking
	Breakalpha	1	Alpha coefficient for wave breaking

	Breakgamma	0.73	Gamma coefficient for wave breaking
	Triads	True	Include triads
	Bedfriction	Jonswap	
	Bedfriccoef	0.067	Bed friction coefficient
	Diffraction	False	Include wave diffraction
	Whitecapping	Komen	
	Refraction	True	Include wave refraction
	Fregshift	True	Include frequency shifting in frequency space
	Waveforces	Dissipation	Method of wave force computation
	Dirspacecdd	0.5	Discretisation in directional space
	Freqspacecss	0.5	Discretisation in frequency space
	Rchhstm01	0.02	Relative change of wave height or mean wave period w.r.t. local value
	Rchmeanhs	0.02	Relative change of wave height w.r.t. model-wide average wave height
	Rchmeantm01	0.02	Relative change of mean wave period w.r.t model-wide average mean wave period
	Percwet	98	Percentage of points included in simulation at which convergence criteria must be satisfied
	Maxiter	15	Maximum number of iterations for convergence
	Writecom	True	Write results to communication file
	Comwriteinterval	60	Interval for writing communication file (min)
	Flowbedlevel	2	Use and extend bedlevel
	Flowwaterlevel	2	Use and extend waterlevel
	Flowvelocity	2	Use and extend
	Flowwind	0	Don't use
	Dirspace	Circle	Directional space
	Ndir	36	Number of directional bins
	Fregmin	0.05	Minimum frequency (Hz)
	Fregmax	1	Maximum frequency (Hz)
	Nfreq	24	Number of frequencies
	Spectrumspec	Parametric	Spectrum specification type
	Spshapetype	Jonswap	
	Periodtype	Peak	Wave period type
	Dirspreadtype	Degrees	Directional spreading type
	Peakenhancefac	3.3	Peak enhancement factor jonswap spectrum

B. INPUT REDUCTION

B.1. CORRELATION AND SPREADING OF ALL COMBINATIONS OF DOUBLE TIDES

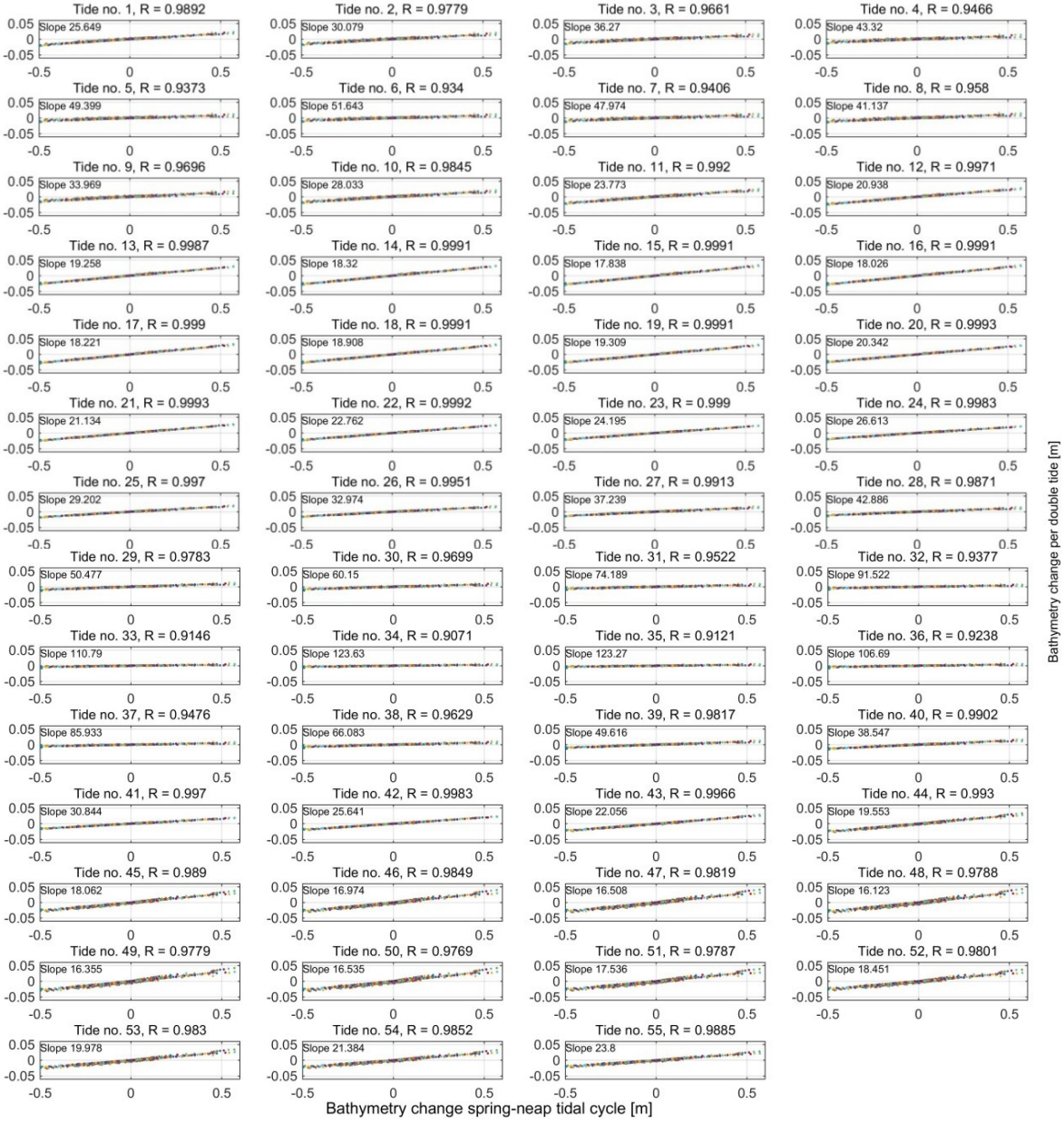

Figure 38 - Correlation and spreading of all consecutive double tides

B.2. SAND TRANSPORT AFTER SPRING-NEAP TIDAL CYCLE

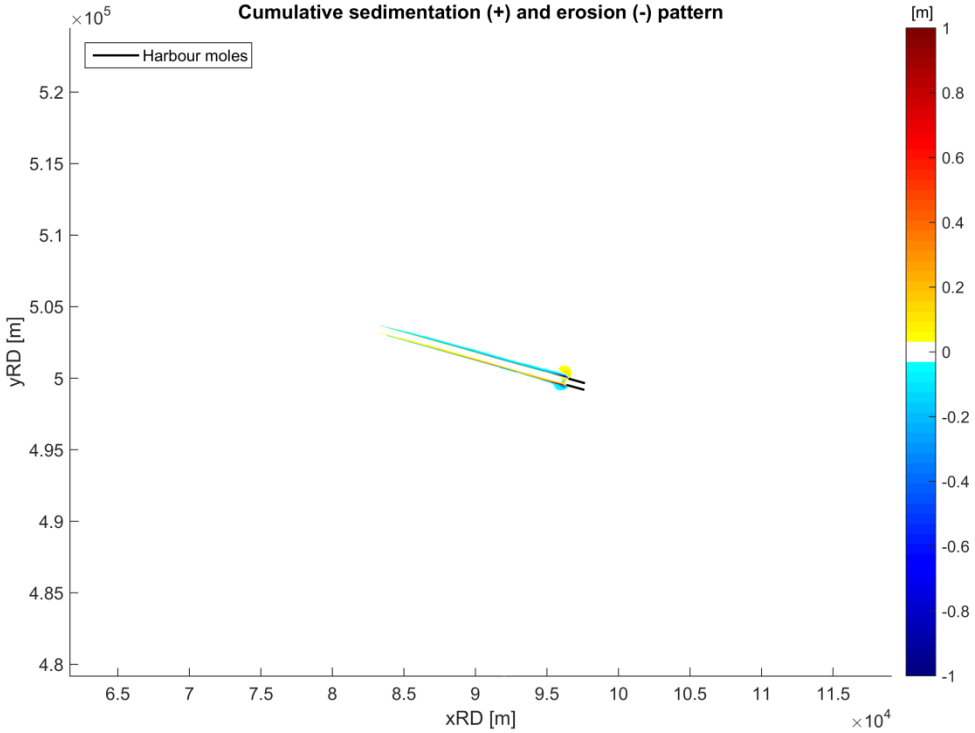

Figure 39 - Cumulative sedimentation (+) and erosion (-) pattern after one spring-neap tidal cycle. The harbour moles (black) are included for clarity

B.3. COMBINATIONS OF REALISTIC AND OCCURRED WAVE HEIGHTS AND DIRECTIONS

Table 12 - Combinations of wave heights and direction as input for OPTI-method

Condition name/no	H (cm)	T (s)	Direction (° w.r.t North, clockwise)	Directional spreading (°)
101	25	3.734361	360	30
102	75	4.34204	360	30
103	125	4.639248	360	30
104	175	4.995438	360	30
105	225	5.420701	360	30
106	275	5.875	360	30
107	325	6.368335	360	30
108	375	6.52414	360	30
109	425	7.16328	360	30
113	25	4.338981	330	30
114	75	4.670998	330	30
115	125	4.939962	330	30
116	175	5.113729	330	30
117	225	5.520334	330	30
118	275	6.142443	330	30
119	325	6.64327	330	30

120	375	6.88	330	30
121	425	7.314359	330	30
122	475	7.911888	330	30
123	525	8.181078	330	30
124	575	7.9	330	30
125	25	3.792467	300	30
126	75	4.117278	300	30
127	125	4.491639	300	30
128	175	4.874611	300	30
129	225	5.365517	300	30
130	275	5.592409	300	30
131	325	6.197083	300	30
132	375	6.237148	300	30
133	425	6.986247	300	30
134	475	7.160589	300	30
137	25	3.571196	270	30
138	75	3.968977	270	30
139	125	4.409549	270	30
140	175	4.81958	270	30
141	225	5.252224	270	30
142	275	5.651257	270	30
143	325	5.991782	270	30
144	375	6.295	270	30
146	475	6.936546	270	30
147	525	7.237448	270	30
149	25	3.463147	240	30
150	75	3.788702	240	30
151	125	4.264668	240	30
152	175	4.760429	240	30
153	225	5.134202	240	30
154	275	5.534664	240	30
155	325	5.992542	240	30
156	375	6.207763	240	30
157	425	6.3386	240	30
158	475	7.018268	240	30
159	525	7.049915	240	30
161	25	3.2975	210	30
162	75	3.601542	210	30
163	125	4.069282	210	30
164	175	4.577204	210	30
165	225	5.029958	210	30
166	275	5.230033	210	30
167	325	5.664806	210	30
168	375	6.075625	210	30
169	425	6.35637	210	30
170	475	6.675	210	30

B.4. DEFINED WAVE CLIMATES BASED ON OPTI-METHOD

Table 13 - Defined scenarios of combinations of wave classes

Amount of wave classes included	Included wave classes (no)	Wave height (m)	Wave period (s)	Wave direction (°) w.r.t North, clockwise	Directional spreading (°)	Weight
0	-	-	-	-	-	-
1	151	125	4.264668	240	30	0.6717
2	116	175	5.113729	330	30	0.2483
	151	125	4.264668	240	30	0.5142
6	102	75	4.34204	360	30	0.221
	103	125	4.639248	360	30	0.1017
	116	175	5.113729	330	30	0.1355
	142	275	5.651257	270	30	0.0854
	151	125	4.264668	240	30	0.1901
	165	225	5.029958	210	30	0.0971
10	102	75	4.34204	360	30	0.1707
	103	125	4.639248	360	30	0.0808
	116	175	5.113729	330	30	0.1347
	126	75	4.117278	300	30	0.0694
	142	275	5.651257	270	30	0.0686
	151	125	4.264668	240	30	0.2386
	162	75	3.601542	210	30	0.0115
	163	125	4.069282	210	30	0.023
	165	225	5.029958	210	30	0.0411
	167	325	5.664806	210	30	0.0302

B.5. VALIDATION RESULTS

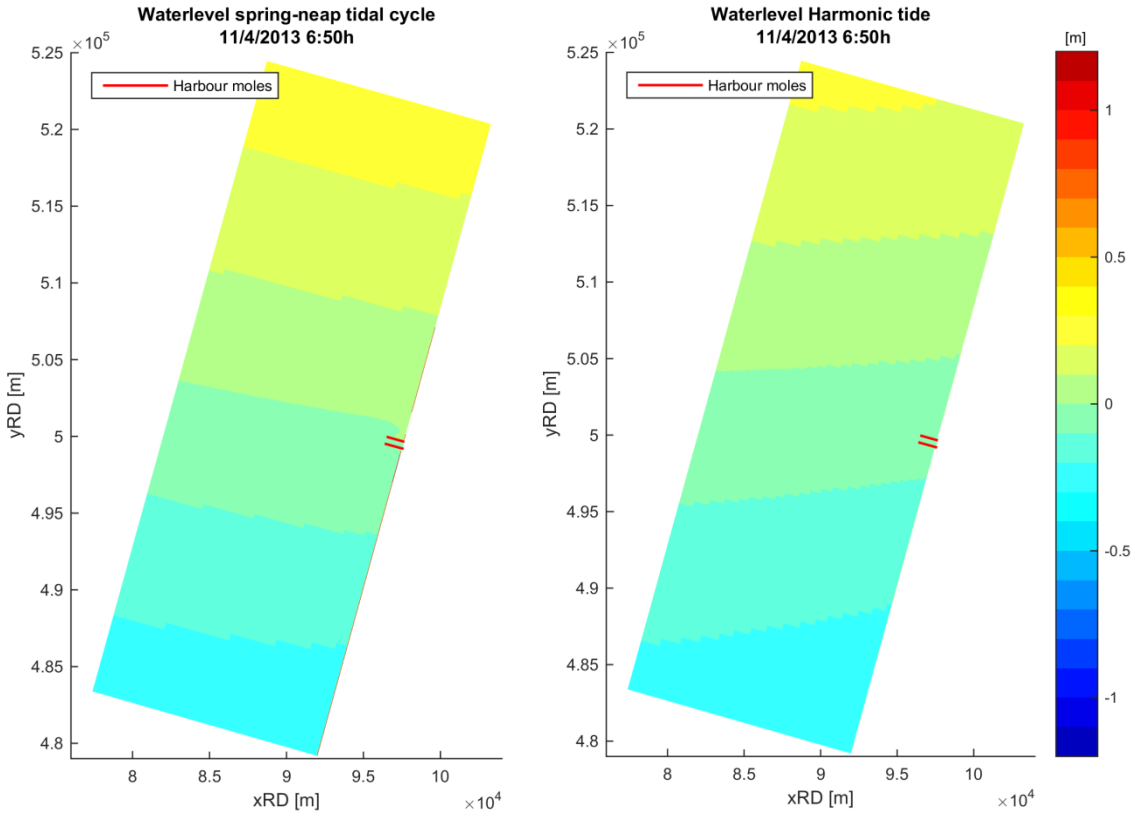

Figure 40 - Comparison water levels spring-neap tidal cycle simulation and harmonic morphological tide simulation

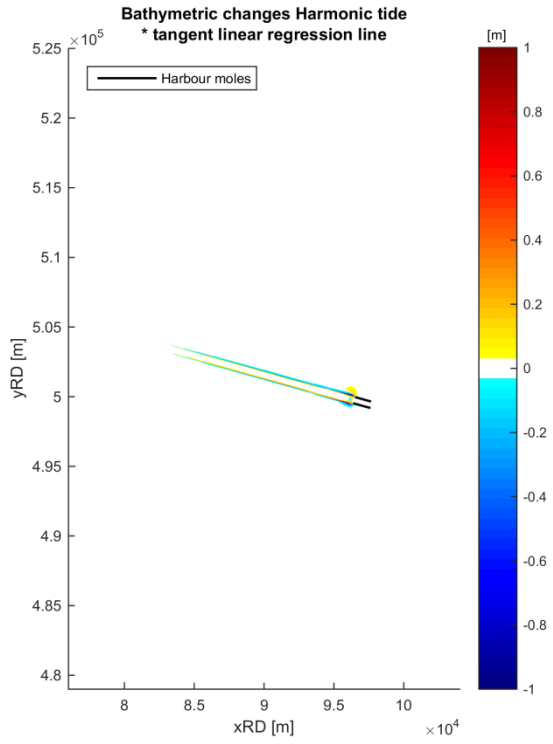

Figure 41 - Bathymetric changes for validation simulations

C. LONG-TERM MORPHOLOGICAL MODELLING

C.1. CROSS SECTION RESULTS FOR DIFFERENT ACCELERATION FACTORS

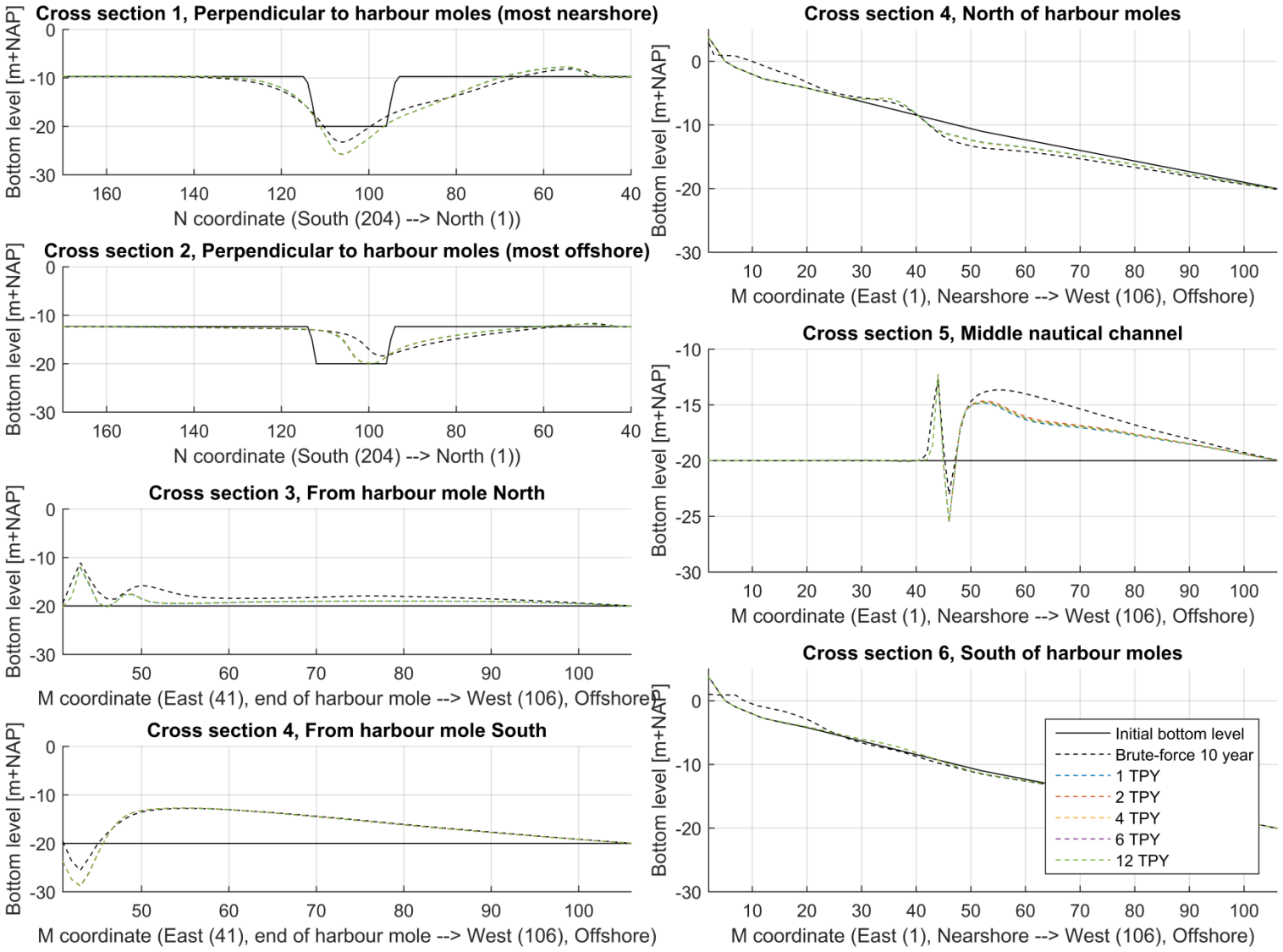

Figure 42 - Cross section results Tide only (no waves), all accelerations (TPY)

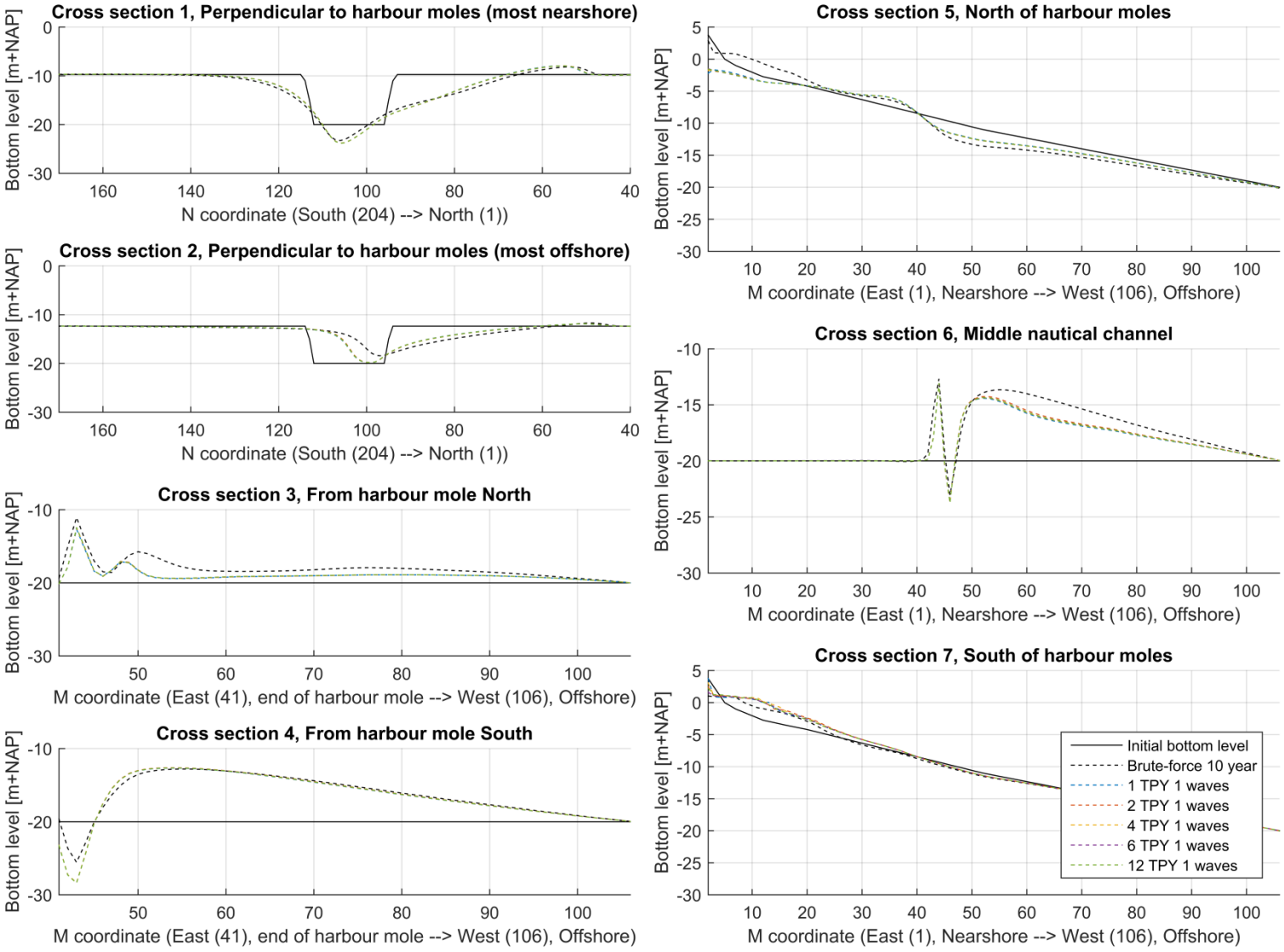

Figure 43 - Cross section results one wave class, all accelerations (TPY)

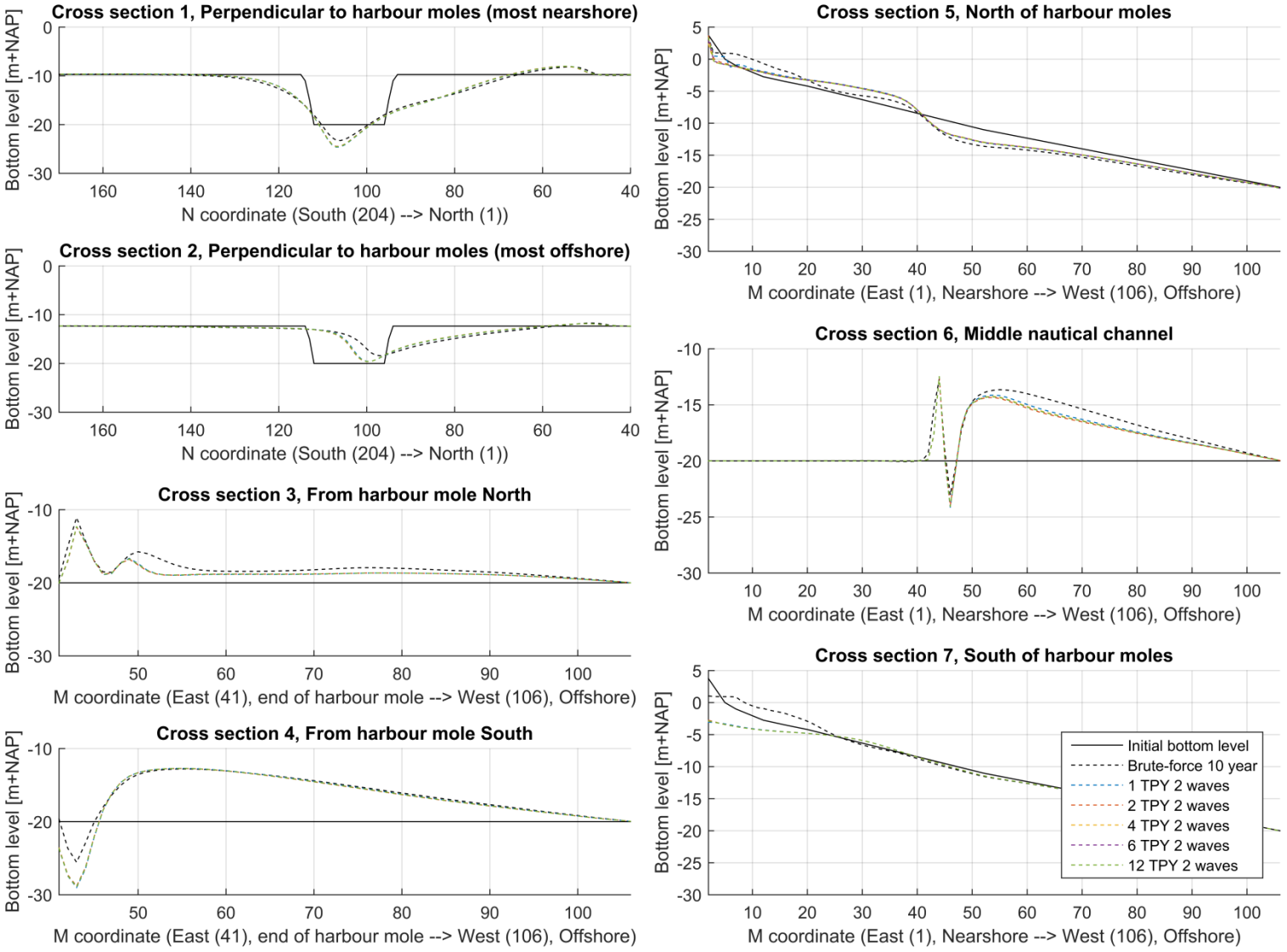

Figure 44 - Cross section results Morfac two wave classes, all accelerations (TPY)

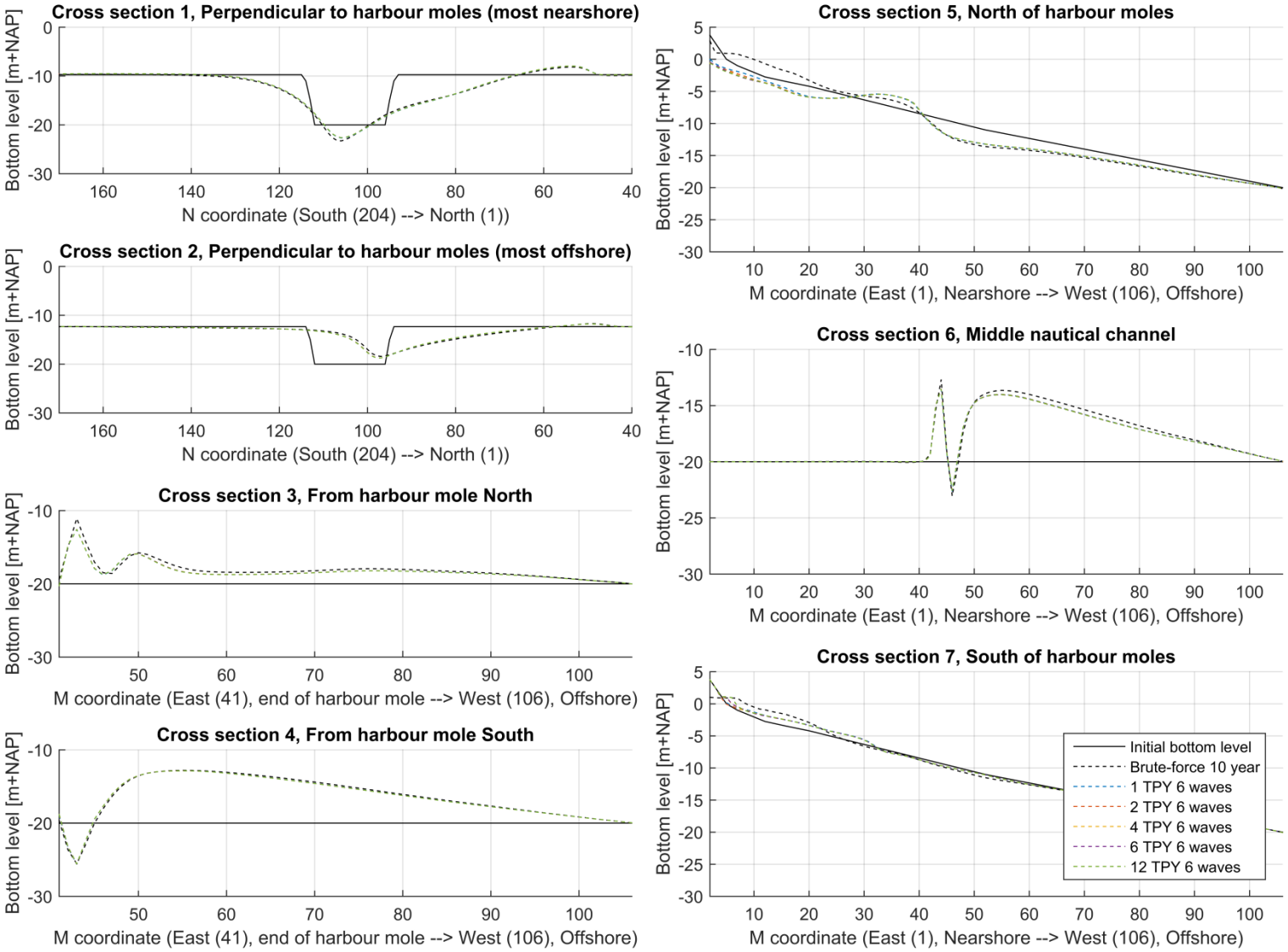

Figure 45 - Cross section results Morfac six wave classes, all accelerations (TPY)

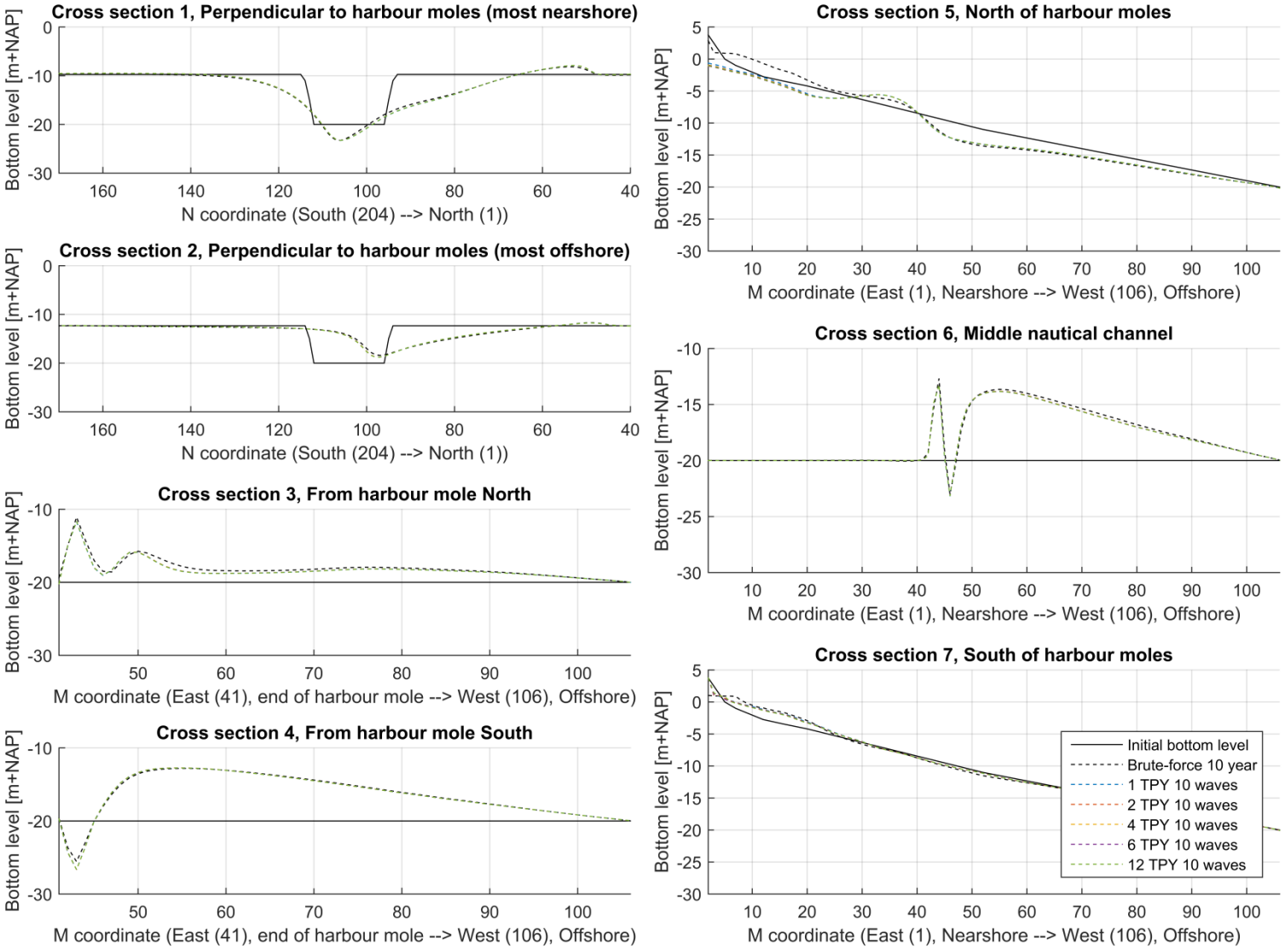

Figure 46 - Cross section results Morfac ten wave classes, all accelerations (TPY)

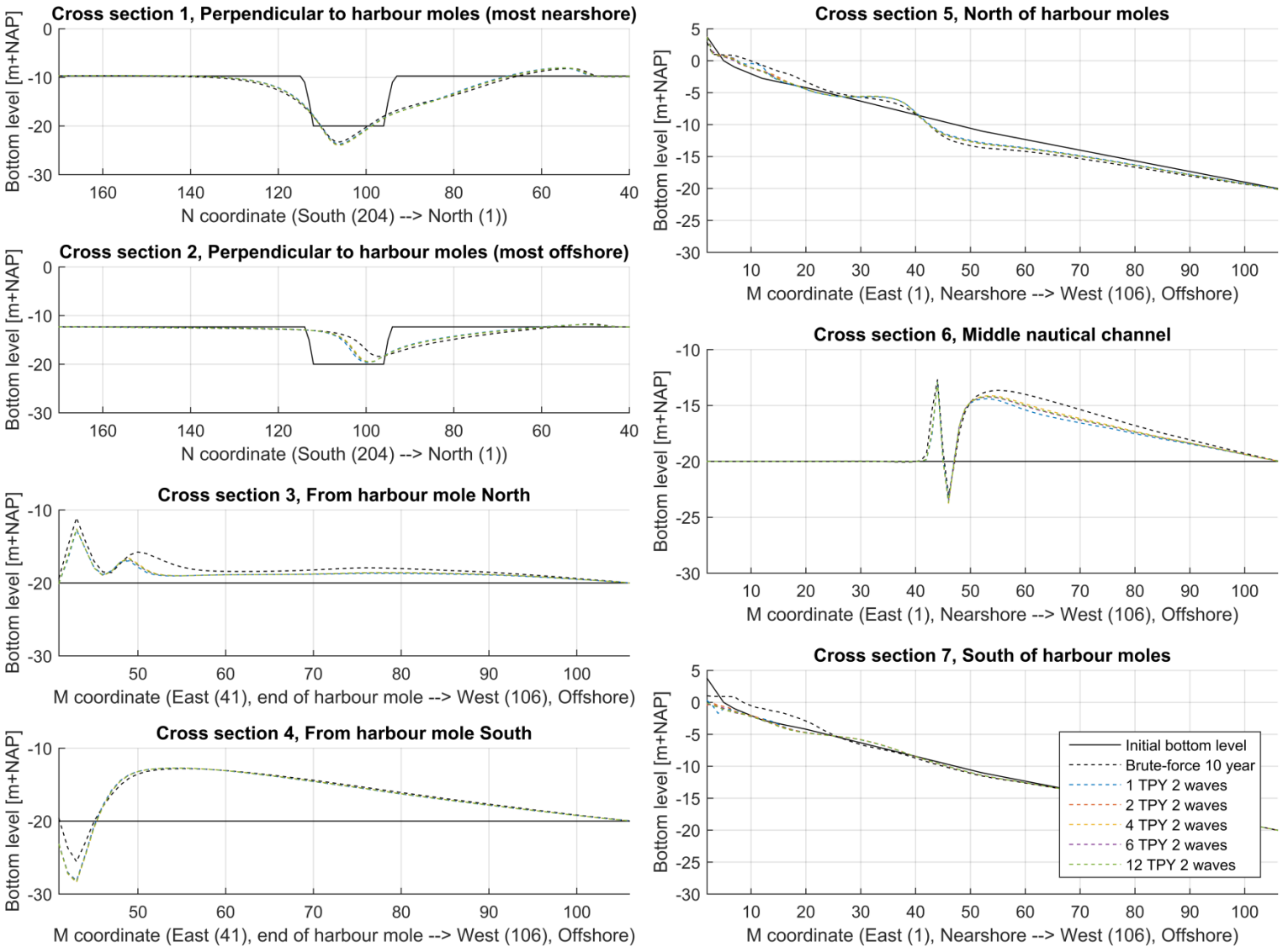

Figure 47 - Cross section results Mormerge two wave classes, all accelerations (TPY)

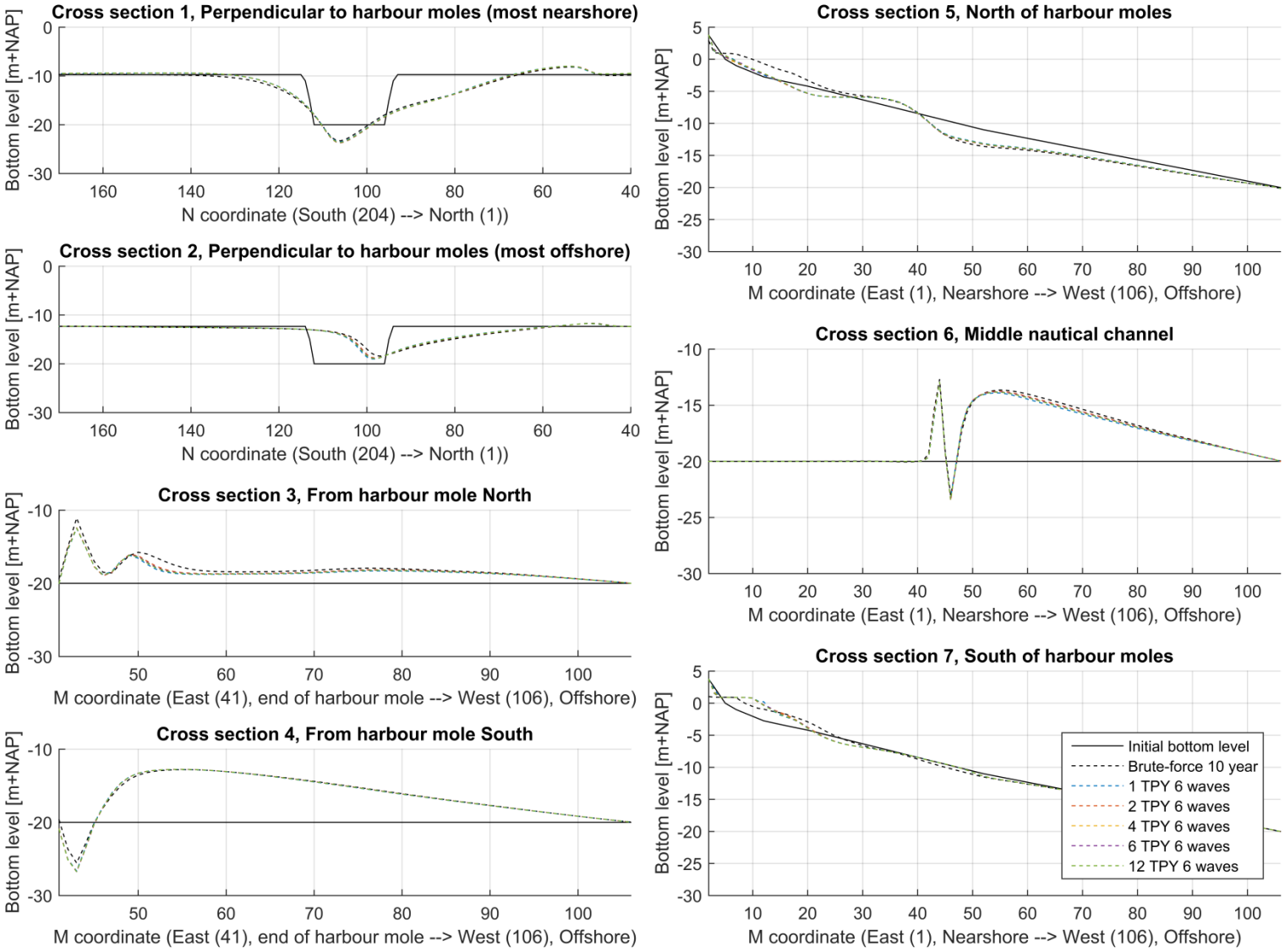

Figure 48 - Cross section results Mormerge six wave classes, all accelerations (TPY)

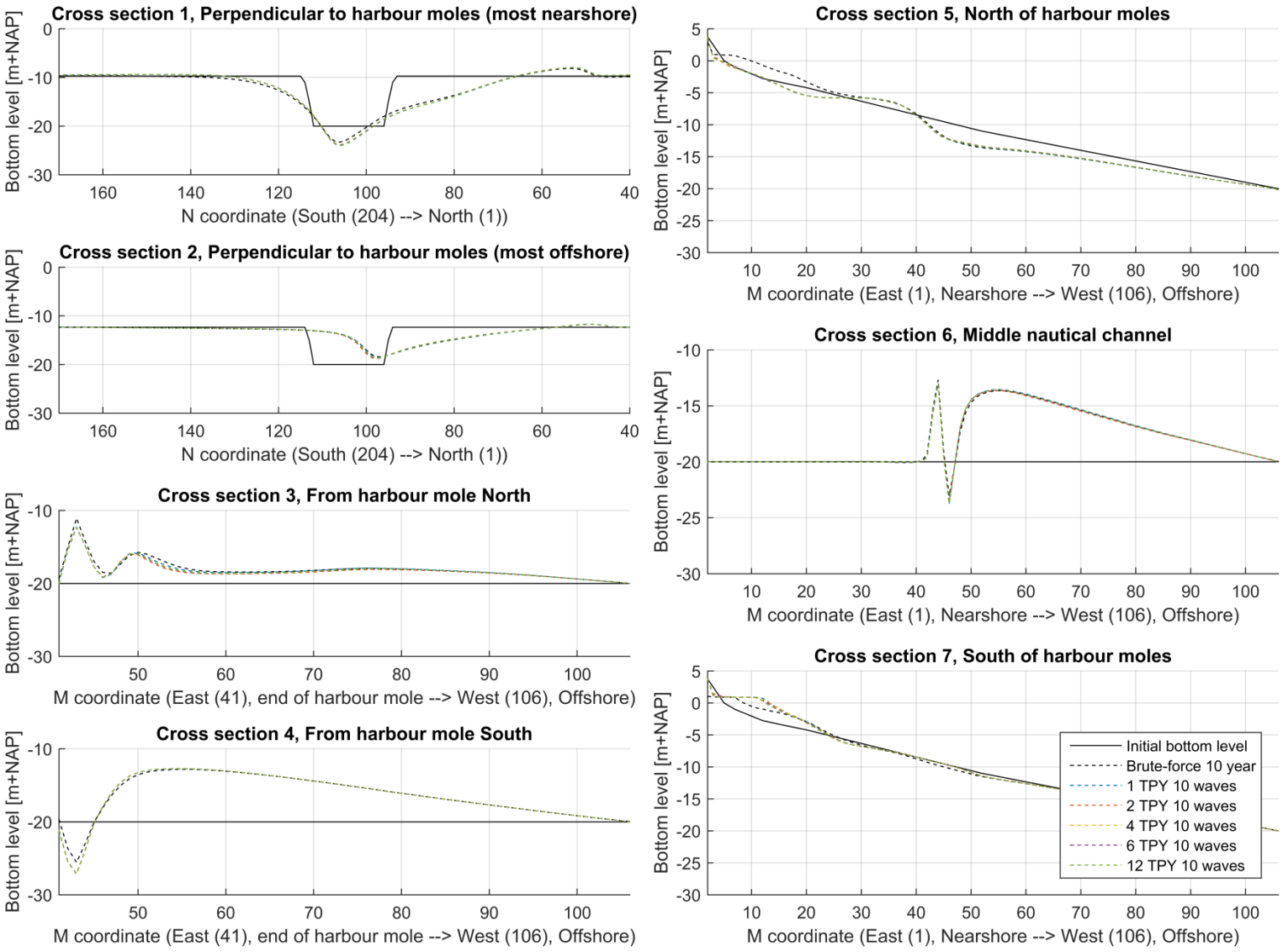

Figure 49 - Cross section results Mormerge ten wave classes, all accelerations (TPY)

C.2. CROSS SECTION RESULTS FOR INCLUSION OF DIFFERENT WAVE CLASSES

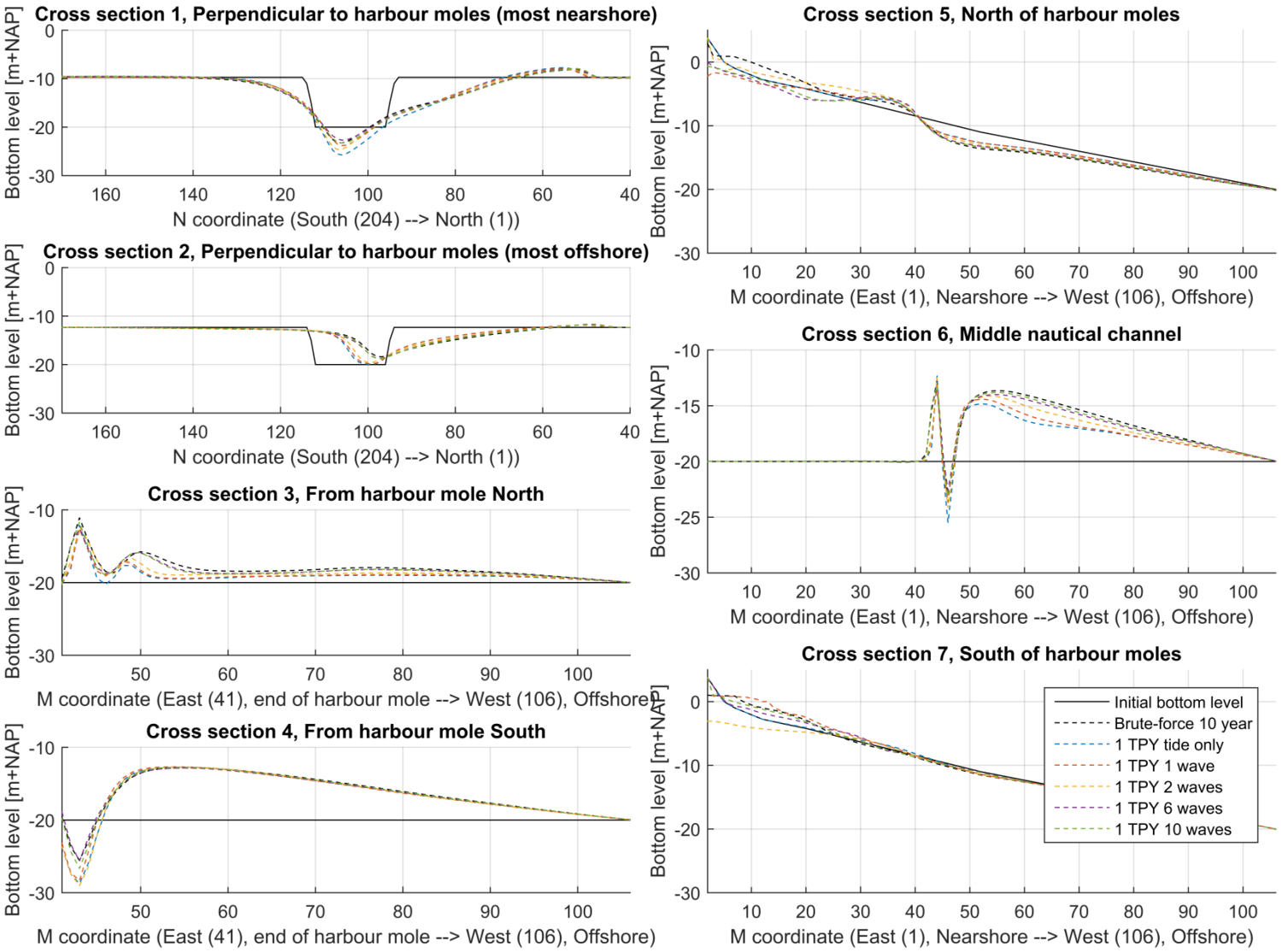

Figure 50 - Cross section results Morfac 1 TPY, all waves

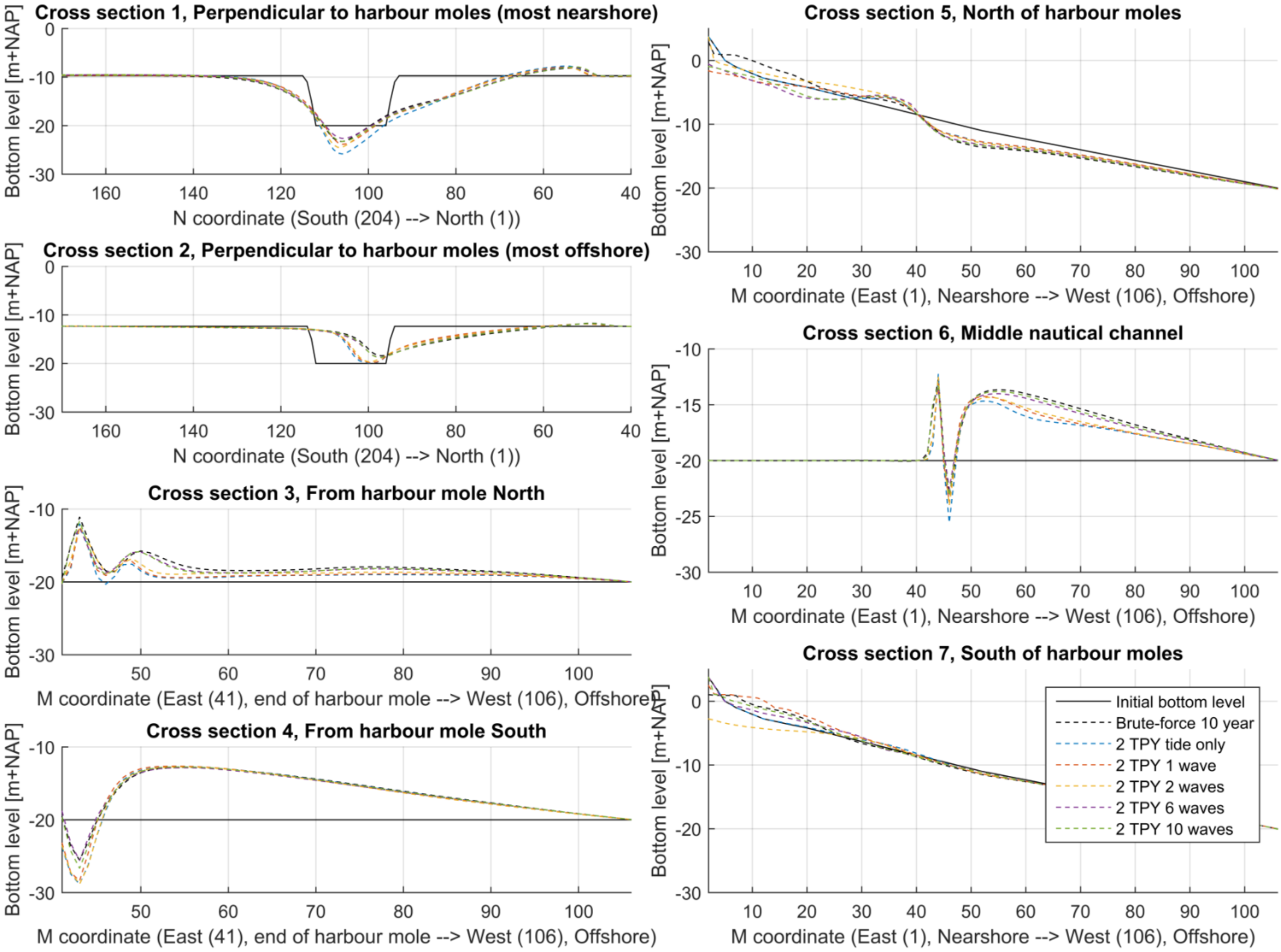

Figure 51 - Cross section results Morfac 2 TPY, all waves

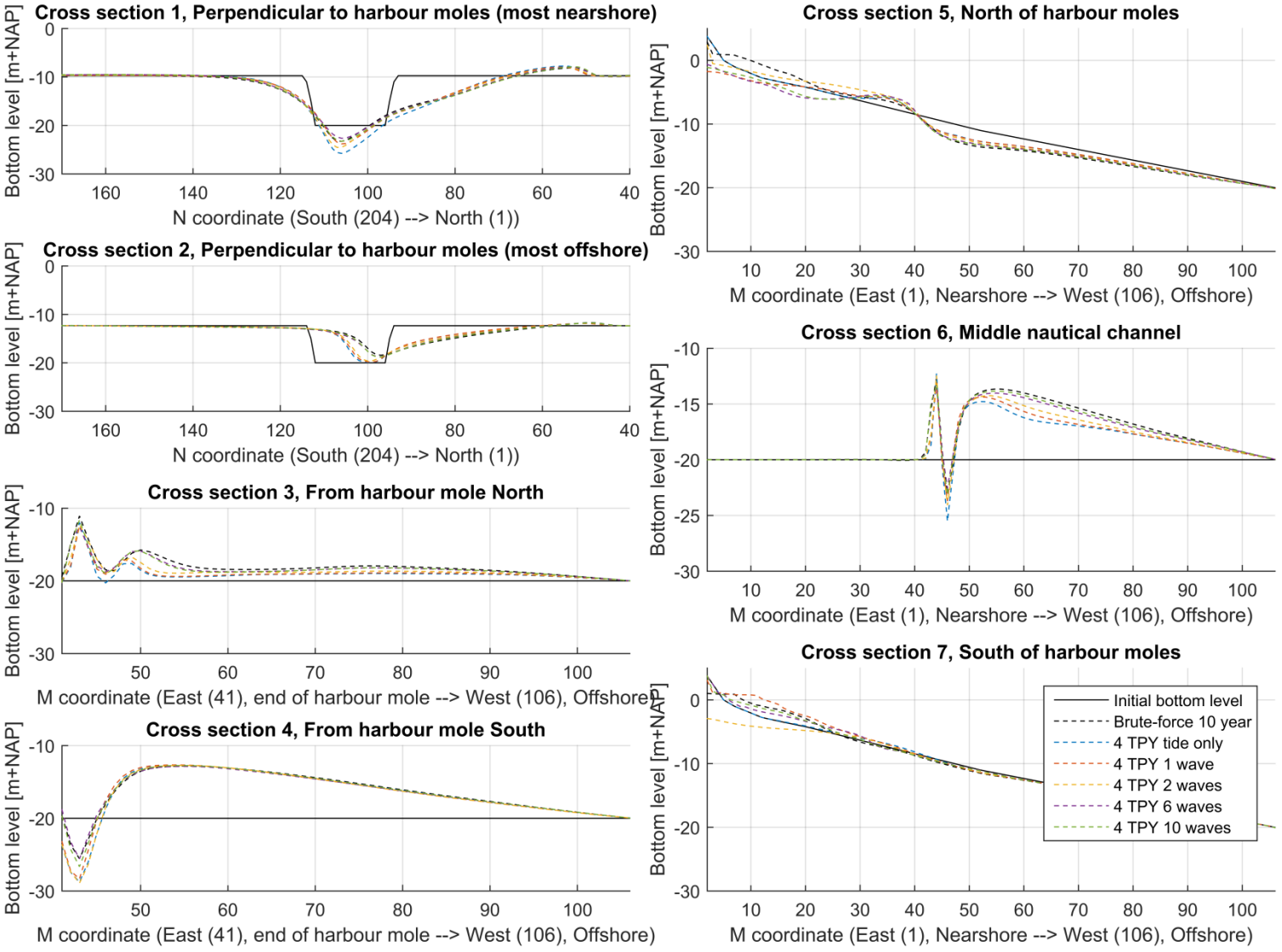

Figure 52 - Cross section results Morfac 4 TPY, all waves

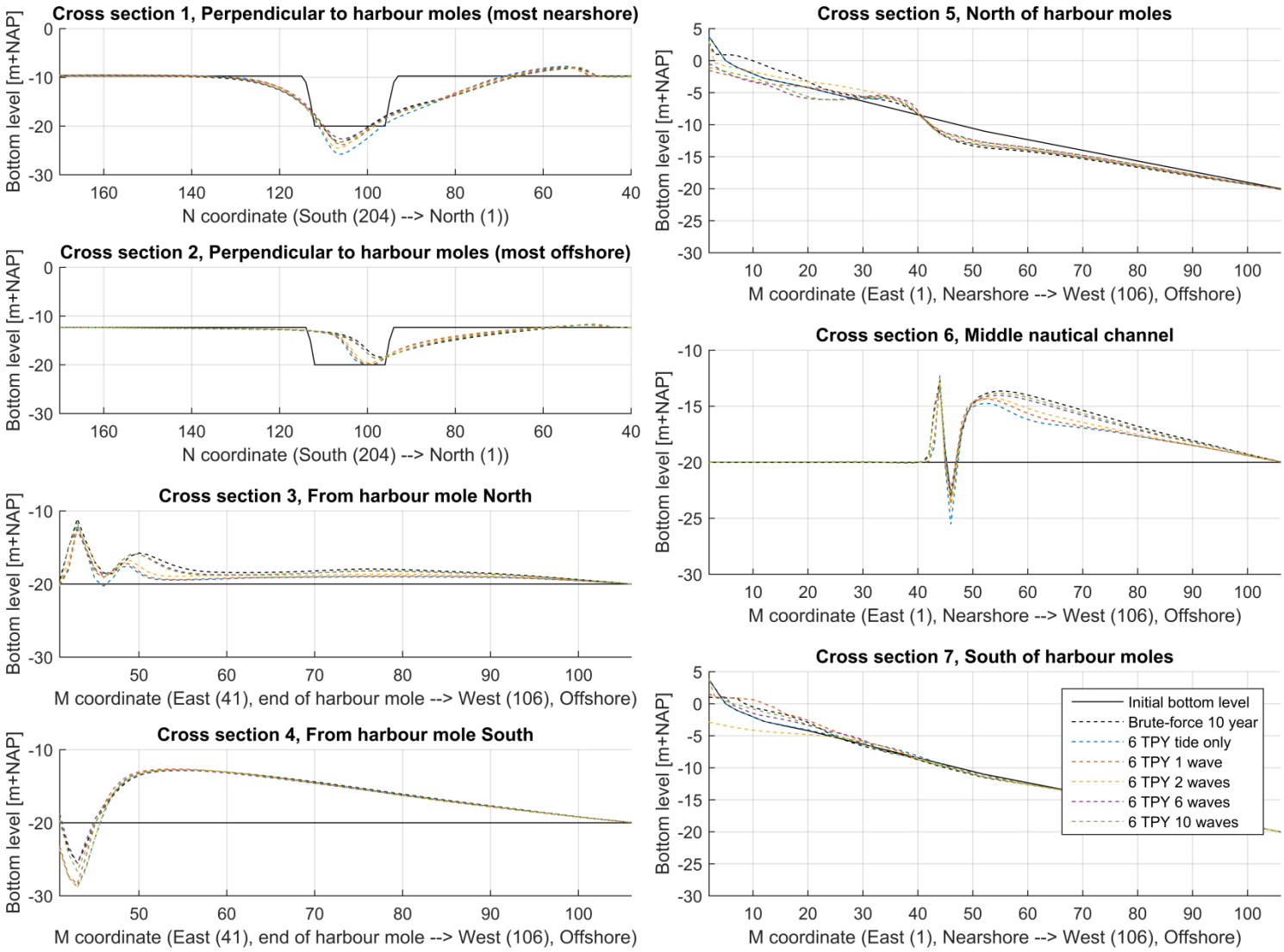

Figure 53 - Cross section results Morfac 6 TPY, all waves

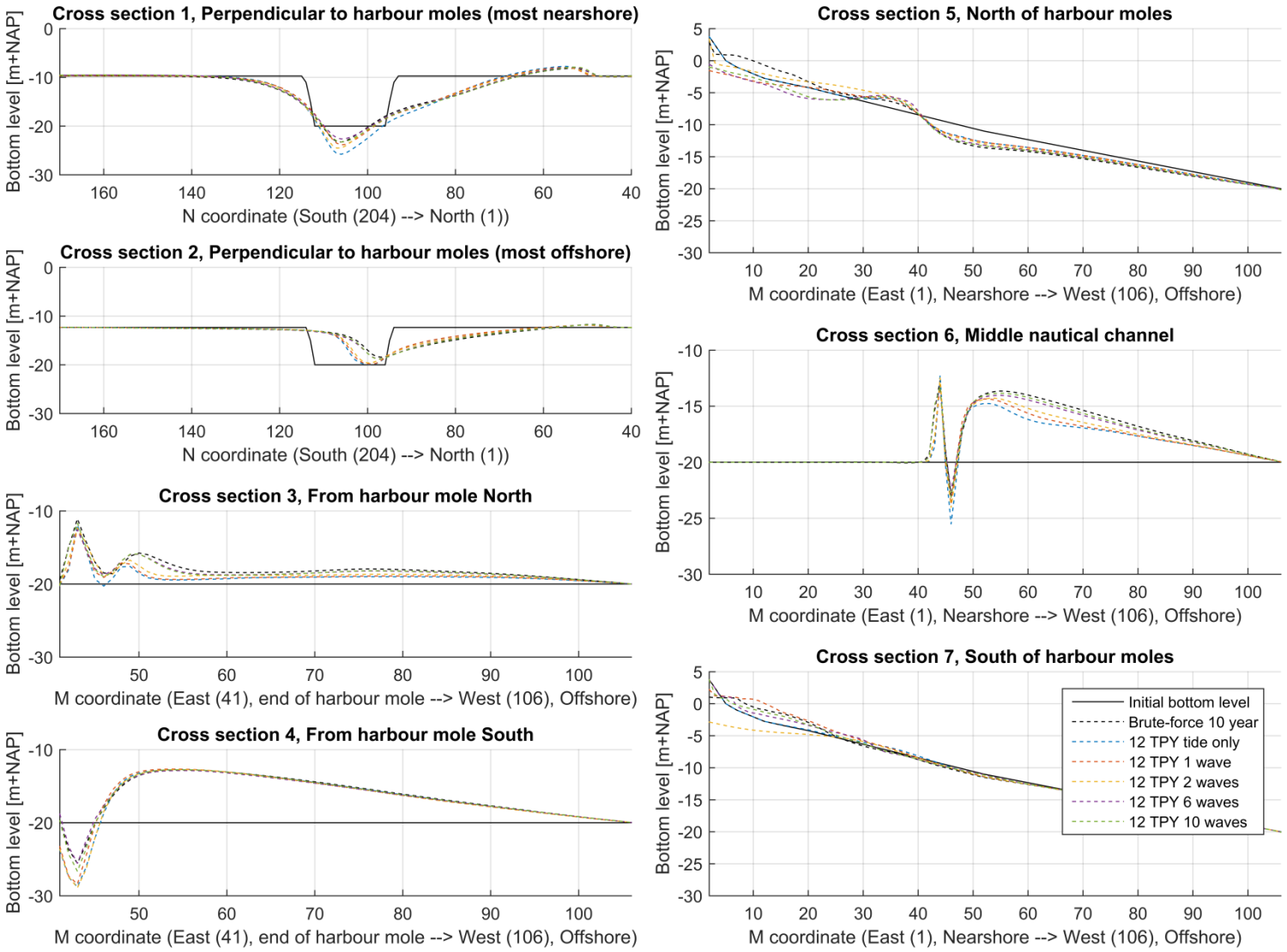

Figure 54 - Cross section results Morfac 12 TPY, all waves

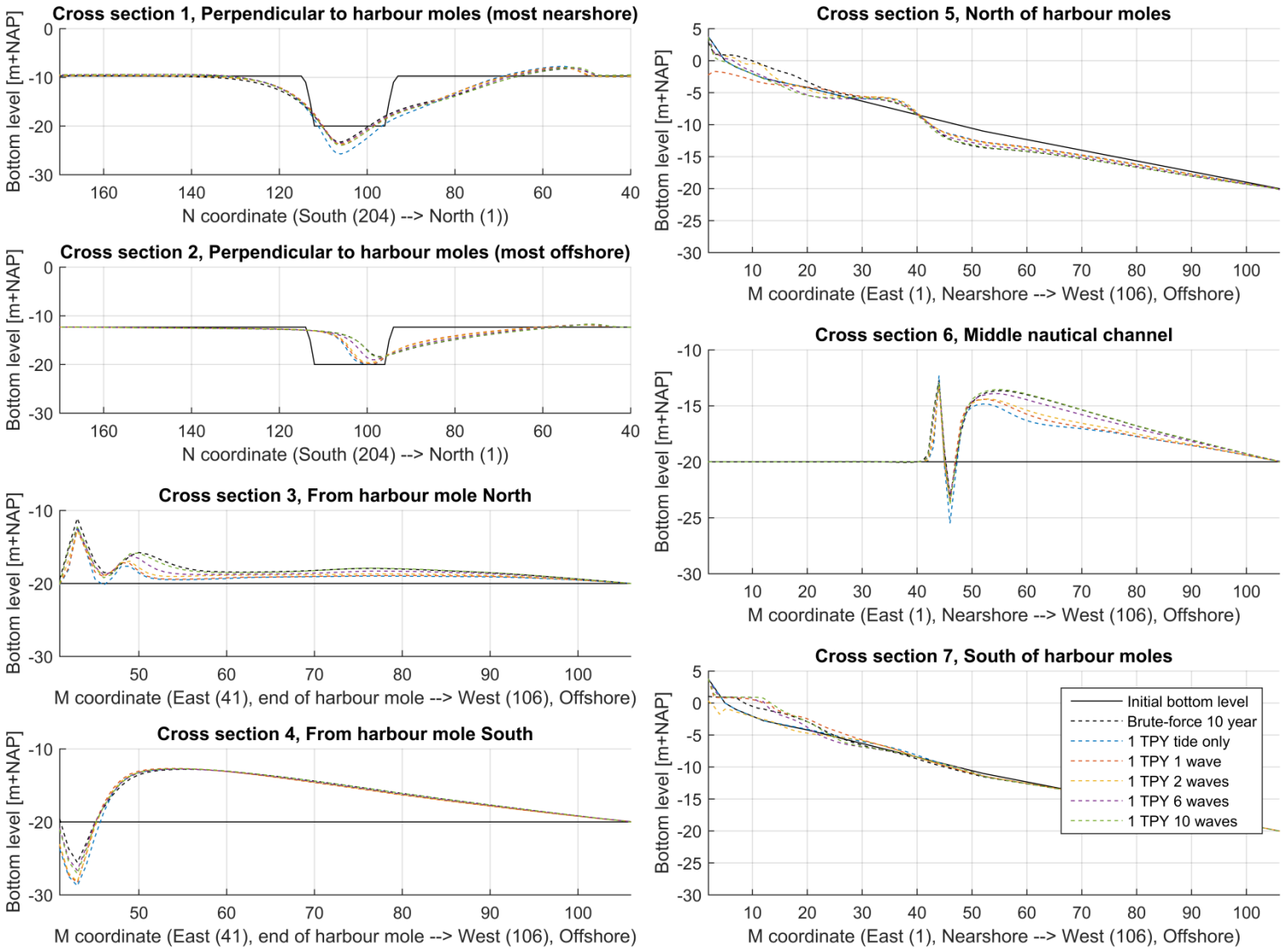

Figure 55 - Cross section results Mormerge 1 TPY, all waves

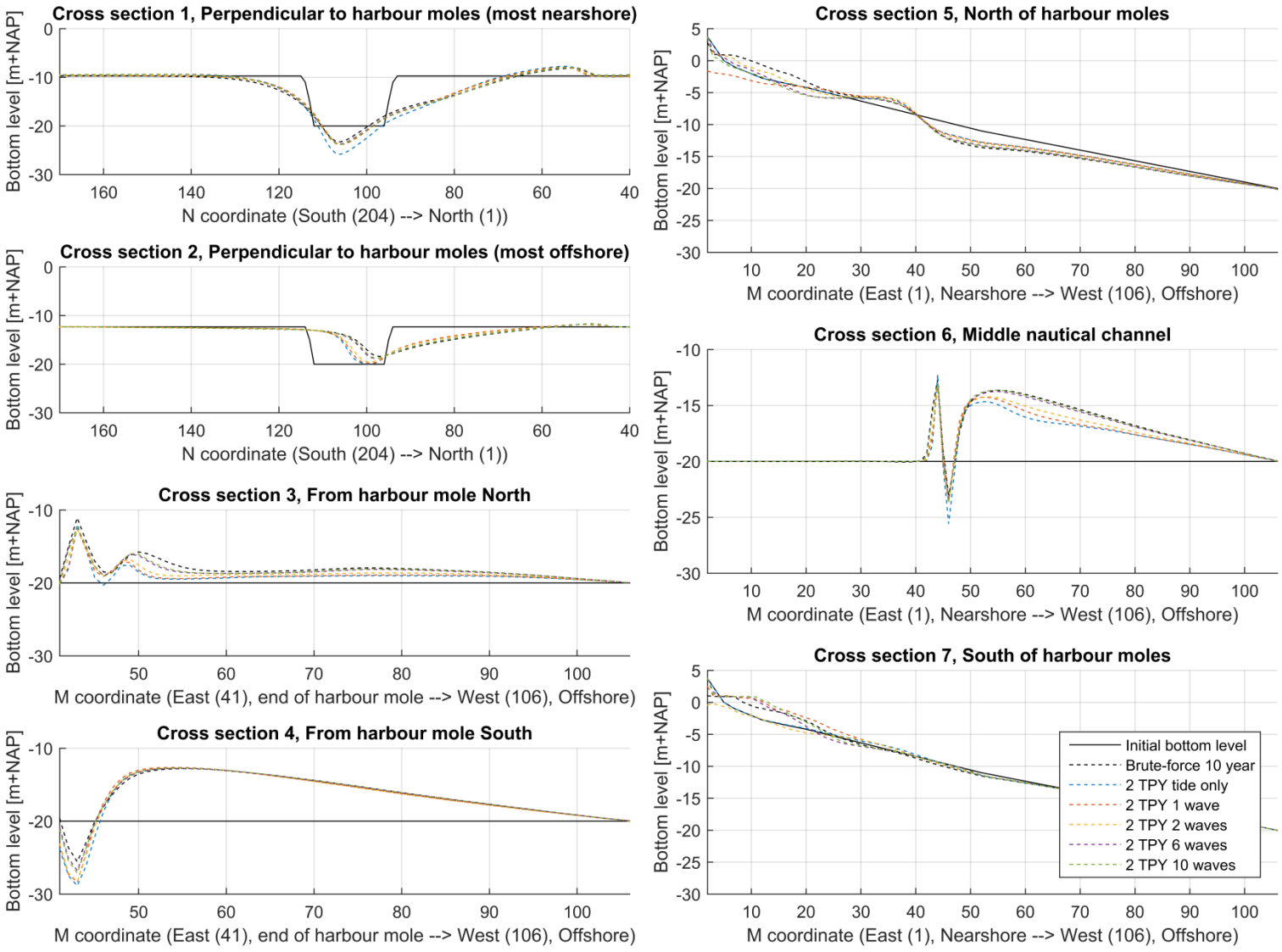

Figure 56 - Cross section results Mormerge 2 TPY, all waves

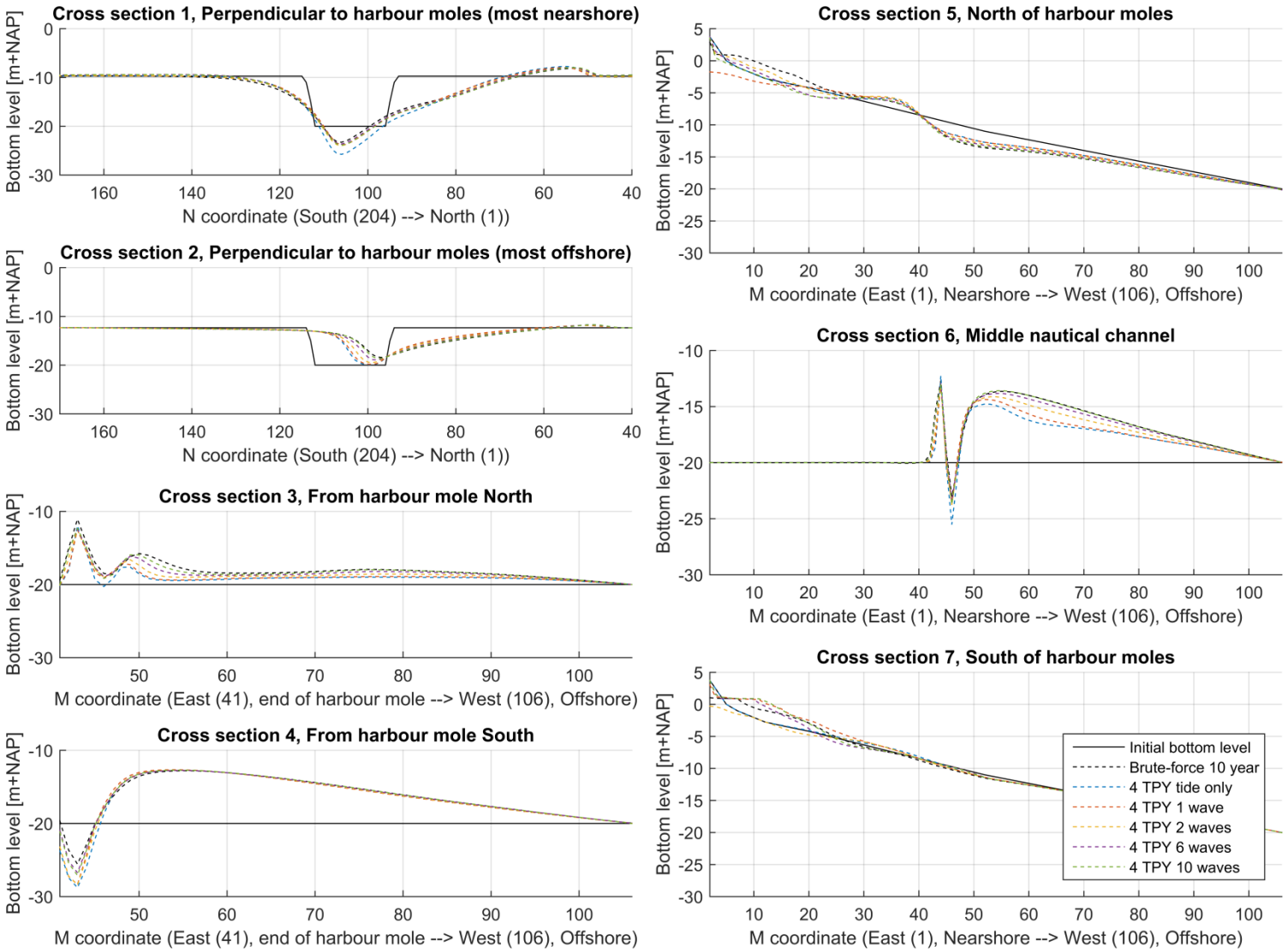

Figure 57 - Cross section results Mormerge 4 TPY, all waves

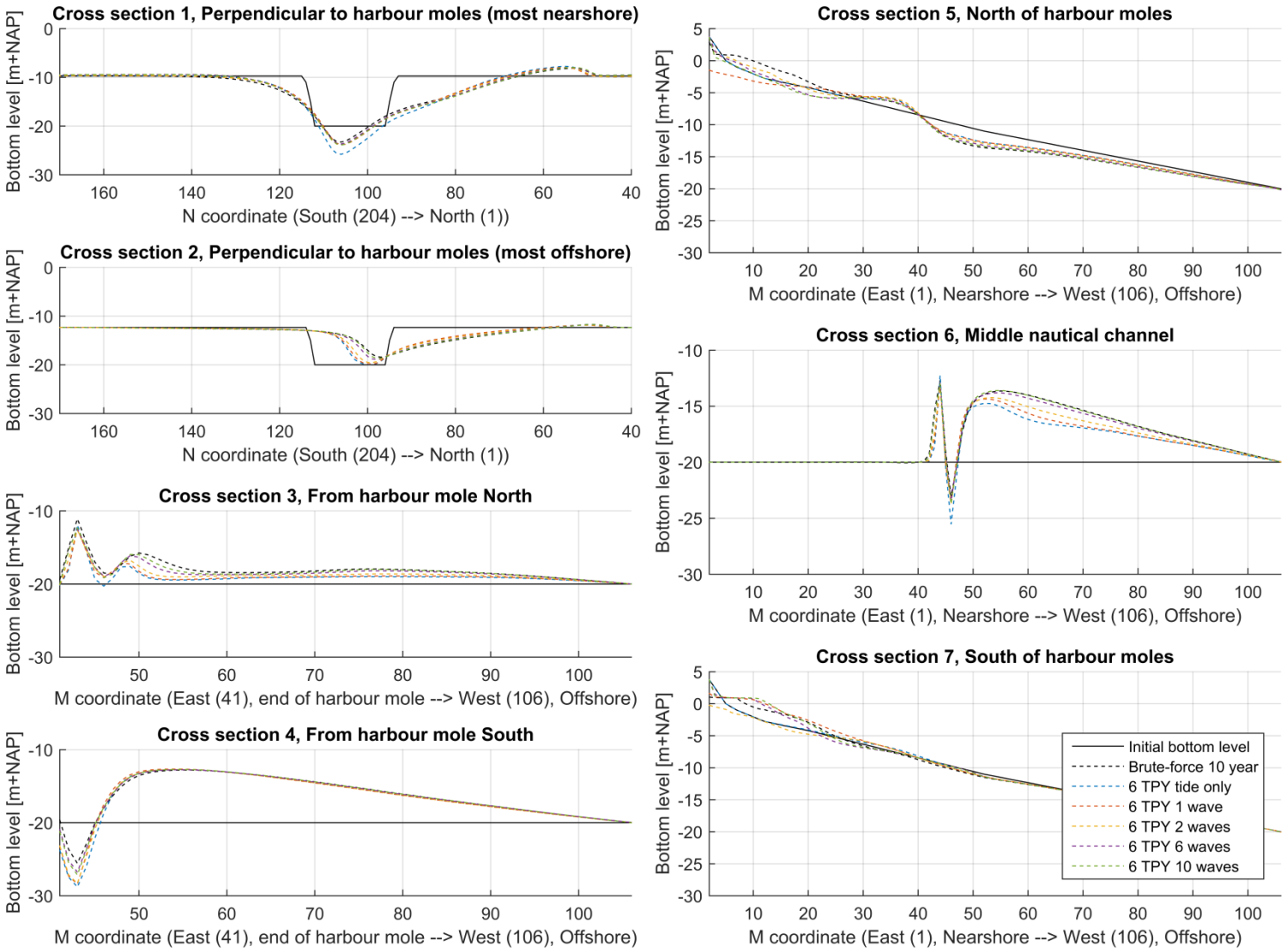

Figure 58 - Cross section results Mormerge 6 TPY, all waves

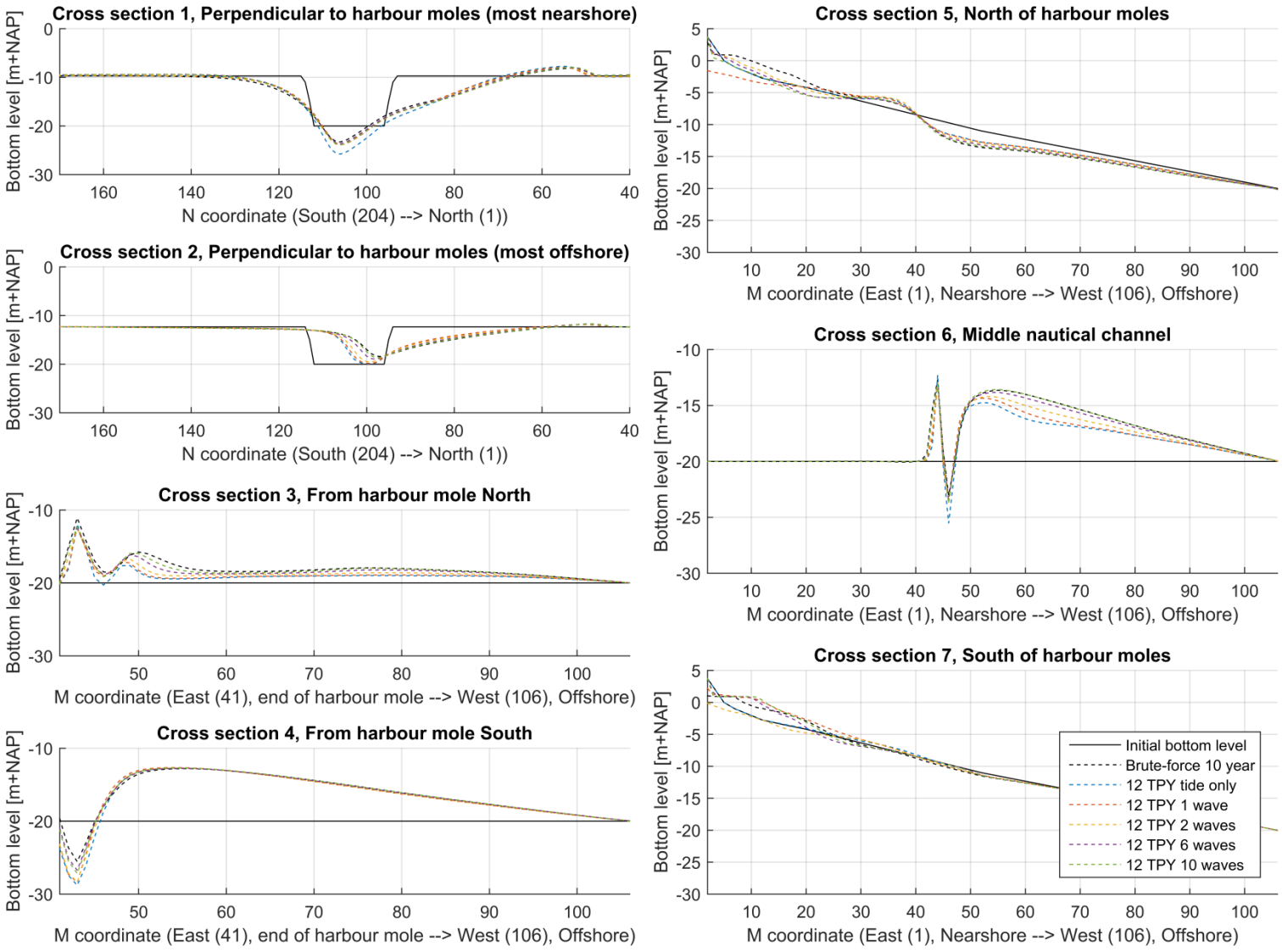

Figure 59 - Cross section results Mormerge 12 TPY, all waves

C.3. CUMULATIVE SEDIMENTATION AND EROSION MAPS

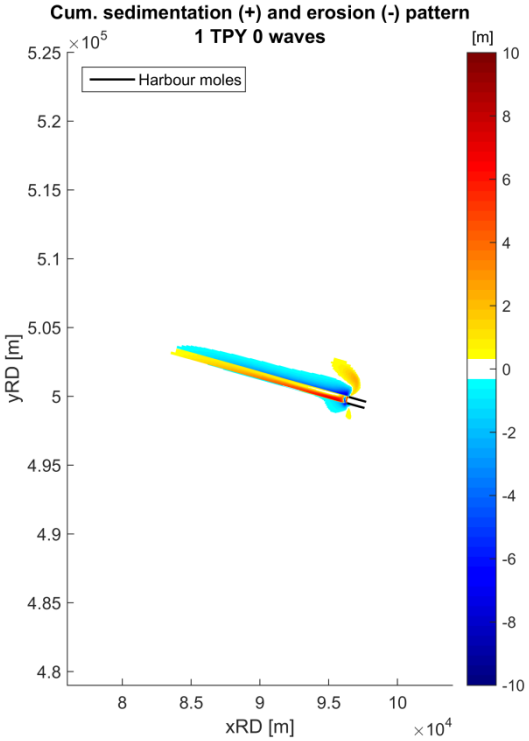

Figure 60 - Cumulative sedimentation (+) and erosion (-) pattern, 1 TPY 0 waves (tide only)

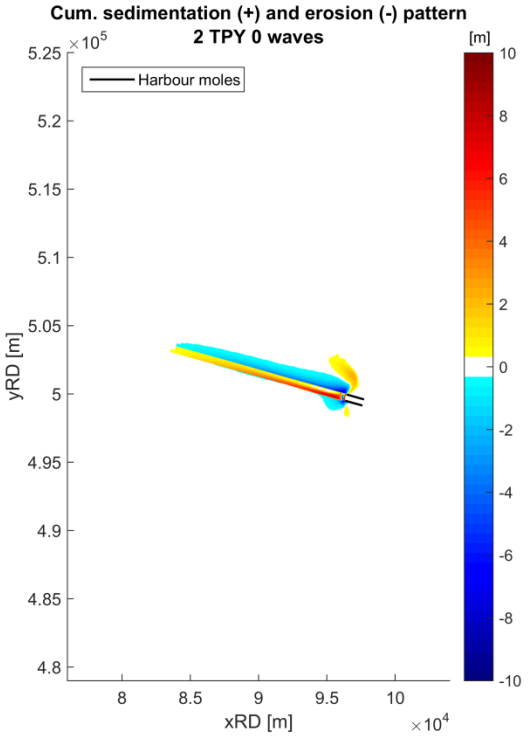

Figure 61 - Cumulative sedimentation (+) and erosion (-) pattern, 2 TPY 0 waves (tide only)

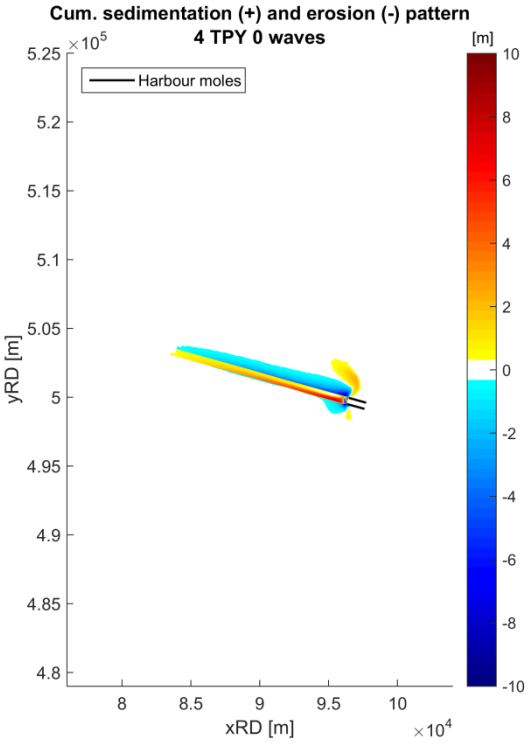

Figure 62 - Cumulative sedimentation (+) and erosion (-) pattern, 4 TPY 0 waves (tide only)

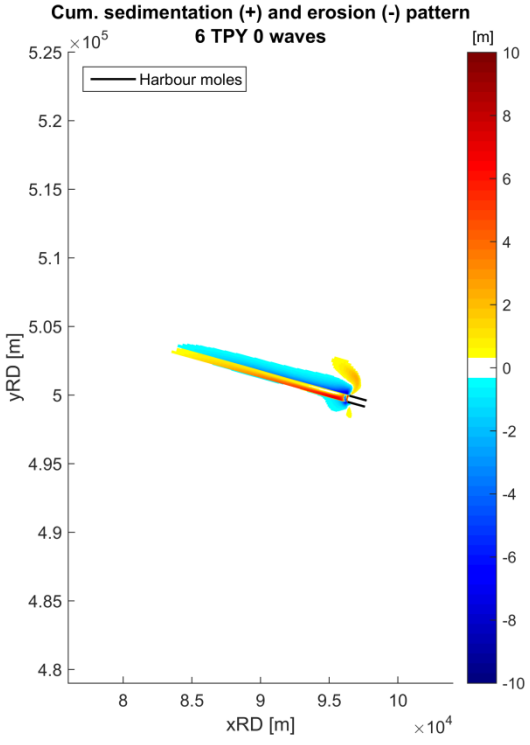

Figure 63 - Cumulative sedimentation (+) and erosion (-) pattern, 6 TPY 0 waves (tide only)

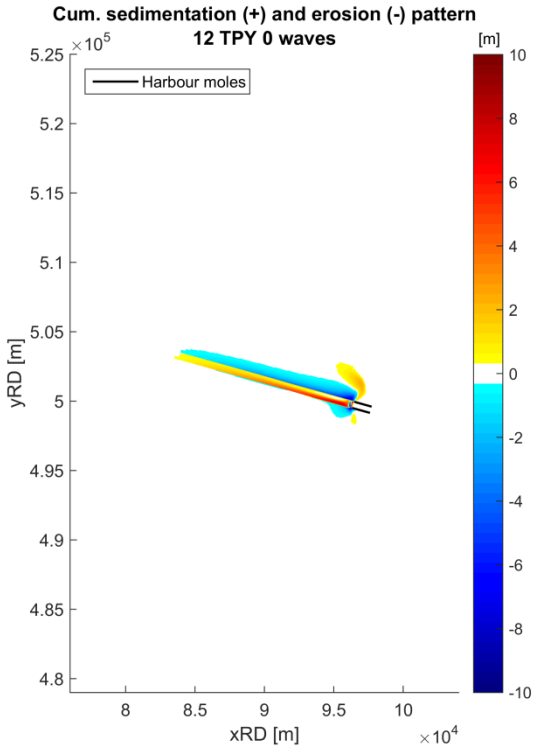

Figure 64 - Cumulative sedimentation (+) and erosion (-) pattern, 12 TPY 0 waves (tide only)

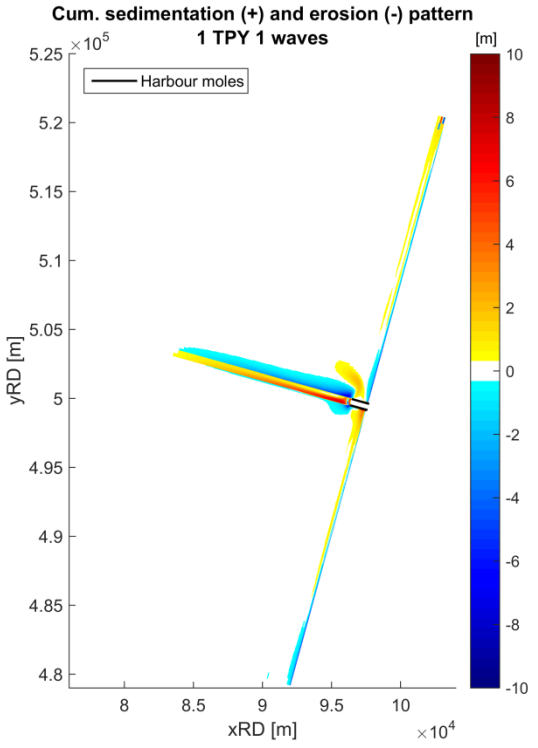

Figure 65 - Cumulative sedimentation (+) and erosion (-) pattern, 1 TPY 1 wave

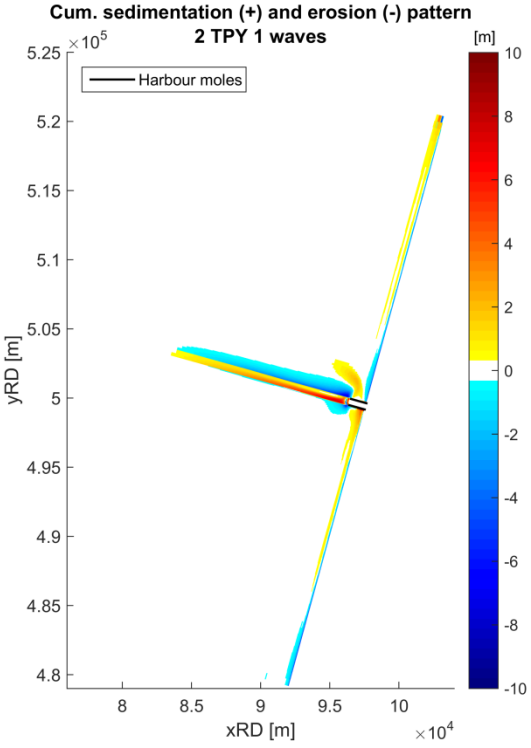

Figure 66 - Cumulative sedimentation (+) and erosion (-) pattern, 2 TPY 1 wave

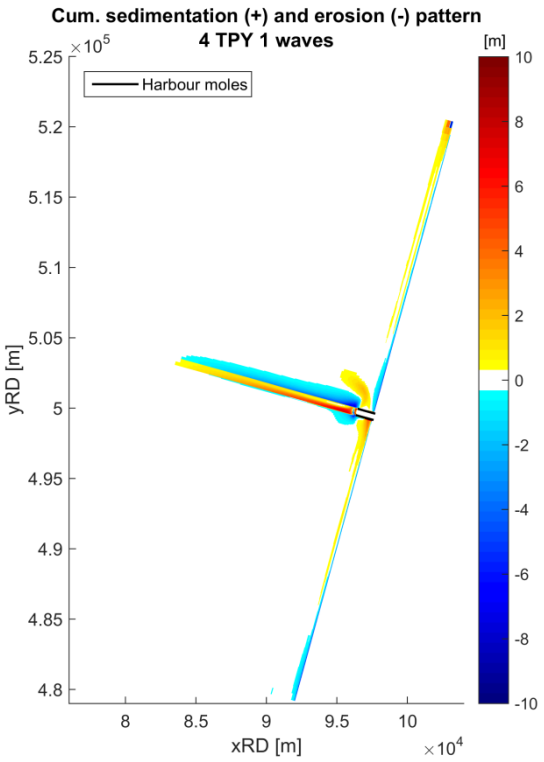

Figure 67 - Cumulative sedimentation (+) and erosion (-) pattern, 4 TPY 1 wave

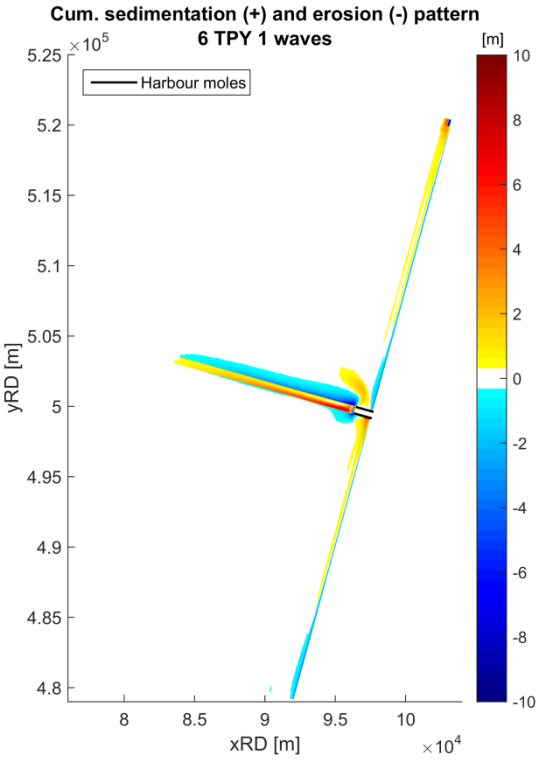

Figure 68 - Cumulative sedimentation (+) and erosion (-) pattern, 6 TPY 1 wave

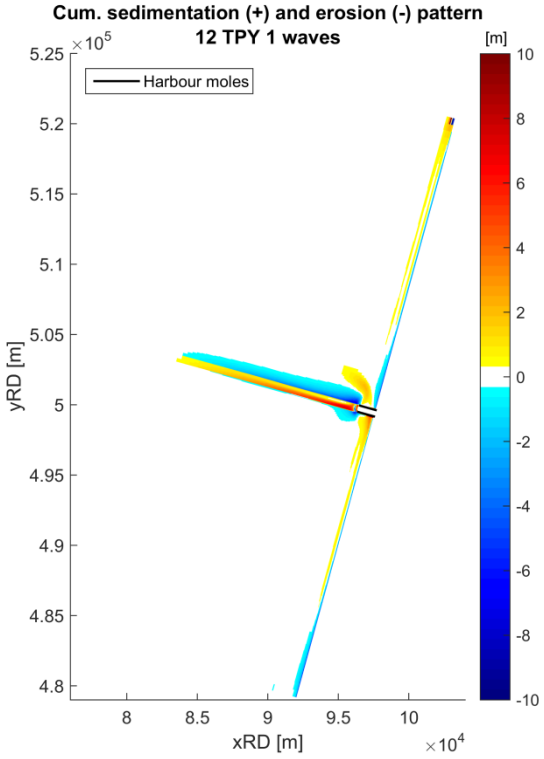

Figure 69 - Cumulative sedimentation (+) and erosion (-) pattern, 12 TPY 1 wave

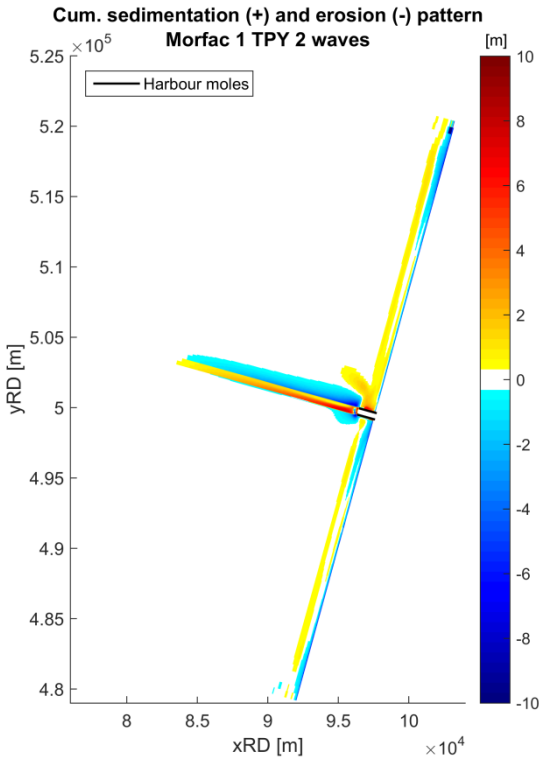

Figure 70 - Cumulative sedimentation (+) and erosion (-) pattern, Morfac 1 TPY 2 waves

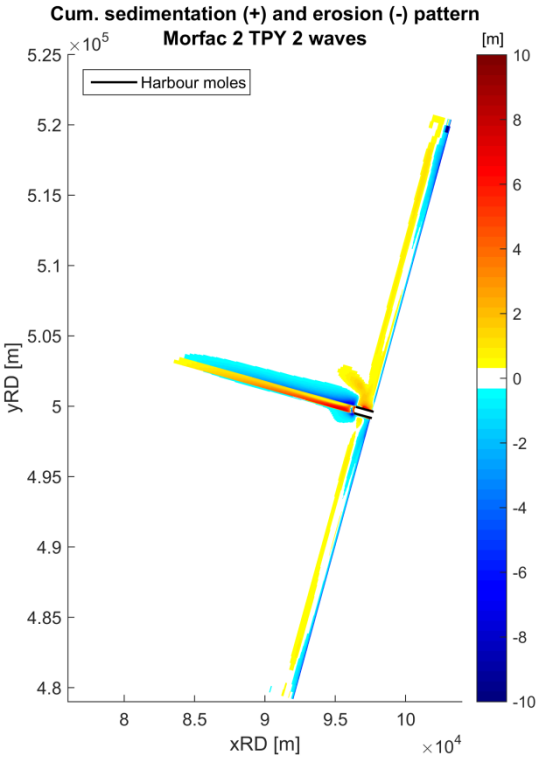

Figure 71 - Cumulative sedimentation (+) and erosion (-) pattern, Morfac 2 TPY 2 waves

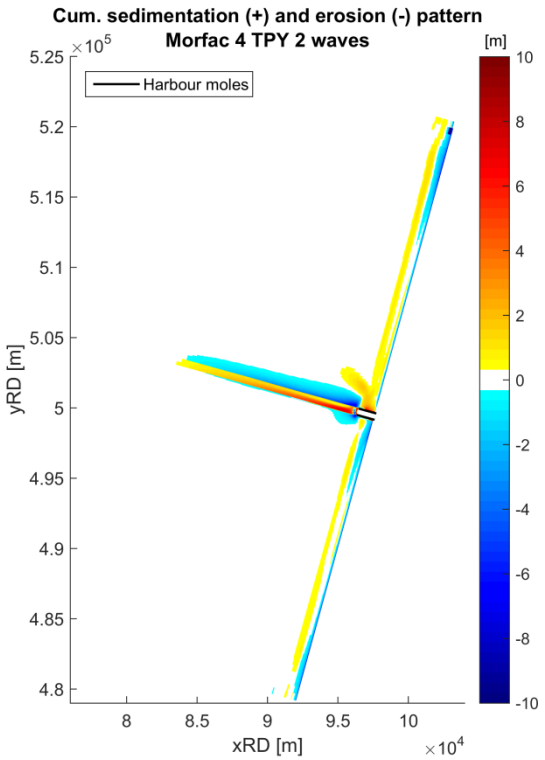

Figure 72 - Cumulative sedimentation (+) and erosion (-) pattern, Morfac 4 TPY 2 waves

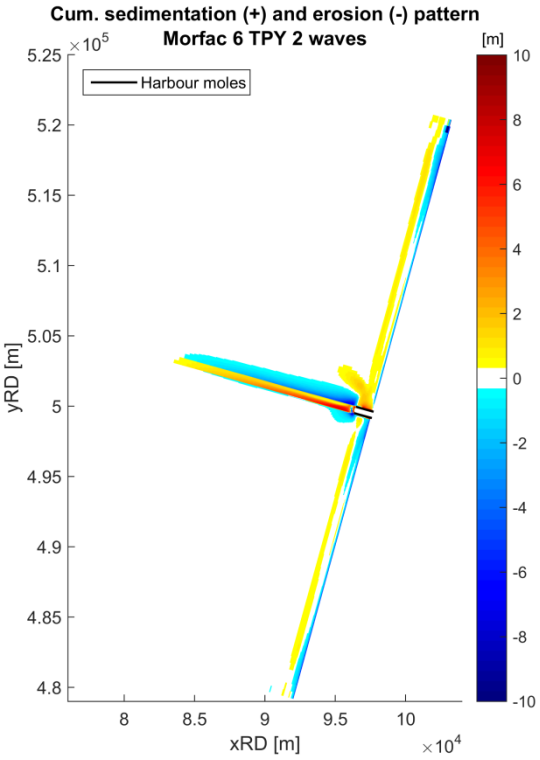

Figure 73 - Cumulative sedimentation (+) and erosion (-) pattern, Morfac 6 TPY 2 waves

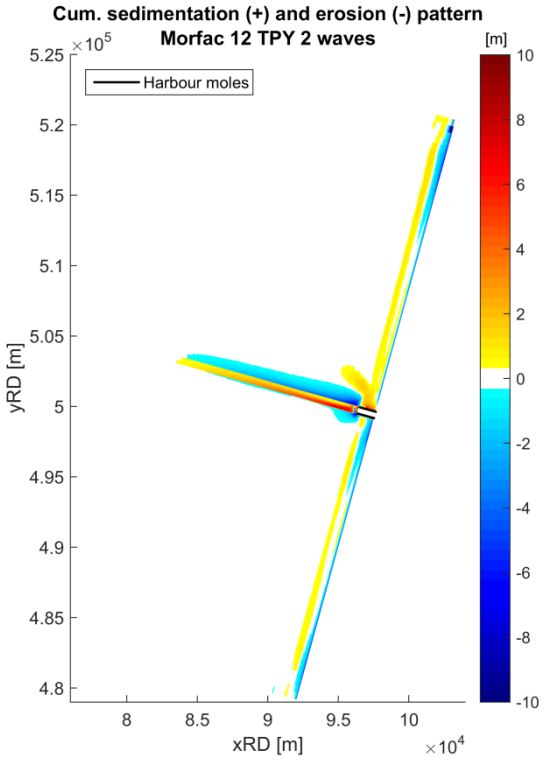

Figure 74 - Cumulative sedimentation (+) and erosion (-) pattern, Morfac 12 TPY 2 waves

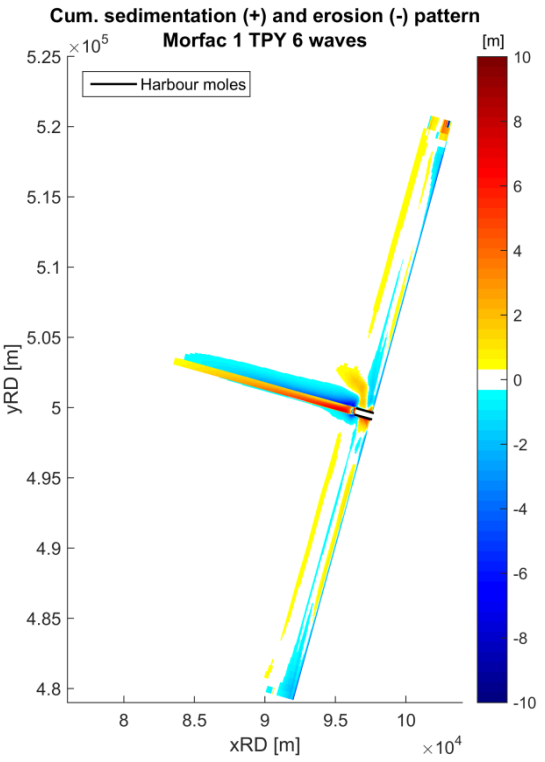

Figure 75 - Cumulative sedimentation (+) and erosion (-) pattern, Morfac 1 TPY 6 waves

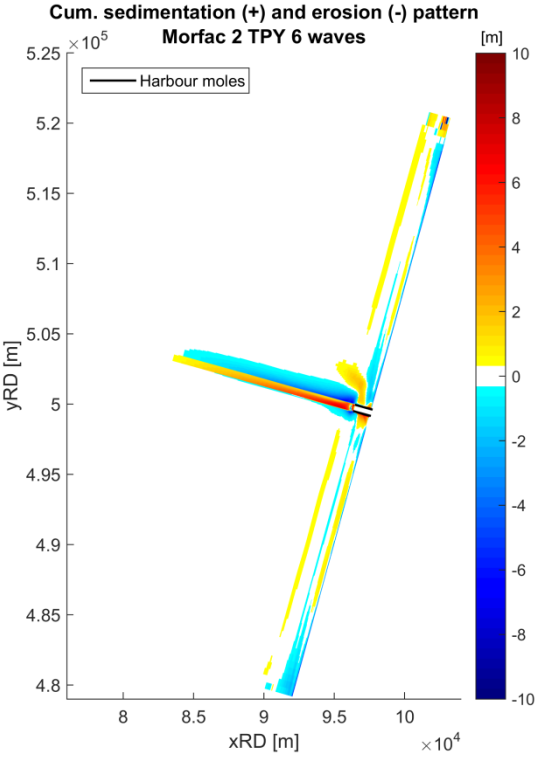

Figure 76 - Cumulative sedimentation (+) and erosion (-) pattern, Morfac 2 TPY 6 waves

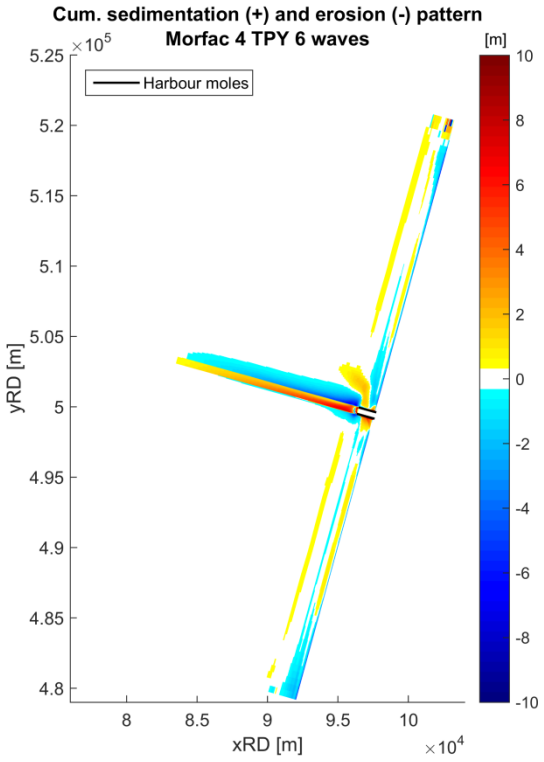

Figure 77 - Cumulative sedimentation (+) and erosion (-) pattern, Morfac 4 TPY 6 waves

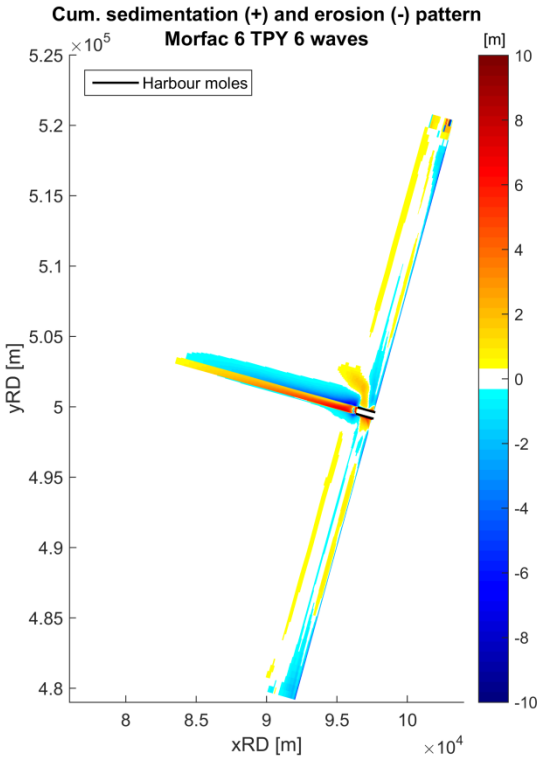

Figure 78 - Cumulative sedimentation (+) and erosion (-) pattern, Morfac 6 TPY 6 waves

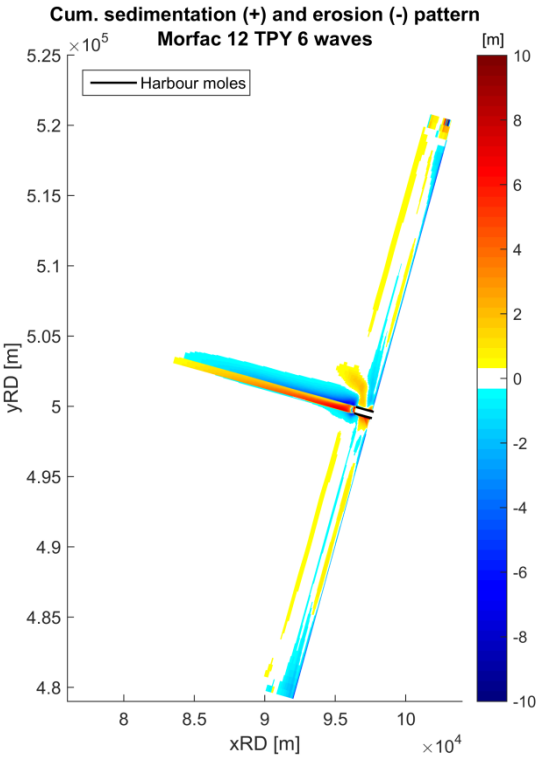

Figure 79 - Cumulative sedimentation (+) and erosion (-) pattern, Morfac 12 TPY 6 waves

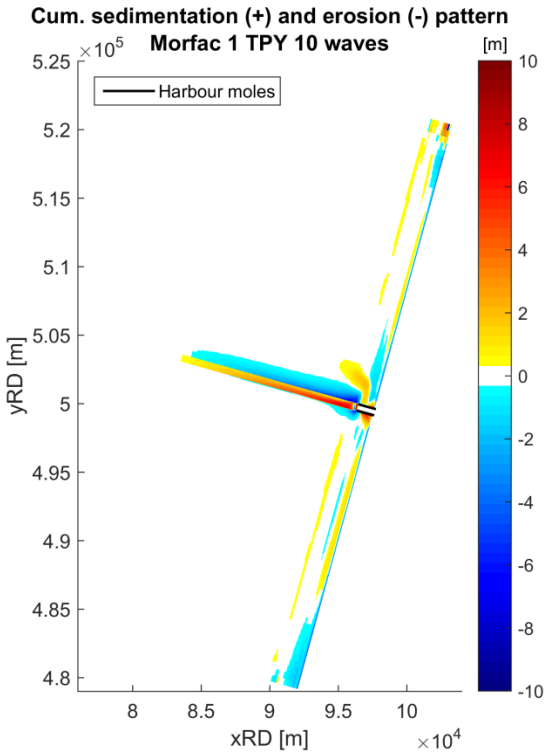

Figure 80 - Cumulative sedimentation (+) and erosion (-) pattern, Morfac 1 TPY 10 waves

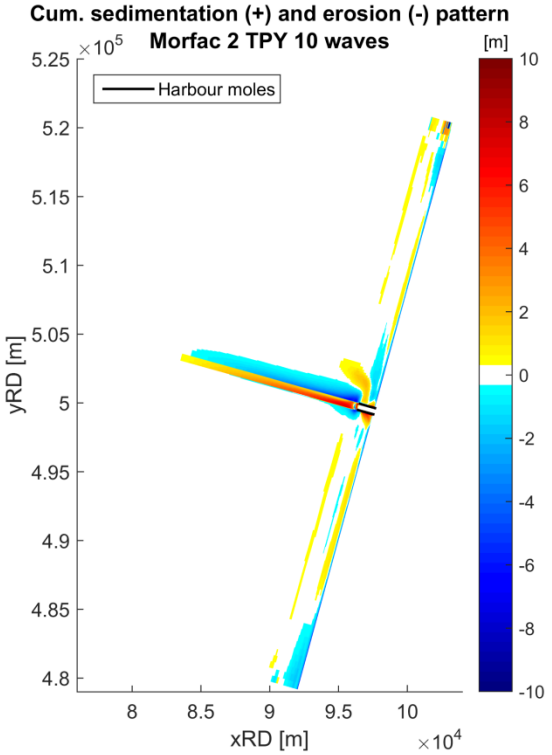

Figure 81 - Cumulative sedimentation (+) and erosion (-) pattern, Morfac 2 TPY 10 waves

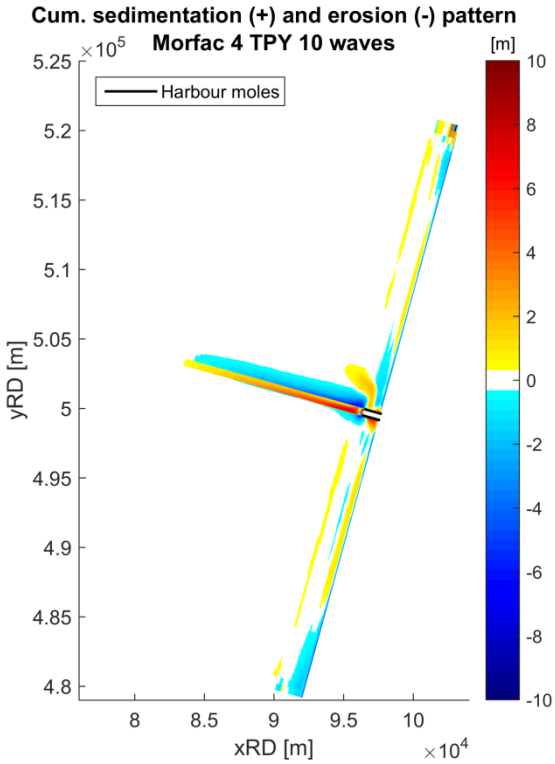

Figure 82 - Cumulative sedimentation (+) and erosion (-) pattern, Morfac 4 TPY 10 waves

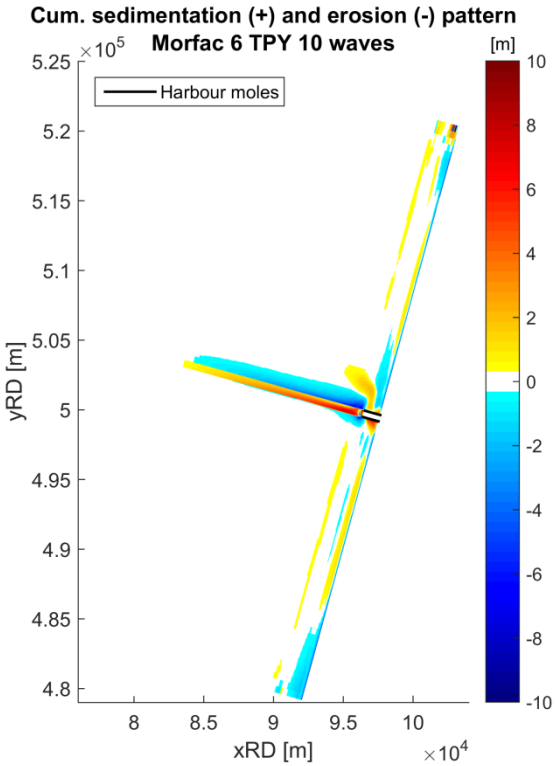

Figure 83 - Cumulative sedimentation (+) and erosion (-) pattern, Morfac 6 TPY 10 waves

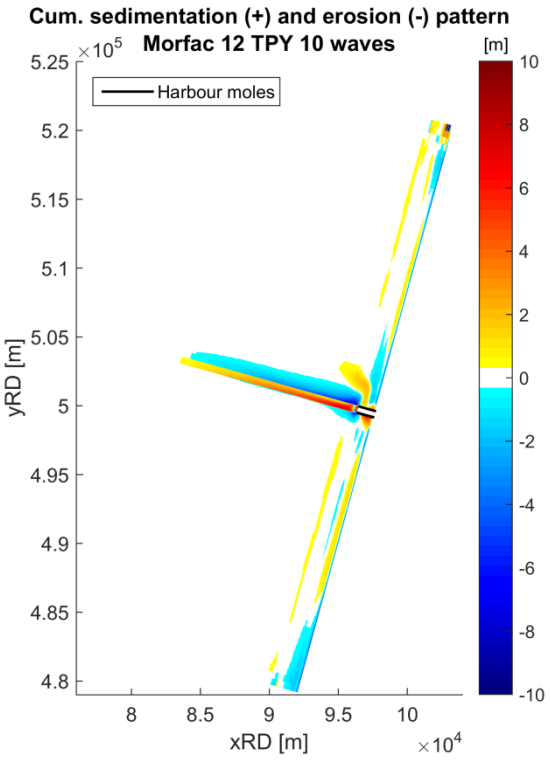

Figure 84 - Cumulative sedimentation (+) and erosion (-) pattern, Morfac 12 TPY 10 waves

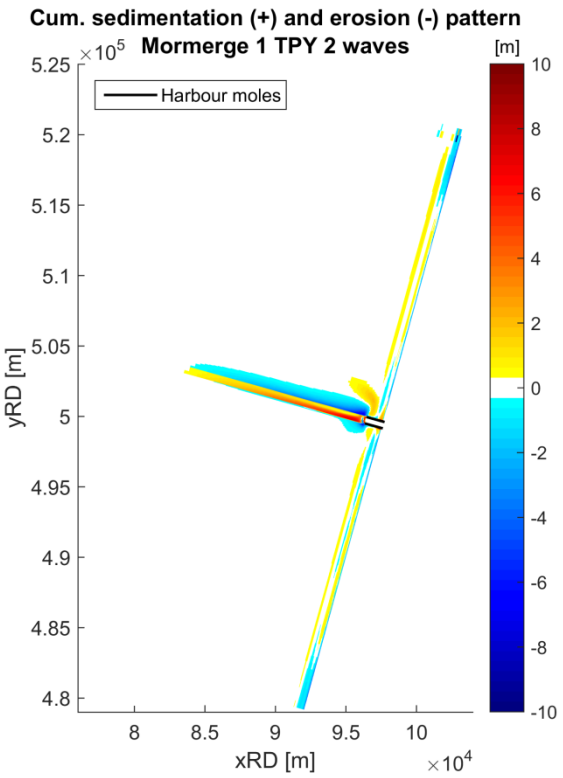

Figure 85 - Cumulative sedimentation (+) and erosion (-) pattern, Mormerge 1 TPY 2 waves

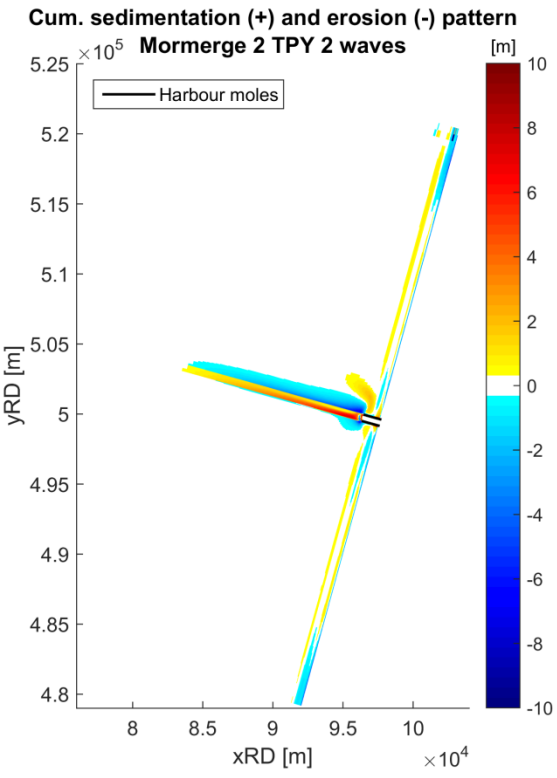

Figure 86 - Cumulative sedimentation (+) and erosion (-) pattern, Mormerge 2 TPY 2 waves

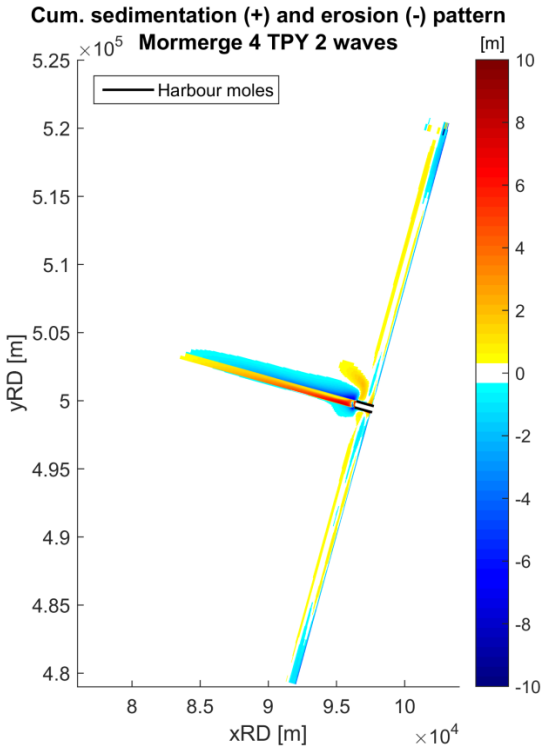

Figure 87 - Cumulative sedimentation (+) and erosion (-) pattern, Mormerge 4 TPY 2 waves

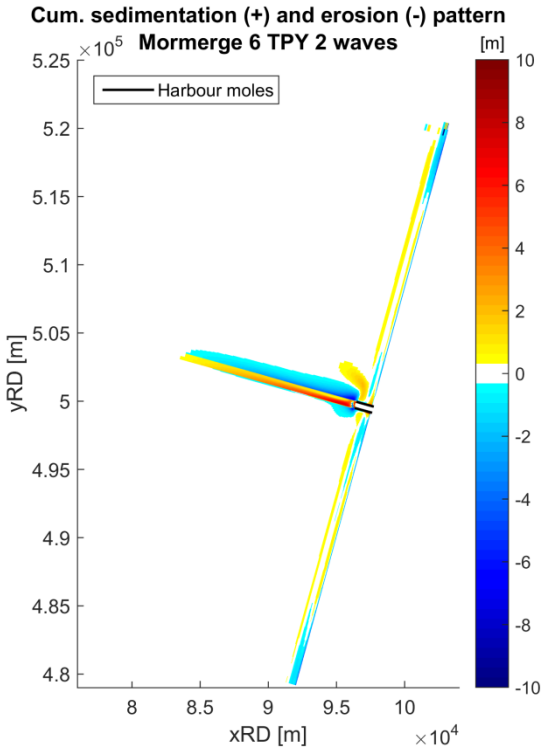

Figure 88 - Cumulative sedimentation (+) and erosion (-) pattern, Mormerge 6 TPY 2 waves

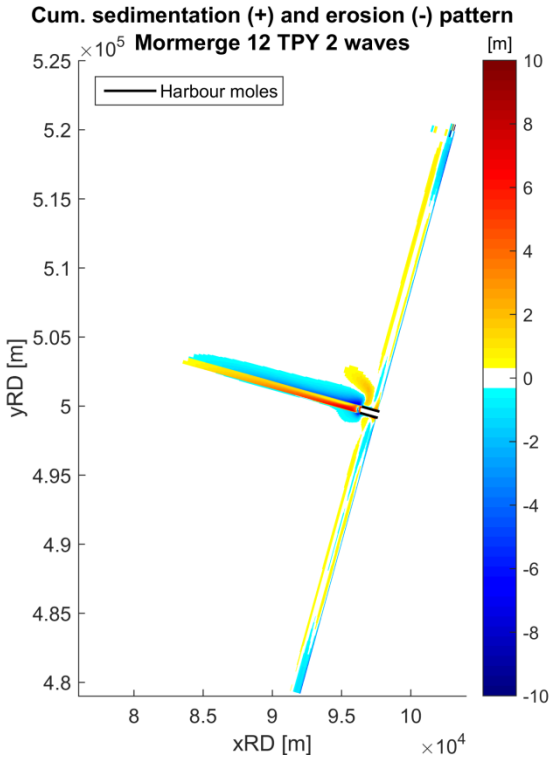

Figure 89 - Cumulative sedimentation (+) and erosion (-) pattern, Mormerge 12 TPY 2 waves

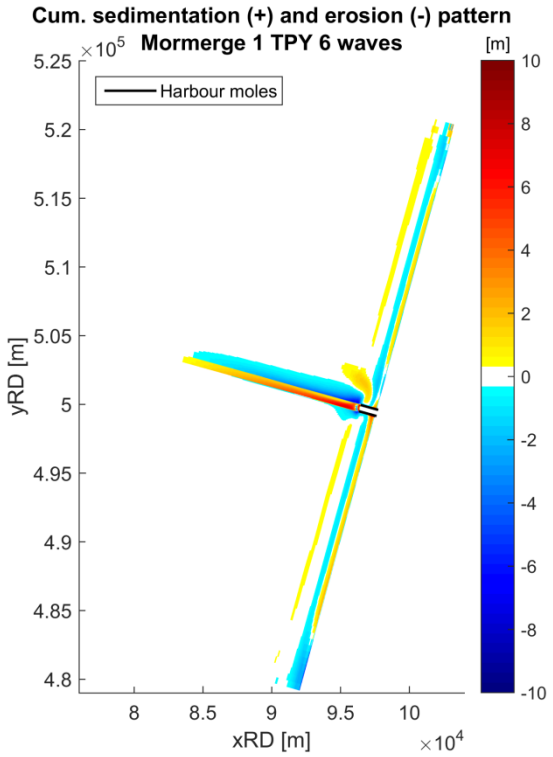

Figure 90 - Cumulative sedimentation (+) and erosion (-) pattern, Mormerge 1 TPY 6 waves

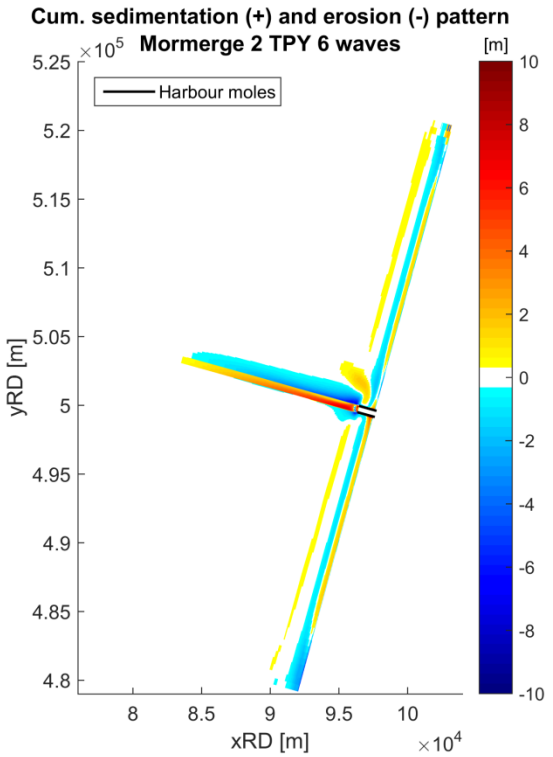

Figure 91 - Cumulative sedimentation (+) and erosion (-) pattern, Mormerge 2 TPY 6 waves

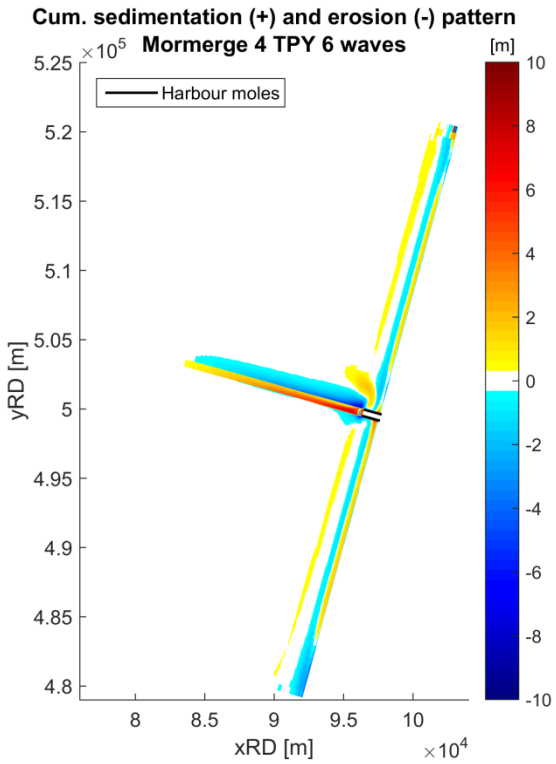

Figure 92 - Cumulative sedimentation (+) and erosion (-) pattern, Mormerge 4 TPY 6 waves

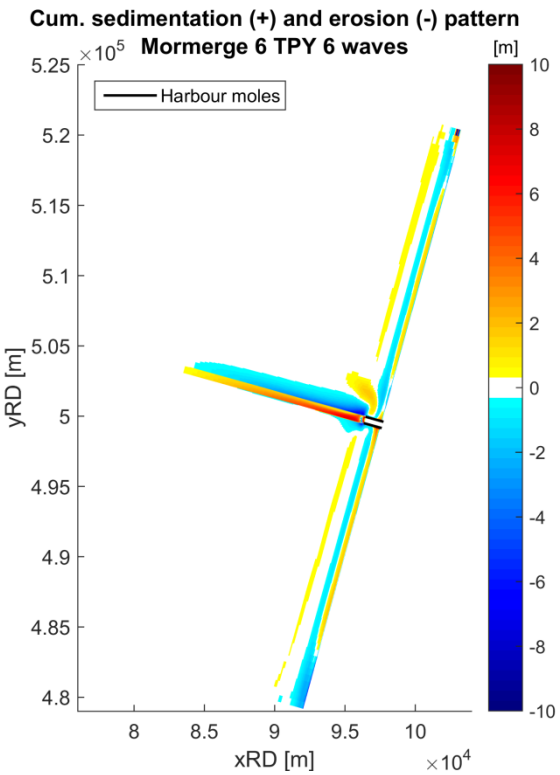

Figure 93 - Cumulative sedimentation (+) and erosion (-) pattern, Mormerge 6 TPY 6 waves

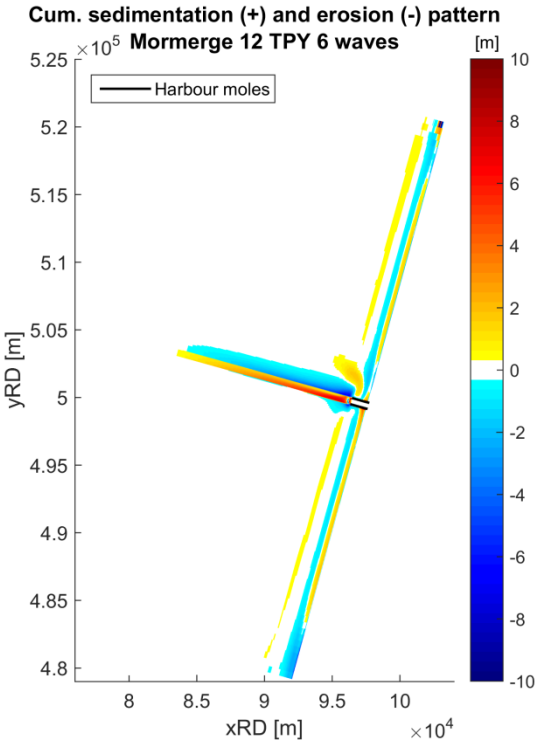

Figure 94 - Cumulative sedimentation (+) and erosion (-) pattern, Mormerge 12 TPY 6 waves

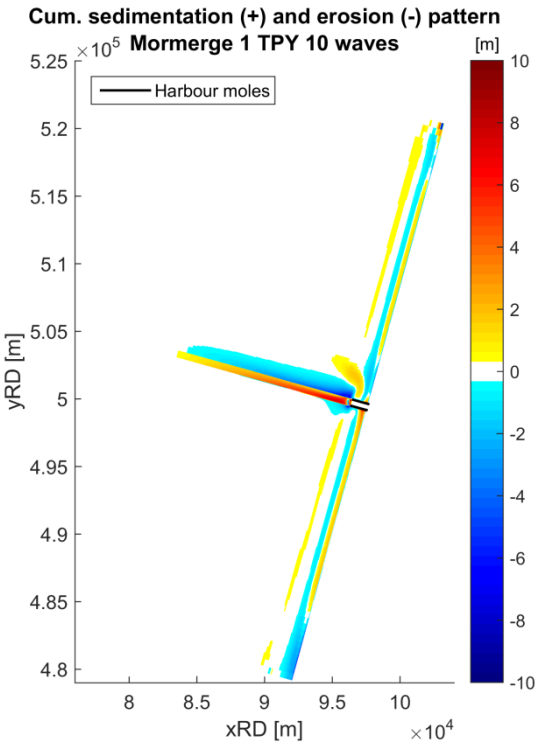

Figure 95 - Cumulative sedimentation (+) and erosion (-) pattern, Mormerge 1 TPY 10 waves

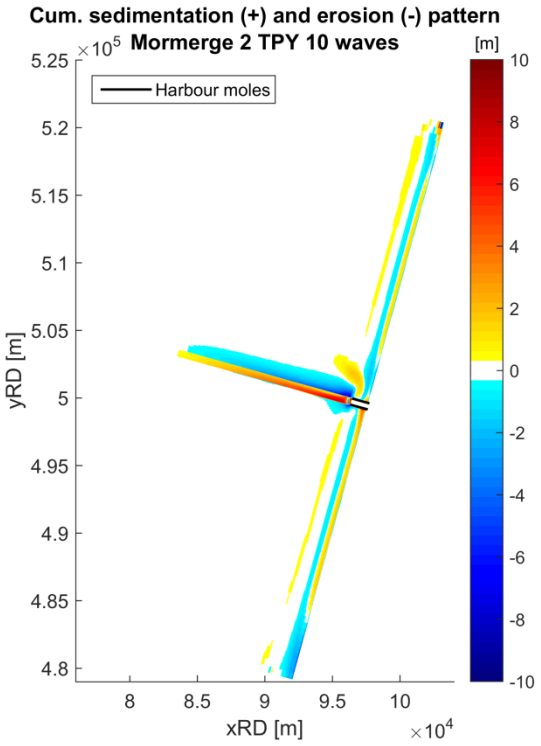

Figure 96 - Cumulative sedimentation (+) and erosion (-) pattern, Mormerge 2 TPY 10 waves

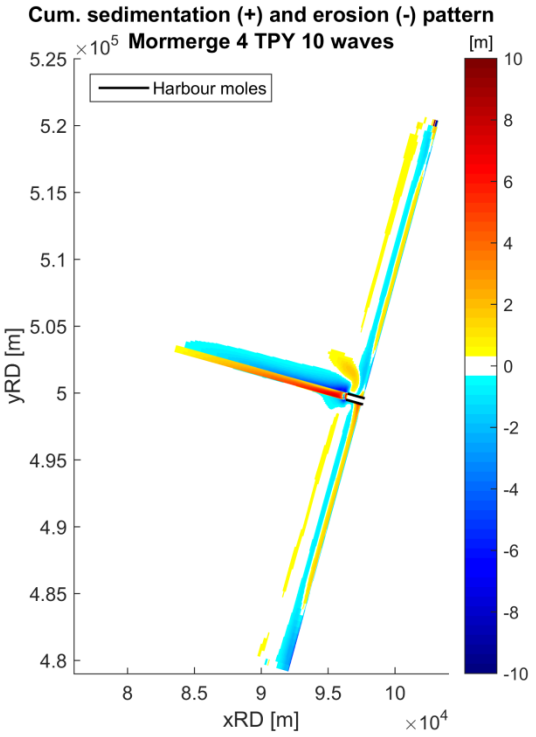

Figure 97 - Cumulative sedimentation (+) and erosion (-) pattern, Mormerge 4 TPY 10 waves

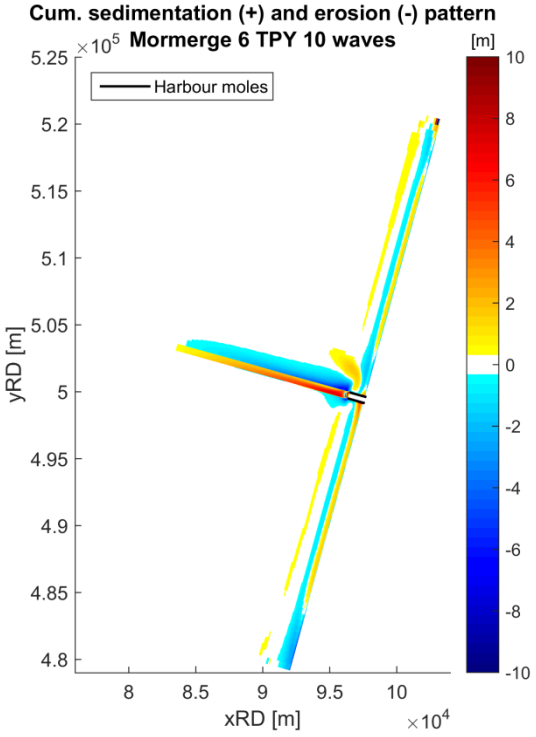

Figure 98 - Cumulative sedimentation (+) and erosion (-) pattern, Mormerge 6 TPY 10 waves

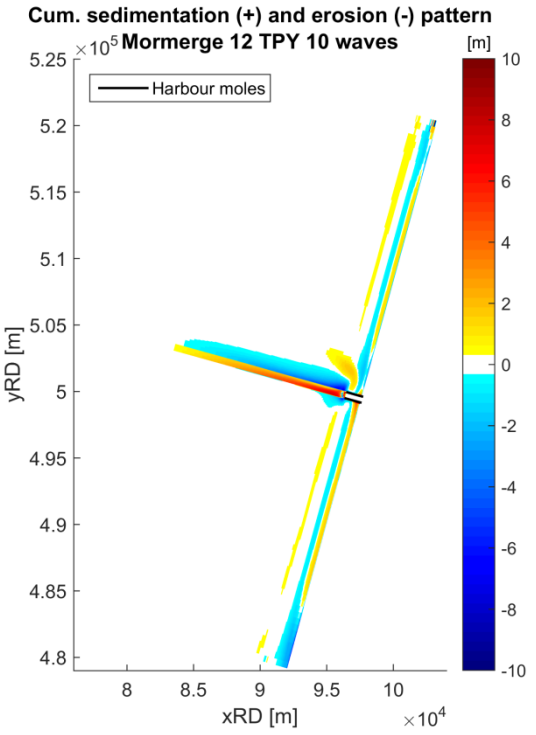

Figure 99 - Cumulative sedimentation (+) and erosion (-) pattern, Mormerge 12 TPY 10 waves